UNIVERSITY OF CALIFORNIA,
IRVINE

Investigating Mitochondrial Responses After Dendrite Injury and Repair

DISSERTATION

submitted in partial satisfaction of the requirements
for the degree of

DOCTOR OF PHILOSOPHY

in Biological Sciences

by

Patrick T Hwu B.A

Dissertation Committee:
Professor Katherine L. Thompson-Peer, Chair
Professor Marcelo A. Wood, Co-Chair
Professor Evgeny Z. Kvon
Professor Grant R. MacGregor
Professor Oswald Steward

2025

DEDICATION

To my mom, dad, and brother for showing me unconditional support.
I hope you are proud of me.
I love you.

TABLE OF CONTENTS

Page

DEDICATION ii
TABLE OF CONTENTS iii
LIST OF FIGURES vii
LIST OF TABLES ix
ACKNOWLEDGMENTS x
Curriculum Vita xii
ABSTRACT OF THE DISSERTATION xiii
Chapter 1 1
More than just the Powerhouse of the Cell 1
Historical Overview of Mitochondria 1
Mitochondrial Transport: *riding the rails* 5
Overview 5
Molecular motors of mitochondrial trafficking: from soma to synapse 6
Mitochondrial tethering: staying put 10
Mitochondrial Morphology: *size doesn't mean everything* 11
Overview 11
Fusing for function 12
Mitochondrial fission: breaking apart 13
Mitochondrial metabolism: metabolic masters of the cell 14
Moving beyond transport: non-canonical regulators of mitochondrial morphology 15
Mitochondrial contact sites: linked by membranes 16
Reactive oxygen species: ROS regulators of morphology 18
Central Controllers of Ion Flow 19
Overview 19
Gatekeepers of calcium: from calcium to catabolism 20
Magnesium matters: messengers for mitochondria 22
Power in potassium 23

Forging signals with iron 24
The sodium switch: a central regulator of ion homeostasis 25
Redox and renewal: a little ROS goes a long way 27
The Dispatcher of the Cell 29
Shape shifts under cell stress 30
The problem(s) 36
The approach 38
Chapter 3 40
Materials and Methods 40
Animals 40
Fly Husbandry and genetics 40
Drosophila larvae collection and handling 40
Larval immobilization for imaging 41
Ice anesthetics 41
Table of Fly Stocks 43
Table of Reagents and Resources 44
Microscopy 45
Confocal imaging 45
Airyscan imaging 45
Live imaging 45
2-Photon laser injury 45
Microtubule imaging 46
MitoGCaMP imaging 47
Table of Microscopes 48
Image analysis 49
Mitochondrial contraction 49
Mitochondrial area quantification 49
Mitochondrial fold-change quantification 50
Mitochondrial shape change index 50
Branching rate and elongation rate quantification 50

Mitochondrial GCaMP analysis 51
Table of Software 52
Chapter 3 53
In Vivo Dendrite Injury Drives Local Mitochondrial Contraction and Dendrite Branching 53
Abstract 53
Introduction 54
Results 56
Laser injury induces local changes in mitochondrial morphology 56
Dendrotomy induces distance-dependent mitochondrial contraction 59
Mitochondria contract independently of changes in microtubules or calcium buffering . 64
Injury-induced mitochondrial contraction scales with dendrite branch order 67
Hyperpolarization via KCNJ2 impairs mitochondrial contraction after primary dendrotomy 71
Complete injury-induced mitochondrial contraction requires Drp1 activity 75
Discussion 80
Chapter 4 87
Structural and Functional Plasticity 87
Introduction 87
Results 90
Investigating dendrite regeneration in genes involved in learning and memory in mice . 90
Proof of concept: SWI/SNF subunits Baf53b enhances dendrite regeneration 93
Baf53a, Baf53b, and Bap55 attenuate self-crossing defects in dendrite regeneration 93
Dendrite extension and retraction is increased during regeneration 95
Neuronal scaffolding during regeneration 97
Discussion 100
Chapter 5 103
Interpretations, Outlook, and Advice 103
Interpretations 103
Outlook for therapeutics 104
Advice for PhD students 105

Discipline 105
Experimental design 106
Data interpretation 106
REFERENCES 108
APPENDIX A: 2-Photon-induced Neurodegeneration 151
APPENDIX B: LCM tissue isolation for downstream genome sequencing 152
APPENDIX C: Miro N-terminal GTPase domain and EF hands are required for dendrite development 154
APPENDIX D: Mitochondrial recovery after dendrotomy 156
APPENDIX E: Characterization of ddaE and ddaD branching order for computational simulations 158
APPENDIX F: Dendrotomy induces ER fragmentation and calcium influx 160

LIST OF FIGURES

Page

1.1 Schematic of injury paradigms 56

1.2 Dendrite injury triggers changes in mitochondrial area 58

2.1 Schematic of injury paradigms and time lapse imaging 59

2.2 Characterization of mitochondrial contraction after proximal primary dendrotomy 60

2.3 Characterization of mitochondrial contraction after distal primary dendrotomy 61

3.0 Characterization of mitochondrial contraction after axotomy 63

4.0 Injury induced mitochondrial contraction can occur independently of EB1 puncta 65

5.0 Dendrotomy induces local global mitochondrial calcium buffering 66

6.1 Schematic of tertiary dendrotomy paradigm and subsequent arbor tracking 67

6.2 Tertiary dendrotomy induces mitochondrial contraction but to a lesser extent 69

6.3 Mitochondrial contraction scales with dendrotomy severity 70

6.4 Injury induced mitochondrial contraction is associated with dendrite branching 71

7.1 Schematic for injury paradigm for KCNJ2 experiments 72

7.2 KCNJ2 inhibits injury induced mitochondrial contraction 73

7.3 KCNJ2 inhibits and prolongs mitochondrial contraction 74

7.4 Presence of contraction in KCNJ2 is sufficient for injury-induced dendrite branching 75

8.1 Injury location and hyperfused mitochondria in Drp1.K38A neurons 76

8.2 Injury induced mitochondrial contraction and branching requires Drp1 77

9.0 Changes in mitochondrial distribution 79

10.1 Exploring how genes involved in learning and memory affect dendrite regeneration 91

10.2 HDAC3 does not inhibit dendrite regeneration in actin rich neurons 92

10.3 Baf53b overexpression does not enhance dendrite regeneration in highly stable neurons 93

11.0 Baf53a, Baf53b, and Bap55 ameliorate self-crossing defects in ddaC dendrite regeneration 94

12.0 Time lapse imaging of dendrite development and regeneration 96

13.0 ddaC and ddaF regeneration in the presence or absence of one another 99

14.0 2PiND (2Photon induced Neurodegeneration) 151

15.0 Zeiss PALM microbeam LCM (Laser Capture Microdissection) for RNA-sequencing 152

16.0 Dendrite regeneration in T25N (N-terminal GTPase) or E234K + E354K miro overexpression 154

17.0 Mitochondrial dynamics + recovery 30mins after dendrotomy 156
18.0 Features of class I dendrite development and in-vivo dynamics 158
19.0 Dendrotomy induces ER fragmentation and calcium influx 160

LIST OF TABLES

	Page
1.1 Fly stocks used during graduate studies	43
1.2 Reagents and resources used during graduate studies	44
1.3 Microscopes used during graduate studies	48
1.4 Software used during graduate studies	52

ACKNOWLEDGMENTS

During my graduate career, I have progressively become quieter, not because I don't enjoy talking about science or sharing my own experiences, but because it is difficult to listen and speak at the same time. I could not afford to miss an opportunity to learn from my mentees, my colleagues, and especially my mentors. So, I listened meticulously, to learn more from the people around me. I am incredibly fortunate to have received the mentorship I had during my graduate career.

Dr. Katherine Thompson-Peer, thank you for allowing me the freedom to play in the lab; to explore any ideas I had, carefully guiding me without influencing the trajectory of the projects based on your own creativities. I appreciate your mentorship, the feedback you gave me, and the fun ideas we could explore together. The countless talks we had about science, and the support (in all aspects) you provided me during my graduate studies. I cannot express my gratitude for your commitment to funding me wholly during my graduate career and although many of the ideas never materialized into tangible publications, I hope these data have helped inform us about the science. You have really helped shaped me into the scientist I am today. Many people enter graduate school with the intentions of pursuing academia but finish their graduate career and pursue industry. However, I am *not* one of those people, and to me, that is the best gift you have given me.

Dr. Marcelo Wood, thank you for being my co-mentor, even though we didn't meet frequently, whenever I needed advice, you were always available. When I asked how to be a better mentor, you praised me for acknowledging my shortcomings and told me that I was already doing the right things to be a better mentor. When I asked you for advice on leading a lab, how to pick the first graduate student, experiments, etc. you told me that when you first started your lab, every single experiment that the graduate student conducted went into a figure. You taught me how to write a manuscript, by funneling down multiple knowledge gaps in the field and eventually the knowledge gap that is addressed in the manuscript. You taught me what you think as the pillars of data supporting the manuscript, where to put them in the manuscript, and how to structure it in a meaningful way. Your perspective on science gave me confidence in myself as a young investigator.

Dr. Evgeny Kvon, thank you for giving me a new perspective in science. I will never forget the weekend when we walked by each other, and you said, "*you're here every day, it's good, I used to be like you during graduate school*" and I said, "*of course I love the science it's fun*". Although we only met once a year, learning how and why you approach science from an evolutionary perspective opened my eyes to a completely new viewpoint of biology. And to be honest, anytime I begin reading about literature now, I start by looking into whether processes are conserved, when they diverge, and why they diverge. I cannot thank you enough for giving me this new perspective on biology.

Dr. Grant MacGregor, thank you for always being attentive during my committee meetings and giving me advice throughout my graduate career. Your advice was blunt, but it was necessary. During my second-year committee meeting, you asked me if I knew how neurons developed (cytoskeletal components, polarity, growth factors, etc.) and I said no, and you responded with "I suggest you pick up any developmental neurobiology textbook and learn the fundamentals" (something of this nature). When you said this, it made me realize how much background I was

lacking, especially coming from Psychology. Your feedback guided my transition from psychology to biology and *shaped* my foundation as a young scientist.

Dr. Oswald Steward, thank you for the senior guidance you provided me. I was lucky to have a committee member like you, who is both an expert in neuronal cell biology and injury signaling. When I first presented my work with dendrite extension and retraction you kept asking me why it matters, why does it matter if dendrite extend and retract more during regeneration? and I never understood why you kept asking me this. But during my 4th year, I realized the reason you kept asking me was because if I never changed the way I designed experiments I would always be left without definitive answers. So, I went back to read the two articles you gave me, one by Platt and one by Douglas whose review of Platt's strong inference. Since then, it completely shifted the way I design experiments.

Dr. Adeela Syed, you watched me grow from an undergraduate researcher with Dr. Ceazar Nave, to a graduate student. You taught me (almost) everything I know about microscopy your dedication to helping others, conducting science, and curiosities truly makes the OBC the place that it is today.

To the members of the Thompson-Peer Lab: Dr. Vinicius Duarte for being a great colleague. The lab is so lively with you in it, and I was so lucky to have someone start this journey with me; Dr. Sydney Prange I remember teaching you some of the microscopy skills early when you first started and every time we moved labs back and forth I was so excited to have you sit next to me; Being able to watch you grow throughout the past 5 years has been pure; Mia Brantley for being such a great, kind friend, the banter we had, and the food runs we went on; Lauren Kim for being such a phenomenal undergraduate. In all honesty, I probably learned more from you than you learned from me, you taught me how to be a better mentor, and you were so incredibly patient and understanding of me. To the friends I've made throughout my graduate career Clark Hendrickson, Grace Bower, Ethan Hollingsworth, Eric Blaes, Jonas Enders, Kathleen Parada, and Raquel Bowman thank you all for always being by my side, providing me emotional support during the times of need (personal obstacles), members of facilities for always getting things done so quickly, Rubin and Scott (people that helped during our move), the Luis and Miguel (the movers), and Gary Roman and Mayra Rubio (admin), and María (facility worker). I would be lucky to be half the people you are today.

And lastly, to my partner Dandan Liu I met you during the most pivotal moment in my life. Thank you for giving me unconditional love and support.

The text of portions in Chapter 3 of this dissertation is an adaption of the materials as it appears in Hwu, P. T, Kim, L.A., Wood, M.A., Thompson-Peer, K.L. (2025). In vivo dendrite injury drives local mitochondrial contraction and dendrite branching. used with permission from Elsevier Publishing. The coauthors in this publication are Patrick T Hwu, Lauren Ashley Kim, Marcelo Andres Wood, Katherine Louise Thompson-Peer. Katherine Louise Thompson-Peer directed and supervised the research which forms the basis for this dissertation.

Curriculum Vita

Patrick T Hwu

EDUCATION

PhD in Biological Sciences, University of California, Irvine — Sept. 2019—Dec. 2025
B.A. in Psychology, University of California, Irvine — June 2016—Dec. 2019

PUBLICATIONS

Hwu P., Kim L., Wood M., Thompson-Peer K. (2025). *In-vivo dendrite injury drives local mitochondrial contraction and dendrite branching.*

Prange S., Bhakta I., Sysoeva D., Jean G., Madisetti A., Le H., Duong L., **Hwu P**., Melton J., Thompson-Peer K. (2024). *Dendrite injury triggers neuroprotection in Drosophila models of neurodegenerative disease. Scientific Reports*. 2024 September 26. doi.org/10.1038/s41598-024-74670-4.

Nave C., Roberts L., **Hwu P**., Estrella J., Vo T., Nguyen T., Pervolarakis N., Bui T., Rindner D., Shaw P., Leise, T., Holmes T. (2021). *Weekend light shifts evoke persistent Drosophila circadian neural network desynchrony*. J.Neurosci. 2021 April 15. doi:10.1523/JNEUROSCI.3074-19.2021.

Stehr D., Zhou X., Tisby M., **Hwu P**., Pyles J., Grossman E. (2021). *Top-down attention guidance shapes action encoding in the pSTS*. Cerebral Cortex. 2021 Feb. 24. doi:10.1093/cercor/bhab029.

TEACHING

D111L Developmental and Cell Biology Lab — Winter 2024
Bio 97 Genetics (Head Teaching Assistant) — Fall 2024
Bio 97 Genetics (Lead Teaching Assistant) — Fall 2021
DCB Teaching Excellence Award
Bio93H Honors DNA to Organisms — Fall 2020

CONFERENCES AND PRESENTATIONS

Annual Society for Cell Biology (Boston, MA) — Dec. 2023
Co-presenter ABRCMS (Phoenix, AZ) — Nov. 2023
Neuroblitz (Irvine, CA) — Dec. 2021
Center for Neural Circuit Mapping (Irvine, CA) — Aug. 2021

UNDERGRADUATE MENTORSHIP

Lauren Kim (Sept. 2022—June 2025; SURP Award 2023), Erika Zagni (Dec. 2022—Dec. 2022), Asal Kalantir (Sept. 2022—June 2023), Claire Stewart (Mar. 2022—Aug. 2022; SURP Award 2022), Rocelyn Lee (Dec. 2020—Mar. 2022), Mansher Dhaliwal (Dec. 2020—Mar. 2022; SURP Award 2021), Miyo Sun (Dec. 2020—Dec. 2021)

ABSTRACT OF THE DISSERTATION

Investigating Mitochondrial Responses in Dendrite Injury and Repair

by

Patrick T Hwu

Doctor of Philosophy in Biological Sciences

University of California, Irvine, 2025

Assistant Professor Dr. Katherine Thompson-Peer Chair

Professor Dr. Marcelo Wood, Co-Chair

Studies have estimated that the global economic burden of neurological disorders costs nearly $1.9 trillion per year and is projected to increase by 4.3% annually[1]. While this fact highlights the macroeconomic burden of public health disorders, these disorders are just as debilitating on a personal level, affecting the patient and their caretakers.

Neurons are the principal cell of the nervous system, they transmit and detect electrochemical signals through their axons and dendrites, respectively. Unlike many other cells, neurons are non-mitotic, presenting an indisputable challenge for renewal and repair when systems become damaged. *Fortunately*, neurons can regenerate their axons[2–10], dendrites[11–18], and even both simultaneously[19]; highlighting a remarkable capacity for repair. However, for cells to initiate repair, a repair stimulus must first be conveyed and subsequently detected. Indeed, cell damage induces several changes in cell homeostasis including organelle fragmentation[20–22], ion imbalance[23–25], and cytoskeletal disorganization[26–29]. Importantly, the damage signal must be within an amplitude that is detectable but not detrimental or cells may not initiate repair.

Using in-vivo time lapse imaging in *drosophila*, combined with genetic tools, we found that mitochondria rapidly contract following laser dendrotomy (dendrite injury). We provide evidence

that this response is regulated by neuronal depolarization and the canonical mitochondrial fission machinery. Furthermore, we found that the presence of mitochondrial contraction following dendrite injury is associated with an increase in dendrite branching. Interestingly, we found that injury-induced mitochondrial contraction scales with injury severity; that is, injury of a primary dendrite elicits a stronger contraction response than injuring a terminal branch. Moreover, *KCNJ2* (*Potassium Inwardly Rectifying Channel Subfamily J Member 2*) decreased the likelihood of injury induced mitochondrial contraction but not the consequence of contraction, if mitochondria contracted after injury, neurons still had an increased branching rate. Moreover, we found that expressing a dominant negative allele of Drp1 (which lacks GTPase activity), in a cell type specific manner prevents injury-induced contraction and subsequently branching. We defined this injury-induced response as an injury signal as evidenced by the decreasing contraction amplitude (mitochondrial further away require a longer time to contract and are less likely to contract than mitochondria close to the injury site) and the stochastic response when we injured tertiary dendrites. In summary, we characterized mitochondrial contraction following dendrotomy and injury induced contraction was associated with dendrite branching. From our studies, we provide evidence that neuronal depolarization and the canonical fission machinery promotes injury-induced mitochondrial contraction. These findings suggest that altered in mitochondrial morphology at baseline, observed in diseases, may impair the cell's ability to detect in mitochondrial shape and subsequently regeneration. This study published will provide a solid foundation for future investigations into this mechanism, whether this increased dendrite branching is associative or causative.

Chapter 1

More than just the Powerhouse of the Cell

Historical Overview of Mitochondria

The first observations of mitochondria date back to 1857, when Albert von Kölliker published his findings on "sarcomeres" which were small granular structures he observed in muscles[30]. In 1890, Richard Altmann used staining techniques to visualize *bioblasts*, which he proposed were independent living organisms within the cell[31]. and in 1898, Carl Benda reported his own observations of both tubular and granular structures living in eukaryotic cells which he coined *mitochondria*[32]. Little did they know that these structures they meticulously investigated, now known as mitochondria, are essential for almost all modern-day eukaryotes.

A mechanistic understanding of mitochondrial function was significantly advanced early in the 20th century. In 1925, David Keilin rediscovered reversible redox-active proteins called cytochromes, (first discovered by Charles MacMunn during his studies on pigmentation) showing that they are imperative components of the respiratory chain complex[33]. Otto Warburg's research throughout 1910—1930[34,35] showed that following fertilization in sea urchins, respiration is

significantly upregulated, providing evidence on how mitochondria utilize oxygen to support life, for which he was awarded the 1931 Nobel Prize in Physiology or Medicine[36]. Warburg's research critically identified that cancer cells preferentially use aerobic glycolysis instead of aerobic respiration to generate ATP (adenosine-triphosphate). Around the same time, Albert Szent-Györgyi isolated Hexuronic acid (also known as, vitamin C) from various plants and the adrenal cortex, elucidating the chronological process of the fumarate–succinate cycle (later found to be crucial for the Krebs cycle), awarding him the 1937 Nobel Prize in Physiology or Medicine[37–40]. In 1937, Hans Krebs described the citric acid cycle (also known as the Krebs cycle or tricarboxylic acid cycle) establishing the central pathway of oxidative metabolism, work which awarded him the 1953 Nobel Prize in Physiology or Medicine[41,42]. In 1945, Fritz Lipmann discovered coenzyme A, a key intermediate metabolite which later showed to be crucial for several metabolic processes, resulting in the 1953 Nobel Prize in Physiology or Medicine[43]. The breakthrough of biochemically isolating mitochondria was achieved by Albert Claude in 1946, who developed cell fractionation and studied various components of mitochondria and other organelles like the endoplasmic reticulum, laying the foundation for organelle fractionation. In 1953, George Palade produced, at the time, the highest resolved image of mitochondria using electron micrographs, revealing their beautifully complex cristae[44]. Christian de Duve, through biochemical fractionation studies, discovered lysosomes in 1955 and peroxisomes in 1965[45,46]. Claude, de Duve[47], and Palade[48] shared the 1974 Nobel Prize in Physiology or Medicine for their contributions to organelle biology.

Mitochondrial bioenergetics greatly advanced throughout the 1960s. Efraim Racker and colleagues purified ATP-synthase between 1961–1967[49,50], establishing the enzymatic basis of oxidative phosphorylation. In 1961, Peter Mitchell proposed the chemiosmotic hypothesis to explain that mitochondria, through catabolism, generate ATP through an electrochemical gradient

across the inner membrane which later won him the 1978 Nobel Prize in Chemistry[51,52]. In 1963, Margit and Sylvan Nass demonstrated that mitochondria react to the same reagents as DNA, visualized through electron microscopy, providing the first evidence for mtDNA[53] (mitochondrial DNA).

By the late 20th century, mitochondria were increasingly linked to human disease. In 1988, Douglas Wallace reported the first disease caused by mutations in mtDNA, linking mitochondrial genome to Leber's hereditary optic neuropathy[54]. In 1992, Paolo Bernardi characterized the mPTP (mitochondrial permeability transition pore) as a Ca^{2+}-dependent inner membrane channel influencing mitochondrial permeability and swelling of the inner membrane[55]. Lastly, work by Boyer[56] and Walker[57] made significant advances on how conformational changes of ATP synthase drives ATP synthesis[58,59] sharing the 1997 Nobel Prize in Chemistry with Jens Skou[60] for his discovery of Na^+/K^+ pumps in 1957[61].

At the turn of the 21st century, mitochondrial dynamics came into focus. In 1998, Janet Shaw's group showed that *Dnm1p* (*dynamin-related protein 1*) controls mitochondrial fission in yeast[62]. In 2001, Alexander van der Bliek's group demonstrated that its mammalian homolog *Drp1* (*Dynamin related protein-1*) is required for mitochondrial division[63]. In 2003, David Chan's group showed that *Mfn1* and *Mfn2* (*Mitofusin-1,-2*) are essential for mitochondrial fusion and embryonic development in mice[64]. Also in 2003, Vamsi Mootha et al., defined the first integrated mitochondrial genome[65]. Finally, in 2011, two groups independently and simultaneously (Baughman et al. (Mootha's lab) and De Stefani et al. (Rizzuto's lab)) identified the mitochondrial calcium uniporter (MCU), the mechanism controlling calcium influx into mitochondria[66,67]. With the improvements in EM (Cryo-EM) there has been significant advancements in understanding the protein structures that regulate mitochondrial transport[68,69], morphology[70,71], ion flux[72–75],

mitophagy[76,77], and metabolism[78–80].

Building upon previous literature, the current ongoing research has uncovered mitochondria's role in development[81–83], cellular maintenance[84,85], injury signaling[86–88], and local translation[89,90]. Because of mitochondria's primary role in ATP production, which is influenced by mitochondrial morphology, trafficking, and distribution, it should not come as a surprise that changes in mitochondrial morphology, trafficking, and distribution—observed in diseases or cellular injury—affects cell homeostasis.

Our understanding of mitochondria today is shaped by an integrative approach, linking their dynamic morphology to cellular function. Mitochondria constantly remodel themselves through Drp1 (Dynamin related protein 1) dependent fission[91–93], Mfn1/2[64] (Mitofusins 1/2) and OPA1 (mediated fusion[71], and cristae restructuring, processes that collectively tune mitochondrial length, branching, and internal architecture. These shape changes respond to fluctuations in membrane potential[94] and calcium[95,96] allowing mitochondria to adapt their bioenergetic output to cellular demands. Importantly, mitochondria are being increasingly recognized as critical regulators of injury signaling[9,95,97–99]. And whilst prior labs have independently studied how mitochondria respond to cell injury or mitochondria's role in repair, no studies (to my knowledge), have directly examined how mitochondria respond at the time of injury and the cells outcome. During my graduate studies, we observed that dendrite injury triggers rapid mitochondrial contraction, injury-induced shape changes in mitochondria is regulated by the neuronal depolarization, the fission machinery (Drp1), and provide evidence injury-induced contraction is regulated by neuronal depolarization. These findings are consistent with previous literature showing that neuronal depolarization causes mitochondria to fragment in a Drp1 dependent manner. Moreover, we observed injury-induced contraction was associated with an increase in dendrite branching,

suggesting that this morphological change in mitochondria we observe may serve as an injury stimulus for neurons to respond to.

In this chapter, I will review how cellular homeostasis is shaped by four interconnected aspects of mitochondrial biology: (1) trafficking, tethering, and subcellular distribution; (2) the regulation and functional significance of mitochondrial morphology; (3) ion homeostasis and redox signaling; and (4) injury-evoked signaling cascades under pathophysiological stress. Together, these processes provide the mechanistic framework for interpreting our observations of injury-induced mitochondrial contraction and help frame how acute shape changes may influence, or be influenced by, local metabolic, ionic, and signaling conditions during neuronal repair.

Mitochondrial Transport: *riding the rails*

Overview

Mitochondria are the primary source of ATP in most cells, and their precise subcellular distribution is crucial in providing local energetic demands. To achieve this, mitochondria are actively transported along microtubule tracks by motor proteins and their adaptor complexes. This trafficking system ensures that mitochondria are delivered to regions of high metabolic load during neuronal outgrowth[100], where ATP production[101] and calcium buffering[102] are most needed. Conversely, when mitochondria fail to reach the right place at the right time, cellular homeostasis is disrupted: local ATP levels fall[103], calcium influx[102] becomes dysregulated, and critical signaling pathways are impaired. Thus, mitochondrial positioning and motility are not merely structural features but central determinants of how neurons and other cells maintain function under both physiological and stressed conditions.

Molecular motors of mitochondrial trafficking: from soma to synapse

Mitochondria are dynamic organelles essential for supplying energy for maintaining energetic demands and ATP for neurite outgrowth during neuronal development. Neuronal outgrowth is an energetically demanding process, as outgrowth requires a significant amount of fuel for ATP-dependent processes like cytoskeleton polymerization and molecular processes such as translation[89,90]. In developing neurons, mitochondria are most dynamic, ensuring that these energetic requirements are satisfied. As neurons develop, mitochondria progressively lose motility, transitioning from highly dynamic organelles in immature neurons to stable organelles in developed neurons[83,100]. For example, in sensory neurons of chick embryos mitochondria halt at mature dendrites, providing energy for local translation[104]. Disrupted mitochondrial motility leads to defects in neuronal patterning, impaired synaptic function, and ultimately neurodegeneration[84,105].

The spatiotemporal organization of neuronal mitochondria is influenced by their structural complexity and neuronal function. In Drosophila horizontal neurons, mitochondria are densely packed in higher-order dendritic branches where their distribution, motility, and speed all decrease with branching order[82]. Change in mitochondrial motility is widely controlled by neuronal activity; and while electrically stimulating neurons is insufficient to drive motility under basal conditions[83,106], it can induce trafficking under pathophysiological conditions. In fact, under basal conditions, local tetanic stimulation or depolarization pushes mitochondria into dendritic spines, decreasing motility and stabilizing them at synapses[107]. In contrast, in RGC (retinal ganglion cells) of *Crx* (*cone-rod homeobox*) null mice, the lack of converging sensory inputs from photoreceptors to bipolar neurons results in spontaneous neuronal activity and subsequently increased mitochondrial motility[83]. These observations illustrate that mitochondrial motility is finely tuned

to the functional and structural demands of neurons. This tight coupling between neuronal depolarization and mitochondrial redistribution provides a mechanistic framework for understanding why injury-evoked depolarization in our model triggers rapid mitochondrial contraction and subsequent dendritic remodeling.

Mitochondrial transport and stability rely heavily on the interactions between motor proteins and cytoskeletal structures such as microtubules and actin filaments. Microtubules serve as railroads for mitochondrial transport and directionality of mitochondrial transport is achieved through motor proteins. For example, kinesin mediates anterograde trafficking towards plus-end microtubules while dynein mediates retrograde trafficking towards minus-end microtubules. The master regulator of mitochondrial trafficking is *Miro1/2* (mitochondrial Rho GTPase-1/2). Miro1/2 (*Miro1/2* in mammals and *dMiro* in Drosophila) is anchored to the OMM (outer mitochondrial membrane) which serves as a motor adaptor for Trak (Trafficking kinesin protein 1, -2; also known as GRIF1/2, *milton* in Drosophila). *Miro1* is a critical regulator of dendrite maintenance as mutations in *Miro1* has shown to prevent mitochondria from being trafficked out of the cell body into subcellular compartments of dendrites[105]. Interestingly, neurons are capable of developing dendrites and axons even when mitochondrial trafficking is severely compromised[105]; it is the absence of locally stable mitochondria in mature neurons which causes neurons to undergo neurodegeneration[84]. In motor neurons of Drosophila larvae, the N-terminal GTPase domain of dMiro is necessary for mitochondrial trafficking in axons and dendrites, and the C-terminal GTPase domain is known to directly regulate retrograde trafficking of mitochondria in the axon[105]. In the axons of Drosophila NMJs (neuromuscular junctions), *dMiro*$^{-/-}$ null larvae have impaired mitochondrial motility[108]. Interestingly, in MEFs (mouse embryonic fibroblasts), *Miro1* knockout severely impairs mitochondrial trafficking, compared to *Miro2* knockouts which

showed minimal effects. The relationship between *Miro1* and *Miro2* is further complicated, as loss of *Miro1* and *Miro2* have a less severe phenotype than just loss of *Miro1*, suggesting antagonistic effects of *Miro* on mitochondrial trafficking[109].

Mitochondrial dissociation from motor proteins is largely controlled by the two calcium sensing domains of *Miro* (EF-hands) and mutations within these domains prevent calcium-dependent halting of mitochondria[110]. In addition to *Miro*, recent studies in C. elegans have shown that RIC7 localizes to axonal mitochondria, trafficked in the anterograde direction[111]. Interestingly, *RIC-7* has no known mammalian homologs but is absolutely required for anterograde trafficking in a Kinesin1 dependent manner in worms. Although RIC7 has no homologs in vertebrates, it would be insightful to identify how RIC7 evolutionary diverged to better mechanisms regulating mitochondrial trafficking.

While the Miro/TRAK complex ensures that mitochondria are marked for trafficking, preferential interactions between TRAK-Kinesin (primarily anterograde) or TRAK-Dynein (retrograde) are formed to ensure that mitochondria are trafficked in the correct directions. In non-neuronal cells (HEK293), wildtype overexpression of *Miro1* sufficiently recruits TRAK1 to mitochondria, providing insight into the role of Miro1/TRAK complex in regulating mitochondrial transport[110,112]. The functional importance of TRAK in mediating mitochondrial trafficking is further supported by mutations in Drosophila, where loss of *milton* (Drosophila TRAK ortholog) causes mitochondria to stall in the cell body[113]. Furthermore, mutations in *milton* prevents KHC (Kinesin heavy chain) localization in photoreceptors, impairing compound eye development[114]. In mouse hippocampal neurons, TRAK1 preferentially binds Kif5b localizing to axons, driving anterograde transport; while TRAK2 preferentially associates with dynein/dynactin in dendrites to promote retrograde transport. Loss of TRAK1 significantly impairs axon but enhances dendrite

development; whilst loss of TRAK2 enhances axon but impairs dendrite. This specificity is conferred by differences in the TRAK N-terminus. TRAK conformational changes (open vs autoinhibited states) regulate motor accessibility, but the TRAK1 vs TRAK2 preference itself is not solely due to TRAK2's N-terminus being "hidden"[115]. TRAK complexes can further confer specificity in mitochondrial transport. For example, *Optn* (*Optineurin*) has shown to connect the C-terminus of the Kif1b motor to TRAK1 during anterograde transport, and loss of this domain significantly impairs anterograde trafficking[4].

In contrast to Kinesins and Dyneins, Myosins regulate actin-based transport. Myo (Myosins) are a family of ATP-dependent motor proteins involved in both antero- and retrograde mitochondrial transport. In Drosophila embryos, *MyoV* (*Myosin 5*) knockout increases bidirectional trafficking, while *MyoVI* (*Myosin 6*) knockout increases retrograde trafficking only[116]. Additionally, *Myo19*, which exclusively associates with mitochondria has been shown to play a critical role in actin-dependent transport[117]. Miro1/2 serve as recruitment platforms for Myo19, by recruiting and stabilizing Myo19 on the OMM, providing evidence that Miro links organelle positioning to actin-based motility[109]. These studies highlight the critical role of motor proteins in regulating mitochondrial transport.

In addition to the established regulators that directly attach motor proteins to mitochondria, many non-transport related genes further regulate mitochondrial dynamics. In Drosophila larval segmental nerves, loss of mitochondrial fusion or fission machinery via *Marf* or *Opa1* RNAi reduces distal mitochondrial distribution in NMJs (neuromuscular junctions)[118]. Furthermore, several other genes that regulate mitochondrial function also influence dynamics: In zebrafish peripheral neurons, expressing *PGC-1α* (transcriptional coactivator of mitochondrial biogenesis) enhances mitochondrial motility[119]; in rat hippocampal axons, *Pink1* or *Parkin* overexpression

reduces mitochondrial motility, with *Pink1-Parkin* acting synergistically[120]; and in mouse striatal neurons, Foxp1 haploinsufficiency decreases mitochondrial trafficking and alters dendrite morphology[121]. In mammalian cell culture, Drp1 controls mitochondrial motility and loss of GTPase activity via Drp1.K38A disrupts mitochondrial distribution in COS-7 cells[122]. While motor proteins and their adaptors serve as the primary regulators of mitochondrial trafficking, mitochondrial trafficking is sensitive to alterations in mitochondrial homeostasis such as morphology and metabolism[123,124].

Mitochondrial tethering: staying put

Proper mitochondrial localization is imperative for regulating cell homeostasis. In mature neurons, mitochondria are primarily stable, ensuring that ATP is abundant across different subcellular compartments. Mitochondria are primarily stabilized through mitochondrial-microtubule anchoring. One well studied protein is *Snph* (*Syntaphilin*), a mammalian specific, neuronal protein that acts as a docking receptor at the interface of mitochondria and microtubules. *Snph* exists as a single gene but confers functional specificity through its N- and C-terminal domains. For example, previous studies have shown that the N-terminus of *Snph* is necessary and sufficient to induce mitochondrial-microtubule anchoring while the C-terminus is required for *Snph* localization to mitochondria[125]. Moreover, *Snph* is required to immobilize mitochondria following KCl-induced depolarization and disrupting Kif5-Snph interactions prevent activity-dependent mitochondrial arrest[126].

In contrast to mitochondria-microtubule tethering, mitochondria are anchored to actin filaments and other organelles. For example, mitochondria are anchored to VAPs (vesicle-associated membrane proteins) in dendrites which ensures local energy synthesis and calcium

buffering[127]. In yeast, RHOT1 (*Miro)* localizes to ERMES (ER–mitochondria encounter structures, also known as MERCS, ER-mitochondria contact sites in mammals and other eukaryotes), where it regulates the number and size of tethering sites[128]. Several ER–mitochondria tethering proteins have been shown to promote MERCS, including PDZD8 (PDZ domain containing 8)[129] and Grp75 (glucose-regulated protein 75), which couples IP3R (inositol 1,4,5-trisphosphate receptor) on the ER to VDAC1 (voltage-dependent anion channel 1) on the OMM (outer mitochondrial membrane)[5]. In the mouse hippocampus, overexpression of *Alex3* (*armcx*, *armadillo repeating containing X-linked protein 3*) results in perinuclear mitochondrial tethering, without affecting calcium buffering capacity or oxygen consumption, highlighting that some proteins can strictly act to regulate mitochondrial trafficking[130]. Together, these findings highlight the complex interplay of mitochondrial tethering and how control of these processes occur at the cytoskeletal and organelle levels to regulate cellular homeostasis[129,131].

Mitochondrial Morphology: *size doesn't mean everything*

Overview

At the most fundamental level, mitochondrial morphology is controlled by a meticulous balance between the fusion and fission machinery. Mitochondrial fusion is the process which combines two individual organelles into a single organelle. This process is critical for preserving mtDNA (mitochondrial DNA)[132], regulating ATP production[133], and preventing organelle dysfunction (as reviewed here[134]). In contrast, mitochondrial fission splits a single mitochondrion into several smaller mitochondria, a regulatory process to remove damaged mitochondria and/or increase trafficking to satisfy energetic demands. Due to the importance of mitochondria in regulating cell homeostasis, changes in mitochondrial morphology have imperative consequences

on the cell, and directly impact mitochondrial's ability to generate ATP consequences on the cell[135]. Consistent with this, we find that dendrite injury induces complete and rapid mitochondrial contraction, which is highly localized to the injured branch, illustrating how acute stress can trigger immediate structural remodeling of mitochondria in vivo.

Fusing for function

The balance between mitochondrial fusion and fission is largely governed by a well-characterized set of dynamin-related GTPases. On the fusion side, Mitofusins (encoded by *Mfn1* and *Mfn2*) localize to the outer membrane to form homotypic (Mfn1-Mfn1 or Mfn2-Mfn2) and heterotypic (Mfn1-Mfn2) complexes, while fusion of the IMM (inner mitochondrial membrane) is controlled by Opa1 (optic atrophy 1) and its proteases Oma1 (overload-mandatory activity 1) and Yme1l1 (Yme1 like 1 ATPase). In C. elegans, mutations in *fzo-1* (mammalian *Mfn1/2* ortholog) and *eat-3* (mammalian *Opa1* ortholog) causes mitochondrial fragmentation[136,137]. Similarly in Drosophila, loss of *Opa1* or *Marf* (drosophila ortholog of *Mfn1/2*) also causes mitochondrial fragmentation in vitro and in vivo[118,138], demonstrating the conserved function of *Opa1* and *Mfns* in regulating mitochondrial fusion. *Opa1* is highly alternatively spliced[139], the alternative transcripts confer specificity in signaling cascades (i.e. the release of cytochrome C in vertebrates[140]) and in Oma1 and Yme1l1 protease activity[139–142]. Opa1 comes in two distinct protein isoforms, and its proteolytic activity is dependent on its GTPase domain. The long isoform of Opa1 (l-Opa1) is unprocessed, inactive, and contains the N-terminal transmembrane anchored tail and the short isoform s-Opa1 lacks its transmembrane anchoring tail, causing it to be active. Loss of Yme1l1 prevents Opa1 cleavage at S2[143], resulting in the l-Opa1 transcript. Interestingly, loss of Oma1 does not affect Opa1 protease cleavage at S1 (encoded by exon 5) nor does it alter

mitochondrial morphology[144], under basal conditions. However, under pathological conditions Oma1 protease is required for S1 cleavage[145], which induces mitochondrial fragmentation and fission. Finally, in the mouse brainstem (pons and medulla), *Parkin* and *Oma1* mediate excessive fusion with age, suggesting age-dependent rewiring of the fusion machinery[146].

Mitochondrial fission: breaking apart

In contrast, fission is orchestrated by *Drp1* (*Dynamin related protein-1*, also known as DNM1L), a highly conserved dynamin related superfamily of proteins. *Drp1* is the master regulator of mitochondrial fission: it contains several domains, including the main GTPase binding domain (which regulates hydrolysis), middle stalk, variable effector domain[147] (confers lipid sensing), and GTPase effector domain. Drp1 is localized cytosolically and GTPase activation causes Drp1 recruitment to the OMM mediated by adaptor proteins[91,148]. Mutations in any of these critical domains impairs Drp1 function and disrupts mitochondrial homeostasis some of which are listed below.

Amongst these adaptors, Fis1 (*mitochondrial fission factor-1, Mff in flies)*, MiD49 and MiD51 (also known as *Mief*, *Mitochondrial elongation factor*) play particularly important roles in recruiting Drp1 to the OMM[149]. Mutations in these adaptors prevents Drp1 recruitment to the OMM, resulting in mitochondrial elongation[92]. For example, deletion of *Fis1* in mouse pyramidal neurons reduces the frequency of mitochondrial fission, resulting in elongated axonal mitochondria[85]. In contrast, loss of MiD49 or MiD51 prevents their localization to the OMM and subsequently Drp1 recruitment, resulting in abnormal mitochondrial elongation[91]. Mechanistic studies have shown that MiD49 directly recruits Drp1 to the OMM to promote Drp1-mediated scission[150]. Furthermore, human patients with mutations in *MiD49* (which present with

neuromuscular degeneration) have abnormally elongated mitochondria[21]. Together, these studies establish the "core" machinery of mitochondrial fusion and fission.

Mitochondrial metabolism: metabolic masters of the cell

While fusion and fission are necessary processes for regulating mitochondrial morphology in all cells, differences in energetic demands further tune mitochondrial morphology[151]. In the hippocampus for instance, mitochondria display striking heterogeneity as opposed to mitochondria in the dentate gyrus and CA1 (hippocampal CA1 region); which house larger and more complex mitochondria than those in less active regions. Within the dentate gyrus, dendritic mitochondria contribute the greatest relative volume compared to mitochondria in axons or the somata[152]. Even within individual CA1 neurons, apical tuft dendrites display a higher mitochondrial area-dendrite length ratio compared to basal dendrites, highlighting compartment-specific differences even within the cell. Electrical activity itself plays a crucial role in regulating mitochondrial morphology at the cellular and organelle level. For example, when the neuron's resting membrane potential is decreased by overexpressing *KCNJ2* (*potassium inwardly rectifying channel subfamily J member 2*), mitochondria become abnormally elongated[153], suggesting that activity dependent signaling promotes small mitochondria. In contrast, directly depolarizing mitochondria can change their morphology. In U2OS cells, mitochondrial depolarization (CCCP treatment) causes mitochondria to transition into donut-like structures, an effect blocked by inhibiting actin polymerization with latrunculin A or cytochalasin D[154]. In H9c2 cardiomyoblasts, loss of inner membrane potential impairs mitochondrial fusion[155]. In MEFs and H9c2 cells, mitochondrial depolarization coincides with transient mitochondrial contraction. Interestingly, loss of OPA1 (involved in fusion) blocks mitochondrial depolarization without affecting transient contraction, providing evidence that

bioenergetics and mitochondrial morphology may occasionally be uncoupled[156]. Altogether, these activity-dependent effects parallel our observation that neuronal depolarization increases the number of small mitochondria; whereas in our studies hyperpolarizing neurons via KCNJ2 suppresses the contraction normally triggered by injury, suggesting that membrane potential of the cell plays a significant role in regulating mitochondrial morphology.

Moving beyond transport: non-canonical regulators of mitochondrial morphology

Mitochondria are tightly coupled to the microtubule network via motor proteins, which not only drives their transport but also influences fission and fusion. Research in yeast demonstrated that KLPs (Kinesin like proteins) regulate microtubule length; where Klp5 and Klp6 promote microtubule catastrophe while Klp4 promotes polarized growth at plus-ends. Furthermore, the loss of Klp5 or Klp6 extends microtubule bundles and elongates mitochondria. In contrast, loss of Klp4 shortens microtubules, resulting in smaller and more abundant mitochondria[157]. These changes in mitochondrial morphology are explained by shifts in fusion and fission frequency, where shorter microtubules are associated with increased mitochondrial fission. Because dendrite injury induces rapid cytoskeletal reorganization, these microtubule-dependent effects may possibly be involved in injury induced mitochondrial shape changes. These findings emphasize that microtubule polarity, length, and stability feed directly into regulating mitochondrial shape[157]. In addition to the influence that motor proteins have in mitochondrial morphology, cytoskeletal proteins can also influence the canonical fusion-fission machinery. In Drosophila neurons, loss of *zipper* and *spaghetti squash* (*MyoII* orthologs) prevents Drp1 from localizing to mitochondria and thus increasing mitochondrial length, an effect that is phenocopied by stabilizing actin. Furthermore, expression of pathological human tau also elongates mitochondria by preventing Drp1 localization

to the OMM[158]. These findings suggest microtubule dynamics indirectly regulates Drp1 to regulate mitochondrial morphology. Such sensitivity of mitochondrial shape to cytoskeletal conditions aligns with the spatially restricted contraction we observed near the dendrotomy site. In HeLa cells, the immunophilin Ppd1 (also known as FKBP52, primarily cytoplasmic and nuclear, but also localized to microtubules) prevents Drp1 from interacting with CypA (cyclophilin A) and calcineurin, inhibiting fission induced by depolarization[159].

Although Miro is primarily involved in mitochondrial trafficking, Miro has also been shown to tune the balance between fusion and fission. In mammalian systems, double knockout of *Miro1/2* in mouse embryonic fibroblasts results in punctate, less elongated mitochondria[109]. Furthermore, mutations in *Miro1's* (R272Q) first calcium sensing domain increases punctate mitochondria[160] and mutations in other calcium sensing domains of *Miro1* prevents MiST (Mitochondrial Shape Transition) induced by cytoplasmic calcium influx[161]. In Drosophila flight muscles, *Vimar* (mammalian ortholog for Rap1 GTPase-GDP dissociation stimulator, *RAP1GDS1*) interacts with *Miro* to regulate mitochondrial fission, and knocking out *Vimar* decreases mitochondrial length[162]. These studies provide a glimpse into the complex interplay between mitochondrial proteins and mitochondrial dynamics; many proteins that have well established roles in regulating one aspect of mitochondrial biology, often influence a secondary aspect, highlighting the intricacies of mitochondrial biology.

Mitochondrial contact sites: linked by membranes

Mitochondria rarely act alone in the cell. In addition to the fusion and fission machinery other linked interactions also regulate mitochondrial morphology. These interactions include physical contacts with membranes (MAMs, mitochondrial associated membranes) such as lysosomes

(MLCs, mitochondrial lysosome contact sites), peroxisomes, and endoplasmic reticulum (MERCS, mitochondrial endoplasmic reticulum contact sites). In both MEFs and HeLa cells, the ER membrane protein PDZD8 forms a complex with FKBP8 which localizes to mitochondria. Overexpression of FKBP8 is sufficient to recruit endogenous PDZD8. While overexpressing FKBP8 increases MERCS, mitochondrial complexity is decreased. This study suggests that the FKBP8-PDZD8 complex have opposing roles in regulating mitochondrial morphology. FKBP8 overexpression promotes excessive ER-mitochondria tethering, thus inhibiting complexity while PDZD8 overexpression suppresses FKBP8 activity resulting in more complex mitochondria[163]. Another gene known to regulate mitochondrial morphology through MERCS interaction is *Arl6ip1* (*ADP-ribosylation factor-like 6 interaction protein 1*). Arl6ip1 is a transmembrane protein that primarily localizes to the cytoplasm and its knockdown reduces MERCS and impaired mitochondrial fission resulting in mitochondrial elongation. Interestingly, *Drp1* overexpression rescues mitochondrial elongation in *Arl6ip1* KO animals, suggesting that *Drp1* and *Arl6ip1* operate in the same molecular pathway but are functionally antagonistic[164]. Given that dendrite injury represents a localized stress event, MERCS-dependent regulation of Drp1 activity may contribute to the rapid mitochondrial contraction we observe after injury. Another study found that mitochondria-lysosome contacts localize to ER and Drp1 positive fission *hotspots* regulated *via* RAB7-mediated GTP hydrolysis[165]. Given that mito-lysosome contacts with the ER regulates Drp1 hotspots, whether ER-lysosome contacts play a role in injury-induced contraction requires further investigation.

MERCS also play a role in stress induced changes in mitochondrial morphology. For example, the phosphatase PGAM5 accumulates at MERCS upon stress activation to suppress Drp1-mediated fission and to upregulate Mfn2-mediated fusion[166]. Mitochondria-peroxisome crosstalk

contributes to mitochondrial morphology as well. For example, deletion of *Pex3* or *Pex5 (peroxisome biogenesis factor 3, -5)* results in highly fragmented mitochondria, suggesting that peroxisomes closely interact with mitochondria to control mitochondrial morphology[167]. Additionally, loss of *Acbd5* (acetyl CoA binding domain 5) –which is involved in peroxisome autophagy—results in mitochondrial elongation[168]. These studies highlight the importance of MAMs in regulating mitochondrial shape.

Reactive oxygen species: ROS regulators of morphology

Lastly, redox signaling is another known mechanism that regulates mitochondrial morphology. During OXPHOS (oxidative phosphorylation), mitochondria generate reactive oxygen species (ROS) such as O_2^- (superoxide anion) and its derivative H_2O_2 (hydrogen peroxide). These species are detoxified in a stepwise manner. First, SODs (superoxide dismutase 1 (matrix), -2 (intermembrane space and cytosol)) convert O_2^- to H_2O_2, while GPXs (glutathione peroxidases) reduce H_2O_2 to H_2O; and GSTs (glutathione S-transferases) conjugate glutathione to secondary oxidative products, limiting downstream cellular damage. Mutations in drosophila *gfzf* (*GST*), results in abnormally elongated axonal mitochondria, suggesting that redox signaling is involved in tuning mitochondrial fusion and fission[113]. In zebrafish, overexpression of the transcriptional coactivator PGC-1α (in humans PPARGC1A, known as the master regulator of mitochondrial biogenesis) increases axonal mitochondrial length, motility, density while decreasing ROS[119]. In mammalian cancer cells, *Myo19* knockout reduces cristae frequency and membrane potential, while epidermal expression of NIX induces fragmentation during differentiation. Blocking fragmentation by inhibiting *Drp1* prevents differentiation, while premature NIX expression induces early differentiation, tying mitochondrial remodeling directly to developmental

programs[169,170]. Although we have not yet determined whether ROS contributes to injury-induced contraction, the strong ROS-morphology link observed in other systems suggests that local redox shifts at the injury site could tune Drp1-dependent remodeling we observed following dendrite injury.

Taken together, these findings demonstrate that while *Mitofusins*, *Opa1* (and its proteases), *Drp1* (and its adaptors) account for the core fusion and fission machinery, the regulation of morphology is far more intricate. Cytoskeletal interactions, proteolytic regulation, and inter-organelle contacts further refine mitochondrial morphology to satisfy energetic demands of the cell. Additionally, less well-studied proteins such as NIX, Arl6ip1, Pdzd8, and slc-25A46 provide fresh perspectives on how mitochondrial shapes are dynamic in response to developmental, metabolic, or stress signals.

Central Controllers of Ion Flow

Overview

Accurate measurement of mitochondrial Ca^{2+} remains technically challenging due to several reasons: 1) GECIs (genetically encoded calcium indicators) have non-linear responses in high levels matrix environment, 2) dyes and genetically encoded calcium reporters perturb normal physiology, 3) these reporters are highly dependent on detectable differences in mitochondrial volume and impacted by mitochondrial morphology, and 4) the inability to capture fast, localized Ca^{2+} microevents relevant for signaling. Moreover, changes in mitochondrial morphology—such as fusion, fission, or injury-evoked remodeling can alter matrix volume and optical properties, complicating interpretation of observed Ca^{2+} signals. These methodological caveats underscore the importance of contextualizing mitochondrial Ca^{2+} measurements within the dynamic structural

state of mitochondria. However, there has been a significant advancement in our understanding of how Ca^{2+} and other ions are regulated by mitochondria and their importance in intracellular signaling cascades.

Gatekeepers of calcium: from calcium to catabolism

Mitochondrial Ca^{2+} flux acts as the central node for ion homeostasis. While mitochondria control the flow of many ions, each of these ions ultimately converge onto shifts in Ca^{2+} homeostasis within the cell and in organelles. Mitochondrial calcium regulates many biological processes including ATP production[171], respiration[172], and oxidative metabolism (as reviewed here [173]). Early evidence in lower vertebrates demonstrated that mitochondria and cytoplasmic calcium signaling are tightly synchronized. In muscle fibers of adult bullfrogs, depolarization induced by extracellular potassium, robustly increased mitochondrial calcium uptake, providing evidence that mitochondria act as Ca^{2+} sinks when calcium is elevated beyond basal levels[174].

Early observations in mitochondria isolated from rat kidneys (1960's) were critical in identifying uniporter activity of mitochondria[175,176] which created the foundation for mechanistic discovery of the MCU[66,67,177] (mitochondrial calcium uniporter) and MICU[178,179] (*essential MCU regulator*, EMRE in invertebrates) in the early 2000's. In Drosophila, the EMRE is required for calcium entry into mitochondria[180]. MCU and MICU function unidirectionally, only permitting mitochondrial Ca^{2+} influx. In addition to increases in cytoplasmic Ca^{2+}, interactions between mitochondria and other organelles, like the endoplasmic reticulum, further regulates intracellular Ca^{2+} homeostasis. For example, loss of MERCS in fly dopaminergic neurons impairs calcium buffering and causing calcium overload in the cell[181]. Whilst *Miro* is predominantly involved in mitochondrial trafficking its functional domains are imperative for buffering calcium when

intracellular levels increase[160]. However, *Miro* overexpression causes calcium overload in mitochondria resulting in bouton defects in the NMJ, highlighting that mitochondrial calcium buffering is precisely controlled. Interestingly, *Pink1* mutants, display abnormally high levels of mitochondrial calcium, which is attenuated by downregulating *Miro*. This *Miro*-dependent calcium signaling regulates both mitochondrial morphology and synaptic morphogenesis at the NMJ, in a pathway that operates independently of the canonical fusion/fission machinery[181]. Furthermore, changes in mitochondrial morphology via loss of Drp1 increases mitochondrial calcium buffering and subsequently cell death[182]. Whether loss of Drp1 activity affects injury induced mitochondrial calcium buffering in our studies requires further. While long mitochondria are associated with increased ATP production[151], it is possible that injury-induced mitochondrial contraction is a protective mechanism to limit mtROS production, by decreasing ATP production, thereby preserving mitochondrial integrity. Lastly, there is an increasing amount of evidence that calcium buffering capacity is decreased in neurological diseases like Huntington's disease[183,184], Alzheimer's disease[184–186], and Parkinson's disease[181,184,187]. However, increasing the capacity of mitochondrial calcium buffering can alleviate symptoms observed in these diseases[181,184,186,188].

In mammalian neurons, the interplay between MERCS and calcium signaling is crucial for synaptic physiology. *PDZD8*, an ER-resident tether, is required for calcium transfer to mitochondria. Knockout of *PDZD8* impairs mitochondrial calcium influx and increases Ca^{2+} retention in the ER and subsequently disrupts calcium dynamics in dendrites[129]. Similarly, overexpression of the chaperone *Grp75* (*Glucose-regulated protein 75*) in primary hippocampal neurons enhances mitochondrial calcium uptake via MERCS and increases both cytosolic and mitochondrial ATP levels[5], providing evidence that ER–mitochondria calcium handling is crucial for energetic homeostasis. Because injury-induced mitochondrial contraction occurs within a

spatially restricted domain near the dendrite injury site, MERCS-dependent calcium transfer may help facilitate where injury-induced contraction occurs.

Mitochondrial calcium buffering is also influenced by canonical fission/fusion proteins. In mouse cortical pyramidal neurons, loss of the fission factor *Mff* increases mitochondrial calcium uptake, without compromising mitochondrial membrane potential or ATP synthesis. Using shRNA against *Mff* produces a similar effect, again increasing mitochondrial calcium uptake without altering their ability to generate ATP or affecting membrane potential[85]. Furthermore, *Mfn2* KO in C2C12 muscle cells increases calcium retention, decreases buffering capacity, and induces mitochondrial fragmentation[189] emphasizing the complex interplay between calcium buffering and mitochondrial morphology. In our system, dendrite injury rapidly elevates mitochondrial calcium levels which coincides with a robust, Drp1-dependent mitochondrial contraction. Although the presence of injury-induced mitochondrial calcium influx is insufficient to drive contraction, the threshold of mitochondrial calcium may likely be involved in regulating contraction, as we observed different levels of mitochondrial calcium influx in contracting mitochondria.

Magnesium matters: messengers for mitochondria

In addition to regulating Ca^{2+} homeostasis, mitochondria also regulate several other ions across the periodic table of life. The regulation and release of these ions are critical for cellular signaling cascades.

Mitochondrial magnesium (Mg^{2+}) homeostasis is primarily regulated by the Mrs2 (mitochondrial RNA splicing 2) channel, which resides in the IMM. *Mrs2*, originally identified in genetic screens in yeast as a factor required for mitochondrial RNA splicing, was later redefined as the major Mg^{2+} transporter in mitochondria[73,74,190,191]. Functional studies have shown that loss

of *Mrs2* markedly reduces mitochondrial Mg^{2+} influx, whereas overexpression significantly increases Mg^{2+} uptake, establishing its central role in Mg^{2+} regulation[190].

The physiological consequences of altered Mg^{2+} availability can influence neuronal function and plasticity. For example, extracellular increase in Mg^{2+} has been shown to amplify NMDA-triggered phospho-CREB (cAMP response element-binding factor), a feature of long term learning and memory formation[192]. In contrast, magnesium supplementation is capable of alleviating neurotoxin-induced apoptosis and promote autophagy, highlighting its neuroprotective capacity under stress conditions[193]. Extending these findings, studies in human SH-SY5Y cells revealed that magnesium supplementation prevents neurotoxicity by reducing excessive mitochondrial activity, dampening the metabolic payload, and subsequently promoting cell survival[193,194]. Together, these findings provide direct evidence that mitochondrial Mg^{2+} homeostasis, is a regulator of cell survival and implicating mitochondrial Mg^{2+} acts as a signaling. This growing body of research is exciting and with a refreshing opportunity to develop novel therapeutics for neurological diseases.

Power in potassium

The existence of ATP-sensitive mitochondrial potassium channels was first provided at the functional level by Inoue and colleagues[195], who patch clamped mitoplasts (mitochondria stripped of their outer membrane) to reveal a selective K^+ channel located in the inner mitochondrial membrane. They showed that the activity of this channel was coupled with free ATP and that blocking ATP availability impaired K^+ influx into mitochondria. Nearly three decades later, the molecular identity of the K^+ channel complex was elucidated. Paggio et al. defined the pore-forming subunit as CCDC51 (renamed MITOK) and *ABCB8* (*ATP-binding cassette subfamily B*

member 8, renamed MITOSUR) as the associated ATP-binding regulatory subunit[196]. Together, these proteins constitute the mitoK$_{ATP}$ complex.

Studies aimed at understanding how mitochondria regulate potassium and subsequently cellular signaling were already being conducted, prior to the characterization of mitoK$_{ATP}$. The effects of mitochondrial K^+ regulation on cell homeostasis is currently being elucidated and will provide insight into K^+ (mis)handling during disease.

Forging signals with iron

Fe^{2+} is indispensable for cellular function, yet potentially toxic if unregulated. To balance these opposing properties, eukaryotic cells employ IRPs (iron regulatory proteins), which bind to IREs (iron response elements) located in the untranslated regions of mRNAs encoding iron metabolism factors. This post-transcriptional regulatory system ensures that iron uptake, storage, and utilization are meticulously integrated into the cell. Amongst its many targets are mitochondrial proteins, highlighting the intimate link between cytosolic iron sensing and iron homeostasis.

Mitochondria are the primary site for both heme biosynthesis and iron–sulfur (Fe–S) cluster assembly, a process that require a dedicated iron import pathway. Early studies in yeast demonstrated that Fe^{2+} uptake across the IMM is driven by the mitochondrial membrane potential, not by ATP hydrolysis because Fe^{2+} transport persisted even when ATP synthase was inhibited by oligomycin[197]. Genetic evidence further uncovered that loss of YFH1 (the yeast homolog of mammalian frataxin, *Fxn*) leads to profound Fe^{2+} accumulation in mitochondria, reflecting impaired iron clustering and delivery. Importantly, this phenotype was attenuated by deletion of *Mrs3* and *Mrs4*, mitochondrial carrier family proteins responsible for iron uptake[198]. These findings established *Mrs3/4* as essential iron importers and revealed how *fxn* deficiency perturbs

Fe^{2+} handling.

In vertebrates, the functional counterparts of *Mrs3/4* are the mitoferrins. Mitoferrin-1 (Mfrn1/SLC25A37) was first identified in zebrafish, where its loss dramatically reduced mitochondrial Fe^{2+} uptake in hematopoietic cells, leading to impaired erythropoiesis[199]. Mitoferrin2 (Mfrn2/SLC25A28), expressed more broadly across tissues including brain, provides basal Fe^{2+} uptake outside the erythroid lineage[200]. Interestingly, *Mfrn1,* but not *Mfrn2* overexpression rescued developmental defects in *frs* (*frascati,* member of the mitochondrial solute carrier 25, *SLC25*) mutant zebrafish, suggesting that *Mfrn1* and *Mrfn2* function non-redundantly[199]. *Mrfn* specificity is further conferred by its interaction with other proteins. For example, ABCB10 (ATP-binding cassette subfamily B member 10) was shown to selectively stabilize Mfrn1, ensuring its stability and function in Fe^{2+} import[201].

Beyond serving as a crucial substrate for mitochondrial energy metabolism, Fe^{2+} also acts as a signaling cofactor, similar to Mg^{2+}. For instance, iron supplementation enhances long-term potentiation (LTP), stimulates phosphoERK1/2, and promotes protein translocation into the nucleus. At the same time, extracellular iron entering the cytosolic labile iron pool (LIP) generates reactive oxygen species (ROS), illustrating the dual role of Fe^{2+} as both a signal potentiator and a source of oxidative stress[202].

Taken together, mitochondrial iron carriers, exporter, and their stabilizers form a coordinated system that integrates iron uptake with mitochondrial metabolism and neuronal signaling. At the cellular level, this ensures that neurons maintain Fe^{2+} in a range that supports growth, synaptic plasticity, and survival, while avoiding the deleterious effects of iron toxicity.

The sodium switch: a central regulator of ion homeostasis

Ca^{2+} handling represents one of the most fundamental roles of mitochondria in neurons. Mechanistic insights into Na^+/Ca^{2+} came from early investigations in mitochondria isolated from rat hearts demonstrating that abundant extracellular Na^+ directly upregulated calcium expulsion from mitochondria, establishing the principle of sodium–calcium coupling[203]. Ca^{2+} enters the matrix through the MCU complex and can be extruded through the Na^+/Ca^{2+} exchanger (called the NCLX, encoded by SLC8B1)[204]. This tight coupling is evident in neurons, where electrical stimulation leads to rapid mitochondrial-Ca^{2+} buffering. However, in neurons that express a SNV (single nucleotide variant) associated with mental retardation, $NCLX^{P367S}$, mitochondrial calcium efflux is significantly decreased and LTP (long term potentiation) is absent[205]. These findings suggest that even though calcium can enter mitochondria, its Na^+-mediated expulsion is critically just as important. Indeed, when sodium entry is compromised, calcium cannot be expelled efficiently, leading to mito-calcium overload, protein aggregation, cognitive decline, and subsequently neurodegeneration[188]. This sodium dependent Ca^{2+} exchange is essential for preventing calcium overload while permitting Ca^{2+}-mediated signaling cascades. Recently, however, the crystal structure of NCLX has been resolved, revealing that the NCLX antiporter preferentially regulates Ca^{2+}/H^+ exchange, not Ca^{2+}/Na^{2+} in mitochondria[206].

In addition to Na^+/Ca^{2+} exchange, mitochondria also express Na^+/H^+ antiporters on the IMM. The earliest evidence of Na^+/H^+ exchange was based on observations of mitochondrial swelling extracted from beef hearts, which is known to be a Na^+/H^+ and/or K^+/H^+ dependent process[207]. Following these observations, *Nha2* (*Nhe6*, in mammals) was identified as essential for mediating Na^+/H^+ exchange, as its deletion or inhibition caused decreased Na^+ uptake into mitochondria[208]. Recent work has demonstrated that CI (Complex I) of the ETC (electron transport chain) functions as a mitochondria-specific Na^+/H^+ exchanger (mNHE), and loss of CI activity impairs Na^+/H^+

pumping despite preserved membrane potential at CII and CIV, highlighting a dedicated sodium–proton exchange at CI[209]. Although it is obvious that sodium mediated ion exchange (Ca^{2+}, H^{+}) is a critical regulator of mitochondrial homeostasis, the consequences of impaired Na^{+}/H^{+} antiporter activity has yet to be directly assessed in relation to neuronal function and will be crucial for identifying if such mutations are associated with diseases.

Mitochondrial ion flux is a central regulator of cellular homeostasis, Ca^{2+} is rapidly buffered by mitochondria which stimulates pyruvate dehydrogenase[210], subsequently boosting the Krebs cycle[211,212]. While Ca^{2+} is a critical regulator of ATP production, the constant upregulation of mitochondrial calcium is detrimental for the cell, as constant upregulation can lead to deleterious effects such as apoptosis[213]. Therefore, the proper regulation of Ca^{2+} into mitochondria is crucial for both providing energy for the cell and as a universal currency which is exchanged for other ions to activate specific signaling cascades. When mitochondria are incapable of exchanging Ca^{2+} for others, cellular homeostasis becomes awry and downstream signaling cascades become abnormal.

Redox and renewal: a little ROS goes a long way

Although ROS (reactive oxygen species) were once viewed exclusively as harmful byproducts of metabolism that drive cellular damage, especially in aging (free radical theory of aging), this notion has largely been dismissed, as ROS are increasingly recognized as signaling molecules that directly regulate cell-cycle progression and developmental programs. During mitosis in mammalian cells, mtROS (mitochondrial ROS) upregulates p-CDK2 enabling cell-cycle progression through S-phase and promoting DNA replication[214]. ROS act as redox switches, they tune enzymatic activity of serine/threonine kinases through reversible oxidation. Loss of redox-

sensitive cysteine residues alters the timing of specific mitotic phases, highlighting the importance of ROS in orchestrating cell cycle[215].

The developmental roles of mtROS extend beyond proliferation to neuronal lineage specification. In neural stem cells, mitochondrial morphology calibrates neuronal identity through differences by tuning ROS production. The presence of long tubular mitochondria is a feature of undifferentiated/uncommitted stem while committed progenitors exhibit distinct ROS profiles. Furthermore, altering mitochondrial fusion is sufficient to drive NSCs towards a biased fate. These findings demonstrate a direct link between mitochondrial dynamics, ROS signaling, and neural fate determination[216].

In postmitotic neurons, mtROS continue to regulate structural development. At the Drosophila NMJ, neuronal activity induced by the temperature-sensitive channel dTrpA1 increases bouton number in a dose-dependent manner. Interestingly, activity induced ROS *via* dTrpA1 activation is amplified when *SOD2* overexpressed, presumably by increasing the quantity of O_2^- that is converted into $H_2O_2^-$, which provides insight into how different ROS signals regulate development. Furthermore, perturbations of mitochondrial redox buffering revealed that either *SOD* or *Catalase* knockdown, is sufficient to drive bouton complexity. Conversely, *Catalase* overexpression which scavenges $H_2O_2^-$, dampened activity-dependent bouton branching. These findings identify O_2^- as a necessary substrate for $H_2O_2^-$ synthesis which signals downstream to promote synaptogenesis[217].

Excessive mtROS, however, can also compromise neuronal viability. In the ventral midbrain of mice, treatment with the Parkinsonian toxin MPP^+ dose-dependently increased in $H_2O_2^-$. Under basal conditions, MPP^+ increases $H_2O_2^-$ without increasing cytochrome release. *However*, when combined with recombinant oligomeric Bax (BCL-2-associated X), the active form of the pro-

apoptotic protein, cytochrome-C (a marker for cell death) is upregulated, providing a mechanistic link between mtROS and neurodegeneration[218]. Finally, mtROS has been shown to regulate organelle transport within neurons. In Drosophila larval motor neurons, exposure to the herbicide paraquat reduced both the distance and frequency of bidirectional mitochondrial trafficking along axons. Remarkably, this impairment was fully rescued by *SOD2* but not *SOD1* overexpression, suggesting that abundant O_2^- disrupts axonal transport, and that mitochondrial redox balance is essential for subsequent downstream processes like mitochondrial trafficking[219].

Together, these findings show that mtROS are not passive metabolic byproducts but active regulators of cell homeostasis. From governing mitotic checkpoints in neural progenitors, to fate specification and shaping neuronal complexity; mtROS serve as versatile redox signals. Their effects are finely tuned by both their abundance and their chemical identity, with $H_2O_2^-$ often acting as a positive signaling molecule, while O^- is a necessary intermediate in moderation but damaging in abundance. We are just now beginning to reconcile the ambiguity in ROS signaling. This balance underscores how mtROS integrates metabolic state with developmental programs and neuronal function across the lifespan.

The Dispatcher of the Cell

Mitochondria regulate ion flux within the cell and between organelles, positioning themselves to match energetic demands in dynamic environments and sustain constant ATP production under stable conditions. Mitochondrial homeostasis is crucial for regulating efficient ATP production, and disruptions in one is unequivocally tied to disruptions in all dimensions. Several principles highlight this interdependence: (1) mitochondrial transport ensures proper ATP distribution, (2) ATP synthesis inherently generates reactive oxygen species (ROS), (3) ATP output is tightly

controlled by mitochondrial morphology, (4) morphology is shaped by ion flux, and (5) ion flux itself governs mitochondrial transport and ionic balance. Together, these processes form a tightly coupled circuit in which perturbation of any single variable propagates across the entire system, creating a self-sustaining feedback loop. Without intervention, the cycle reinforces itself: calcium influx drives transport arrest, morphology changes, and energetic stress, of which regulates each other directly or indirectly.

Whether this cycle resolves or persists depends on proper detection when processes become awry. Failure to correct the disturbance locks the system into a pathological state, which may cause irreversible damage due to dysregulated ion homeostasis, ROS accumulation, and energetic overdrive. Thus, mitochondria function not only as the battery of the cell, but also as central integrators of cell stress, with their feedback loops acting as pivotal decision points between cellular repair or collapse.

Shape shifts under cell stress

Studies ranging from cultured in vitro mammalian cells to in vivo vertebrate systems converge on the conclusion that mitochondrial morphology, calcium buffering, and redox signaling regulate cellular responses to stress. These processes are directly influenced by changes in mitochondrial morphology, motility, mtROS production, and ion transport.

Some of the most critical insights come from observations visualizing mitochondrial morphology in cells under stress. For example, mitochondria become fragmented during apoptosis and blocking mitochondrial fragmentation by expressing *Drp1.K38A* (GTPase dead) increases cell survival by preventing downstream release of cytochrome c[220,221]. Notably, the pro-apoptotic regulator BAX[222] is known to spatiotemporally accumulate at mitochondrial fission sites[223],

suggesting that increased fission in mitochondria may activate apoptosis. This interpretation is further evidenced by literature examining mitochondria in post-mortem cortical samples of AD (Alzheimer's disease) patients which present an increase in fragmented in mitochondria compared to non-AD patient samples. This fragmentation was shown to be directly caused by pathological aβ25-35 fragments (in humans and mice) which promotes SNO (S-nitrosylation, a type of PTM [post-translational modification]) of Drp1 through C644. Furthermore, loss of this PTM site in C644A protects against stress-induced mitochondrial fragmentation. These observations further support the idea that stress-induced changes in mitochondrial morphology may toggle a molecular switch to regulate cell survival and cell death[224]. These early studies served as foundational pillars linking mitochondrial morphology to apoptotic signaling. Understanding how mitochondrial morphology regulates apoptotic signaling, creates an opportunity to intercept the apoptotic signaling cascade before cellular damage becomes irreversible.

More recently, studies have shown that changes in mitochondrial morphology is directly linked to repair pathways. For example, injuring the plasma membrane causes mitochondrial fragmentation which is crucial for initiating the repair response. In myoblasts and non-muscle cells, focal membrane damage triggers mitochondrial calcium buffering[225]. Mitochondrial calcium uptake is known to upregulate ATP synthesis and subsequently O_2^- production[226]. Inhibiting mitochondrial calcium uptake genetically (*mcu* mutant) or pharmacologically (sodium azide) inhibits mtROS production. These changes in mtROS are critical for repair: preventing mtROS production inhibits wound repair, while amplifying its production accelerates RhoA mediated F-actin accumulation, and subsequently repair[225]. Complementary studies in mouse embryonic fibroblasts (MEFs) demonstrate that injury-induced shape changes in mitochondria is a determinant of repair. These shape changes are controlled by the master regulator of fission, *Drp1*

and *MiD49* (Drp1's adaptor) because mutations that impair either of their activity prevents WIMF (wound induced mitochondrial fragmentation) and repair[21]. More critically, mitochondria in *Drp1* knockout cells lose their capacity to buffer excessive calcium and even the addition of exogenous ROS cannot rescue repair. These findings highlight that WIMF and mitochondrial calcium buffering act synergistically to upregulate ROS, whereas bypassing these processes and directly upregulating ROS is not sufficient in driving repair[21]. Similarly, in embryonic day 7 chick DRGs (dorsal root ganglion neurons), injury induces mitochondrial fragmentation and requires the MCU[227]. Excessive mitochondrial calcium uptake is known to contribute to oxidative stress and subsequently apoptosis[180], linking calcium uptake to mitochondrial dysfunction. More recently the effects of injury on mitochondrial morphology have been directly observed in human i3Neurons. Laser axotomy (axon injury) induces rapid mitochondrial calcium buffering and fragmentation, which is dependent on phosphorylation of *Drp1* via *DLK* (*Dual Leucine-Zipper Kinase*)[228]. Interestingly, treating human i3Neurons with vincristine triggers mitochondrial ROS production, which drives axonal degeneration. Treatment with the Drp1 inhibitor mDivi1 mitigates ROS production and delays degeneration, illustrating a mechanistic link between mitochondrial division, oxidative stress, and neurodegeneration[229]. These in vitro studies have been crucial for establishing that mitochondrial morphology is highly sensitive to cellular stress across different cell types in various organisms.

In contrast, many of the previous in vitro findings have been successfully translated into in vivo models. These in vivo studies have further advanced our understanding of how mitochondria are involved in the repair response. For example, in C. elegans axotomy of the VNC (ventral nerve cord) causes mitochondria to accumulate in the damaged axon at 6- and 24-hours after injury, suggesting that mitochondria are actively recruited to the damaged axon to promote repair[6,7].

Indeed, this hypothesis was further supported by genetic manipulations in *Miro1,* where its knockdown decreased the number of axonal mitochondria and significantly impaired axon regeneration. In contrast wildtype *Miro1* overexpression, increased the number of mitochondria in the intact injured axon, thereby enhancing regeneration[7]. In the epidermis of C. elegans, injury (blunt force and laser) triggers shape changes in mitochondria and increases cytosolic and mitochondrial Ca^{2+}. Downstream of mitochondrial Ca^{2+} influx is mtROS production. The production of mtROS is functionally important in regulating Rho1 (Rho/Rac small superfamily of GTPases in mammals) activity via C16 and C20, as loss of this redox sensitive motif (C16A, C20A) impairs wound closure. Unsurprisingly, loss of mitochondrial calcium buffering in *Mcu1* null mutants decreases mtROS production and subsequently epidermal wound closure[97]. Further studies have elucidated findings that support the notion that changes in mitochondrial morphology serves as a signal to mount a repair response. For example, laser and needle wounding in C. elegans triggers mitochondrial fragmentation. And although *Miro1* is predominantly known for its function in mitochondrial transportation, *Miro1* was surprisingly required for WIMF. Additionally, *trpm* mutants, which have impaired ion handling (Ca^{2+}, Mg^{2+}, and Na^{2+}) reduced fragmentation, while *mcu1* mutants show normal fragmentation, suggesting that cytosolic calcium but not mitochondrial calcium is required for WIMF. Moreover, *fzo1* (mammalian ortholog *MFN1/2*) mutants, which display chronic mitochondrial fragmentation, elevated mtROS levels, and have accelerated wound healing. These findings suggest that shape changes are caused by elevated cytosolic Ca^{2+}, which is regulated by the fusion/fission machinery, to upregulate mtROS, required for initiating the repair response[86]. The premise that mitochondrial shape changes are critical for jumpstarting the repair cascade is further supported by studies in the Drosophila epidermis. Mutations in the fusion/fission (i.e. *drp1*, *opa1*, *marf*, *fis1*, and *gdap-1*) machinery impairs injury-induced Ca^{2+} flux (cytosolic and

mitochondrial), F-actin accumulation, and subsequently epidermal wound closure, further implying that mitochondrial morphology is a critical signal for cells to coordinate epidermal wound closure[95].

Mitochondrial morphology is highly plastic. In addition to the well-studied canonical fusion and fission machinery, mitochondria can shorten, contract, fragment, and swell. Laser axotomy in the CNS and PNS of live mice have shown that injury induces mitochondrial fragmentation and contraction. This injury-induced mitochondrial remodeling is dependent on mitochondrial calcium influx but not changes in microtubule cytoskeleton. Injury-induced fragmentation and contraction are accompanied by an upregulation in mtROS detected (Grx1-roGFP biosensor) preceded by calcium influx into mitochondria[230]. Additionally, in rat models of TBI (traumatic brain injury), mitochondrial fusion and fission proteins are differentially regulated depending on injury severity. Mild TBI upregulates *OPA1*, *MFN2*, *YME1L1*, and *PARL*; whereas severe TBI upregulates *OMA1* and *FIS1* while downregulating *MFN1* and *DRP1* expression relative to controls. These findings suggest the proteins regulating the fusion and fission machinery act combinatorially, under various conditions. In a mild injury, mitochondrial fusion is upregulated through OPA1, proteolytically processed by YME1L1, with IMM fusion being executed through MFN2. In contrast, a severe injury triggers fission by upregulating OPA1 and its protease OMA1 which induces fission while simultaneously suppressing MFN1-mediated fusion. Notably, the suppression of Drp1 suggests that there is a molecular brake, as Drp1 mediated fission is key regulator of apoptosis. In addition to these acute regulators *Pink1* expression increases over time in both mild and severe TBI, though with temporal variability relative to controls, while *Parkin* declines over time in mild TBI but increases in severe TBI[231]. These changes in gene expression suggest that the balance between fusion, fission, and mitophagy pathways dictates whether mitochondria adapt or collapse under

injury stress. In rats, corticospinal tract (CST) neurons exhibit decreased axonal mitochondrial length after spinal cord injury. The Drp1 inhibitor mDivi1 blocks injury-induced mitochondrial fragmentation both in vitro and in vivo (somatosensory cortex, 4 weeks prior to CST transection) and decreases the number of retraction bulbs, a hallmark for unsuccessful regeneration.

Alongside fragmentation, mitochondrial swelling represents another hallmark phenotype observed under cellular stress. Mitochondrial swelling is caused by abnormal ion homeostasis from opening of the mitochondrial permeability transition pore (mPTP)[232]. Mitochondrial swelling is associated with loss of membrane potential, expansion of the matrix, and eventually membrane rupture[233]. In mouse models, cerebral ischemia induces mitochondrial swelling, a process that can be attenuated by genetic ablation of CypD (cyclophilin D), a regulator of permeability transition pore opening. Loss of CypD limits pore opening and consequently reduces infarct size caused by calcium overload[234]. Similarly, in sciatic nerve transection models, mitochondrial swelling accompanies axon degeneration, whereas inhibition of the mPTP using CsA (cyclosporin A) delays degeneration[235]. Complementary experiments show that energy supplementation with NAD protects axons from Wallerian degeneration, but this protection is blocked by ETC (electron transport chain) inhibitors such as antimycin A, indicating that NAD requires intact respiration. Mitochondrial swelling is also influenced by changes in microtubule dynamics. In sciatic nerve explants, preventing microtubule polymerization (Taxol) or depolymerization (vincristine) through chemotherapeutic drugs both exacerbate mitochondrial swelling and subsequently axonal degeneration[236].

Mitochondria are also regulated by pathways governing autophagy. In zebrafish sensory neurons, laser axotomy halts mitochondria motility in the severed axon. Loss of *Pink1* (*PTEN induced kinase 1*) or expression of Wld^{s} (*Wallerian degeneration slow*) can both increase

mitochondrial motility following axotomy. Although downregulation *Pink1* or upregulation of *Wld*^{s} can rescue mitochondrial motility, only *Pink1* has functional consequences; its loss increases axon degeneration. Conversely, overexpressing PGC-1α (master transcriptional co-activator of mitochondrial biogenesis), enhances mitochondrial motility decreases ROS production, and promotes cell survival[119]. Similarly, in mouse hippocampal neurons, axon stimulation following axotomy induces mitochondrial fragmentation and targets Parkin-Pink1 labeled mitochondria to LC3-positive autophagosomes (E3 ubiquitin ligase, involved in mitophagy) at the injury site. This mitophagic targeting is dependent on Pink1-mediated recruitment of Parkin which is necessary for clearing out dysfunctional mitochondria[237].

Mitochondria evolved from an ancient endosymbiotic relationship with their host nearly two billion years ago. In all extant eukaryotes, the crucial role that mitochondria have in providing ATP makes them indispensable for cellular function. In addition to ATP production, they regulate ion homeostasis; hoarding ions when they are plentiful and trading in to trigger downstream signaling cascades during stress. If the predominant function of mitochondria is to provide energy for the cell, then they must possess mechanisms to discriminate changes in energetic demand, sustain at sites of need, and importantly adapt their activity under stress. It is now increasingly evident that mitochondria also participate in injury signaling, yet the field faces ambiguity in reconciling how some mitochondrial proteins can both be inhibitory for cell survival in some contexts but promote repair in others . Perhaps the answer is not uniform, but rather dependent on the cellular context: which cell type is involved, what are its energetic requirements, what is the organization of its cytoskeleton, and what ionic environment does it experience? Only by addressing these contextual variables will we be able to uncover the full potential of repair.

The problem(s)

Dendrites and axons are the primary detectors and transducers of signals in the nervous system, orchestrating precise cellular responses that regulate physiology and behavior across the lifespan. Neuronal function is tightly linked to cell-type specific architecture, ensuring that structural organization parallels functional demands[238]. As a result, abnormal changes in neuronal architecture alters the firing frequency of action potentials in neurons[239].

In neurological disorders and diseases, these structural disturbances present as functional changes in behavior. Subtle phenotypes like disrupted circadian rhythms which are some of the first symptoms to arise (in neurodegenerative disorders), typically precede more severe impairments like memory loss. Physical trauma to the cortex, such as TBI (traumatic brain injury), similarly alters neuronal architecture with profound consequences. At the cellular level, disease and trauma disrupt baseline neuronal activity (excitotoxicity)[240], destabilize ion homeostasis via calcium overload, trigger cytoskeletal disorganization[241,242], causes organelle fragmentation[87], upregulates inflammation[243], and ROS production[244,245]. Structural and molecular insults are detrimental for cell function and our understanding of the physiology remains incomplete.

Santiago Ramón y Cajal is widely recognized as the father of modern-day neuroscience. In 1906, Santiago Ramón y Cajal (along with Golgi) was awarded the Nobel Prize in Physiology and Medicine for their seminal discoveries of the nervous system, the *neuron doctrine*. In 1913, Cajal published his book on "*Degeneration and Regeneration of the Nervous System*" which was translated in 1928. In this book, Cajal does a comprehensive review of the field of neuroscience, highlight key facts conducted by him and his colleagues (Strobe, Lugaro, Vanlair, Waller, Golgi, Nageotte, Ranvier, Bethe, and many more). One of the earliest obstacles of regeneration that Cajal eluded to was defective routing during repair (p.112-113)[10], a key defect still observed in modern day research (discussed in **Chapter 5**). Defective axon guidance during regeneration has been

observed across multiple species, from rodents to cats. Dendrites, too, elicit a robust regenerative response. When all initial dendrites are removed from the neuron, new dendrites are regrown; patterning a new dendrite architecture distinct from its architecture prior to any injury. However, dendrite regeneration is imperfect because the newly regrown architectures have significant self-crossing defects. While static snapshots of regenerated structures reveal the endpoints of repair, we lack a fundamental understanding of the mechanisms regulating regenerative initiation and outgrowth. Identifying the mechanisms that regulate injury detection, will allow us to activate repair when systems become damaged and tune regrowth pathways when systems become awry.

The approach

Drosophila melanogaster is a powerful tool to study cellular process in vivo because of their short lifespans, ease of genetic manipulations, and stereotyped patterning. In particular, type I multidendritic-dendritic arborization (md-da) neurons of the Drosophila PNS includes diverse cell types to answer fundamental questions in cell biology in vivo[246]. These highly stereotyped neurons allow us (scientists) to genetically manipulate specific cells in an otherwise wildtype animal. In addition to the genetic utility that Drosophila provide, their translucent bodies allow light to penetrate deep into the tissue, bypassing the need for tissue histology.

Combining the genetic utility and optical imaging techniques provides a powerful tool to revisit fundamental mechanisms of repair, the field has begun uncovering differences (and similarities) in axon vs dendrite regeneration[2], how extrinsic factors vs intrinsic factors affect regeneration[17], and outgrowth during dendrite development vs dendrite regeneration[11]. Even though axons and dendrites exhibit divergent mechanisms in repair, some signaling pathways are conserved[13]. And while identifying novel pathways involved in axon and dendrite regeneration creates new

opportunities to target repair, one knowledge gap is how cells even detect injury which is a critical intermediate between injury and repair.

It is well established that axon and dendrite injury triggers membrane depolarization[247], a surge of calcium influx[12,13,248], cytoskeletal disorganization[26,27,242], and organelle fragmentation[119,227,249,250]. In non-neuronal cells, injury too triggers a surge of calcium influx[21,97], cytoskeletal disorganization[28], and organelle fragmentation[86,251]. It is imperative to determine whether which of these (if any) injury-induced changes are involved in regulating the signaling cascade so that further damage is mitigated, and repair pathways are capitalized.

During my graduate training, I conducted live-imaging, and characterized how mitochondria respond to dendrite injury. The rationale for investigating mitochondria is that following axon or dendrite injury, there is an increase in both cytoplasmic and mitochondrial calcium influx[12,13]. Furthermore, others have found that mitochondria fragment following laser injury[21,86,228] and that injury-induced mitochondrial fragmentation requires calcium influx into the mitochondria[227]. Whether induced changes in mitochondrial morphology at the time of dendrite injury affects the neuron's outcome remains to be investigated until my thesis work.

Chapter 3

Materials and Methods

Animals

Fly Husbandry and genetics

Adult flies were reared at ~22.5˚C and fed a standard yeast diet.

Drosophila larvae collection and handling

Male and female Drosophila larvae were collected from synchronized egg lays on 4.0% grape agar plates (750ml H2O; 18.75g BD DifcoTM Agar, Mfr. No. 214010; 250ml Welch's 100% grape juice; 25g sucrose; 1.5g methyl p-hydroxybenzoate, ReagentPlus®, Mfr. No. H5501-100G) supplemented with yeast paste (made from active dry yeast + dH2O). The plates were maintained at room temperature (22.5°C), and larvae were aged for 72 hours after egg laying (AEL).

For regeneration experiments, individual larvae were transferred to petri dishes containing 4.0% grape agar and yeast paste after injury. Before imaging, larvae were washed in distilled water (dH_2O).

Larval immobilization for imaging

Early third instar larvae were transferred to glass wells containing dH2O to wash off yeast. Class IV (ddaC) Drosophila PNS sensory neurons33 were imaged by immobilizing larvae dorsally on a ~4.0% gelatinous agarose pad (prepared using dH_2O and LE Quick Dissolve Agarose, GeneMate, Cat. No. E3119-500), with a small volume of glycerol (Glycerol, ReagentPlus®, Mfr. No. G7757-500ML) which was sandwiched between a microscope slide (Fisherbrand, Cat. No. 125441, 75 × 25 × 1 mm) and a No. 1.5 coverslip (Epredia, Cat. No. 22-050-218, 22 × 22 mm) as previously described[252].

Late third-instar larvae were immobilized using the same method, with the addition of vacuum grease (DuPont Molykote®, Electron Microscopy Sciences, Cat. No. 60705) and Scotch® tape. This immobilization method was used to generate data for Fig. 2-5, S2-S4. Larvae were immobilized using the LarvaSPA method, as previously described35, with ice as a temporary anesthetic instead of isoflurane.

Ice anesthetics

Drosophila larvae were placed in a glass spot plate with ~1ml of water that was cooled on ice for 5 minutes before individual larvae were transferred onto the spot plate for ~1min for brief anesthetization. After larvae stopped making large movements, larvae were removed from the cold water, dried on a kim wipe, and placed on a slide where they were permanently immobilized using UV-cured glue and PDMS blocks (the larvaSPA technique, where the trunk of the animal is constrained but the head and tail are free to move in the open air). This brief anesthetic was enough to prevent the animal from making whole body contractions, in order to keep the animal still as the glue was being UV-cured, as the mouthhooks began moving within 50 seconds. Between

animals, the spot plate was placed on the bench top to equilibrate back to room temperature.

Table of Fly Stocks

STAR★Methods		
REAGENT OR RESOURCE	**SOURCE**	**IDENTIFIER**
Fly stocks		
D. melanogaster y[1] v[1]; P{y[+t7.7] v[+t1.8]=TRiP.JF02991}attP2	*Bloomington Drosophila Stock Center*	BDSC#28355
D. melanogaster y[1] w[1] ; wg[Sp-1]/CyO, y[+] ; M{w[+mC]=UAS.Bap55.T}ZH-86Fb	*Bloomington Drosophila Stock Center*	BDSC#34488
D. melanogaster y[1] w[1] ; wg[Sp-1]/CyO, y[+] ; M{w[+mC]=UAS.BAF53a.T}ZH-86Fb	*Bloomington Drosophila Stock Center*	BDSC#34489
D. melanogaster y[1] w[1] ; wg[Sp-1]/CyO, y[+] ; M{w[+mC]=UAS.BAF53b.T}ZH-86Fb	*Bloomington Drosophila Stock Center*	BDSC#34490
D. melanogaster w[*] ; ; UAS-EB1-GFP}3	*Bloomington Drosophila Stock Center*	BDSC#35512
D. melanogaster y[1] w[*] HDAC6[KO]	*Bloomington Drosophila Stock Center*	BDSC#51182
D. melanogaster w[*]; P{w[+mC]=UAS-Drp1.D}3	*Bloomington Drosophila Stock Center*	BDSC#51647
D. melanogaster w[*] ; P{w[+mC]=UAS.HDAC3.H140A}3-2 ;	*Bloomington Drosophila Stock Center*	BDSC#55069
D. melanogaster w[*]; P{w[+mC]=UAS-HDAC3.N}2a-6/TM3, Sb[1]	*Bloomington Drosophila Stock Center*	BDSC#55078
D. melanogaster w[*] ; P{UAS-Dscam1.A-17.2-19+23GFP}attP40/CyO	*Bloomington Drosophila Stock Center*	BDSC#66201
D. melanogaster w[*] ; P{y[+t7.7]w[+mC]=UAS-5'UTR-Dscam1.A-17.2-19+23GFP-3'UTR}attP40/CyO	*Bloomington Drosophila Stock Center*	BDSC#66202
D. melanogaster w[*] ; P{UAS-EGFP.Dscam1.3'UTR}attP40	*Bloomington Drosophila Stock Center*	BDSC#66205
D. melanogaster w[1118] ; UAS-mCherry.mito.OMM}2/CyO ;	*Bloomington Drosophila Stock Center*	BDSC#66532
D. melanogaster w[1118] ; ; UAS-mCherry.mito.OMM}3/TM6b,Tb[1]	*Bloomington Drosophila Stock Center*	BDSC#66533
D. melanogaster y[1] w[*]; PBac{y[+mDint2] w[+mC]=UAS-hAPOE.4.R112.R158}VK00037	*Bloomington Drosophila Stock Center*	BDSC#76607
D. melanogaster w[*]; M{RFP[3xP3.PB] w[+mC]=17xUAS-ER-GCaMP6-210}ZH-86Fb/TM6B, Tb[1]	*Bloomington Drosophila Stock Center*	BDSC#91397
D. melanogaster w[*] ; UAS-GCaMP5g.mito}243 ;	*Bloomington Drosophila Stock Center*	BDSC#93059
D. melanogaster w[*] ; UAS-Drp1.K38A.HA}3 ;	*Bloomington Drosophila Stock Center*	BDSC#95247
D. melanogaster w[*] ; UASHsap\KCNJ2.EGFP}7 ;	*Bloomington Drosophila Stock Center*	BDSC#9595
D. melanogaster w[*] ; ppk-GAL4 ;	*Grueber et al., 2003*	Jan Lab
D. melanogaster w[*] ; ppk-cd4-tdgfp[8] ;	*Han et al., 2011*	Jan Lab
D. melanogaster w[*] ; ; ppk-cd4-tdtomato[10a]	*Han et al., 2011*	Jan Lab
D. melanogaster w[*] ; ; GAL4-19-12, UAS-CD4-tdGFP, repo-Gal80 / TM6B	*Yan et al., 2013*	Jan Lab
D. melanogaster w[*] ; ; GAL4-2-21, UAS-CD4-tdtomato / TM6b		Jan Lab
D. melanogaster w[*] Sp / CyOweep ; Tm2/TM6b	*Jan Lab*	Jan Lab
D. melanogaster w[*] ; UAS-Miro.E234K ;	*Russo et al., 2009*	Zinsmaier Lab
D. melanogaster w[*] ; UAS-Miro.E354K ;	*Russo et al., 2009*	Zinsmaier Lab
D. melanogaster w[*] ; UAS-Miro.T25N ;	*Russo et al., 2009*	Zinsmaier Lab
CantonS		

Fig. 1.1 Fly stocks used during graduate studies

Table of Reagents and Resources

REAGENT OR RESOURCE	SOURCE	IDENTIFIER
Chemicals, equipment, reagents		
Drosophila mounting		
DuPont Molykote®	*Electron Microscopy Sciences*	Cat. No. 60705
No. 1.5 coverslip 22 ×22 mm	*Epredia*	Cat. No. 22-050-218
Microscope Slide 75 ×25 ×1 mm	*Fisherbrand*	Cat. No. 125441
Glycerol	*ReagentPlus®*	Cat. No. G7757-500ML
Scotch® tape	*Scotch®*	N/A
Metal chamber	*Ji and Han 2020*	N/A
UV glue	*Norland products*	Cat. No. 6106, NOA 61
UV lamp	*Maxxeon*	MXN02003
Sylgard 184 kit	*Electron Microscopy Sciences*	24236-10
CapSure HS LCM caps	*Molecular Devices*	LCM0213
MembraneSlide PEN	*Zeiss*	415190-9081-000
MicroTube	*Zeiss*	415190-9221-000
Tissue-Tek-O.C.T.	*SakuraUS*	Cat No. 4583
4.0% Grape plates		
750ml H2O	*N/A*	N/A
18.75g BD Difco™ Agar	*Becton Dickinson*	Cat. No. 214010
250ml Welch's 100% grape juice	*Welch's*	N/A
1.5g methyl p-hydroxybenzoate	*ReagentPlus®*	Cat. No. H5501-100G
Fisher Scientific Education™ Yeast, active, dry	*Fischer Scientific*	Cat. No. S25632A
Agarose pads		
100ml H2O	*N/A*	N/A
4.0g LE Quick Dissolve Agarose	*GeneMate*	Cat. No. E3119-500

Fig. 1.2 Reagents and resources used during graduate studies

Microscopy

Confocal imaging

Confocal imaging on the Zeiss LSM980 was used to acquire static images of the dendrite architecture before injury and immediately after injury. A Zeiss LSM700 confocal microscope equipped with a 488 nm and 561 nm laser line was used to acquire static images 24hr after injury using a ×20/0.8 N.A. air objective.

Airyscan imaging

A Zeiss LSM900 equipped with a 488 nm and 561 nm laser line was used to acquire static images of mitochondrial morphology before and after injury. The imaging settings are as follows: ×63/1.4 N.A. oil-immersion objective, with an imaging speed of ~4.63 Hz and a 28.80 × 28.80 μm frame size (~216.19 ms frame time, ~3.05 μs pixel dwell time).

Live imaging

Live imaging was performed by collecting z-stacks using Airyscan imaging or manual z-plane focusing with regular laser scanning confocal microscopy over 200 cycles using a ×63/1.4 N.A. oil-immersion objective. In the cases of z-drift during z-stack acquisition, imaging was paused, refocused, and resumed.

2-Photon laser injury

A Zeiss LSM780 and LSM980 inverted microscopes, equipped with 488 nm and 561 nm laser lines and a tunable Ti:Sapphire 2-photon laser (Mai Tai, Spectra-Physics), were used for laser injuries. Early third instar larvae were immobilized using the methods described above. For

proximal primary dendrotomies, distal primary dendrotomies, and tertiary dendrotomies, a Zeiss LSM980 with a Z-piezo stage was used to image neurons and mitochondria and to perform injuries in third-instar Drosophila larvae, as previously described[252].

On the Zeiss LSM980, injuries were performed using a ×63/1.4 N.A. oil-immersion objective, with an imaging speed of ~11.43 Hz and a 44.9 × 44.9 µm frame size (~75.97 ms frame time, ~0.46 µs pixel dwell time, 200 cycles). A 0.4 × 0.4 µm ROI, focused on a dendrite, was injured using a laser at 820 nm with a measured power of ~84.1 mW for 1 iteration. For 400 ms imaging and injury parameters, injuries were performed using a ×63x/1.4 N.A. oil-immersion objective, with an imaging speed of ~8 Hz and a 22.4 × 22.4 µm frame size (~121.65 ms frame time, ~1.49 µs pixel dwell time, 200 cycles). A manually controlled 0.4 × 0.4 µm ROI was positioned over an axon and injured using a laser at 820 nm with a measured power of 101.5 mW for 6 iterations.

For injury-induced branching experiments two neurons were used per animal, one injured and one uninjured. For the injured neuron, a z-stack was acquired of the entire neuron architecture before conducting live-imaging of dendrotomy. We ablated neurons between and adjacent to injured and uninjured neurons (i.e. ablate - A1; dendrotomy - A2; ablate - A3; uninjured control - A4; ablate - A5).

On the Zeiss LSM780, a 0.5 × 0.5 µm ROI was created over an axon or dendrite and injured for ~2 sec at 915 nm with a measured power of ~79.6 mW.

Microtubule imaging

Homozygous EB1-GFP animals were immobilized and injured using the techniques described above. A single Z-plane was acquired with an imaging speed of ~1.43 Hz. The imaging frame was manually adjusted for focus.

MitoGCaMP imaging

Heterozygous MitoGCaMP animals were immobilized and injured using the parameters techniques described above.

Table of Microscopes

Microscopy		
Zeiss LSM 700 Confocal Microscope	*Zeiss*	N/A
Zeiss LSM 780 Confocal Microscope w/ tunable 2-photon laser	*Zeiss*	N/A
Zeiss LSM 900 Confocal Microscope w/ Airyscan imaging	*Zeiss*	N/A
Zeiss LSM 980 Confocal Microscope w/ Airyscan imaging and tunable 2-photon laser	*Zeiss*	N/A
Zeiss PALM Microbeam LCM (Laser Capture Microdissection)	*Zeiss*	N/A
Zeiss Elyra 7 Lattice SIM	*Zeiss*	N/A

Fig. 1.3 Microscopes used during graduate studies

Image analysis

All quantifications were conducted using the open-source software: ImageJ/Fiji (https://fiji.sc).

Mitochondrial contraction

Mitochondrial distance from the injury site was measured in ImageJ/Fiji using the segmented line tool to trace the dendritic length from the injury site to each mitochondrion within the proximal intact dendrite. Contraction onset was defined by the first morphological shift from a tubular to a circular structure following 2-photon laser dendrotomy or axotomy. The end of contraction was marked by the first frame in which mitochondria appeared fully circular, and contraction duration was calculated as the time between initiation and completion. Mitochondria lacking a sustained tubular-to-circular transition were classified as non-contracting.

Mitochondrial area quantification

The following quantification was performed in ImageJ/Fiji using the freehand selection tool. The total mitochondrial area was quantified in ImageJ/Fiji using the freehand selection tool to trace mitochondria with consistent position and visibility before and after 2-photon laser injury within the imaging ROI (~28.80 × 28.80 μm; 336 × 336 pixels). Subjects were blinded to experimental conditions using a custom renaming script (renamer.py) developed for this study (see Data Availability for source code).

To track the change in mitochondrial area acquired from time lapse imaging, the freehand selection tool was used to outline individual mitochondria. Each mitochondrion was manually traced (ROI) for 30 consecutive frames after first appearing and for the last 30 frames before the end of image acquisition. Changes in mitochondrial area were calculated as the area of a single

mitochondria at any frame, divided by the starting area when mitochondria first become visible.

Mitochondrial fold-change quantification

Mitochondrial fold change was quantified by counting the number of mitochondria before and after dendrite injury within the injured branch in Fiji.

Mitochondrial shape change index

Quantification was performed in ImageJ/Fiji using the line tool. Mitochondrial minimum and maximum lengths were measured using the line tool in ImageJ/Fiji before and after injury. The starting shape before injury was measured in the intact proximal distal severed and dendrite by measuring mitochondria prior to the injury frame and at their last visible frame post-injury following primary dendrotomy. Subjects were blinded to experimental conditions using a custom renaming script (renamer.py) developed for this study (see Data Availability for source code).

Branching rate and elongation rate quantification

Control neurons and injured neurons were imaged on the day of injury and 24 hr after injury to generate branching and elongation rates. Neurons were categorized for changes in branching rates based on contracting vs non-contracting mitochondria, where contracting groups had at least one contracting mitochondria. Growth rates were calculated by tracing a primary branch and its tertiary branches in an uninjured dendrite of an injured neuron and in control neurons using the Simple Neurite Tracer (SNT) plugin in Fiji. The branching rate calculation is determined by the following equation:

(branch #injured neuron 24hr after injury / branch #injured neuron day of injury)

×

(branch #uninjured neuron day of injury / branch #uninjured neuron 24hr after injury)

To determine the elongation rate, total dendrite length was used instead of branch #.

Mitochondrial GCaMP analysis

Using the ROI created for tracing the baseline mitoGCaMP intensity (f_0) was defined as the average maximum fluorescence over the first T-10 frames where T = time before mitochondria become visible. Changes in GCaMP fluorescence (f/f_0) were calculated as the maximum intensity at any frame divided by f_0. 10 frames before injury, 30 frames immediately after injury, and the last 30 frames were plotted.

Table of Software

Software and source code		
FIJI (ImageJ)	*Schindelin et al., 2012*	https://fiji.sc/
Scrambler.py	This study	https://github.com/pthwu/scrambler
Imaris	Oxford Instruments	

Fig. 1.4 Software used for analysis

Chapter 3

In Vivo Dendrite Injury Drives Local Mitochondrial Contraction and Dendrite Branching

The content of this **Chapter 3** is published in XXX.

Authors: Hwu, P.T, Kim L. A., Wood, M.A. and Thompson-Peer., K.T.

Abstract

Mitochondria regulate cellular homeostasis in development and disease, and mitochondrial morphology plays a role in local injury signaling and wound repair. How mitochondria respond during dendrite injury remains an open fundamental question. Here we show that mitochondria undergo rapid morphological changes, transitioning from tubular to spherical structures, rapidly and locally after laser-induced dendrite injury (dendrotomy) in live Drosophila larvae. We term this process "mitochondrial contraction" based on the reduction in mitochondrial length and increased circularity. In the proximal intact dendrite, the extent of mitochondrial contraction diminishes with increasing distance from the injury site. We report that injury-induced mitochondrial contraction differs based on primary vs tertiary dendrite injury and that immediate

contraction after injury correlates with increased dendrite branching during repair. Additionally, we find that mitochondrial contraction can be inhibited by KCNJ2 (potassium inwardly rectifying channel subfamily J member 2) overexpression, providing evidence that mitochondrial contraction is regulated by neuronal membrane potential. Mechanistically, we show that expressing a dominant negative form of Drp1 (Dynamin related protein 1) impairs injury-induced mitochondrial contraction and subsequent branching, providing evidence that the fission machinery is also involved in this injury response. These in-vivo findings characterize how mitochondria respond to dendrite injury and suggest that such morphological changes may contribute to dendritic repair processes.

Introduction

Cells constantly encounter mechanical and chemical injuries that trigger adaptive or pathological intracellular responses. Successful cellular repair relies on precise spatiotemporal localization of injury signals and detection of abnormal physiology[21,86,97,221,225,253–256]. Neuronal homeostasis is disrupted in many conditions, from normal aging[152,257] to neurodegeneration[184], and physical injuries like spinal cord[258] and traumatic brain damage[259]. Central to these conditions is disrupted mitochondrial homeostasis, resulting in decreased ATP production, excessive calcium buffering, and increased mtROS (mitochondrial reactive oxygen species)[260]. Thus, studying changes in mitochondrial integrity is critical for understanding how neurons are jeopardized during injury and disease.

Mitochondrial morphology is essential for maintaining local ATP production, protein and calcium homeostasis, and stress responses[184,224,261,262]. To sustain proper function, mitochondria are continuously remodeled by fusion and fission machinery, which facilitates the recycling of

damaged components and removal (mitophagy) of dysfunctional organelles[223]. Fusion is regulated by the interaction of MFN1 and MFN2[64] on the outer mitochondrial membrane, while OPA1[142] and its protease OMA1[145] mediate inner membrane fusion. In contrast, fission is primarily driven by the translocation of DRP1 from the cytosol to the outer mitochondrial membrane, where its activity is regulated by OMM-anchored receptor proteins[93,263]. This dynamic process is critical for cellular function under basal conditions, and under stress, adopts adaptive roles such as buffering calcium and inducing reversible morphological changes[21,97,225]. These acute adaptations influence whether a cell undergoes apoptosis or initiates repair. Despite the importance of mitochondria in injury signaling, the mechanisms regulating mitochondrial dynamics after neuronal injury and subsequently repair are incompletely understood.

Neuronal injury is known to induce microtubule catastrophe, calcium influx, and changes in mitochondrial morphology. Within seconds of axotomy, intracellular Ca^{2+} is upregulated, microtubules are destabilized, organelle homeostasis is disrupted, and mtROS (mitochondrial reactive oxygen species) are produced[26,27,228–230,264]. After axon injury, mitochondria localize to the injured axon to support regeneration[7,8]. Whether dendrite injury triggers changes in mitochondrial morphology, and more critically whether such changes contribute to dendrite repair, has yet to be elucidated.

Here, we investigate how mitochondria respond to laser-induced dendrite injury (dendrotomy) in living Drosophila larvae. Using in vivo time-lapse imaging, we reveal that mitochondria in the intact dendrite, near the injury site undergo rapid morphological changes, transitioning from tubular to a spherical shape, in a distance-dependent manner. We term this process “mitochondrial contraction” based on the apparent reduction in mitochondrial length and increased sphericity. We demonstrate that this contraction response scales with injury severity and can occur independently

of cytoskeletal disruptions or sudden mitochondrial calcium buffering. Furthermore, we show that disrupting neuronal ability to depolarize or inhibiting mitochondrial fission machinery attenuates injury-induced mitochondrial contraction. Importantly, we observe that mitochondrial contraction correlates with enhanced dendrite branching during the repair process. These findings suggest that injury-induced changes in mitochondrial morphological changes may serve as an early signal that promotes dendrite repair rather than simply representing a consequence of cellular damage.

Results

Laser injury induces local changes in mitochondrial morphology

To assess how neuronal mitochondria respond to injury, we imaged mitochondria in class IV *Drosophila* PNS sensory neurons in live animals before and after injury[246,265]. We adapted LarvaSPA, an immobilization technique that preserves respiration during laser injury, because hypoxia can alter mitochondrial morphology (see materials and methods)[252,266].

Axotomy (axon injury) is known to trigger cytoskeletal changes across the neurons architecture

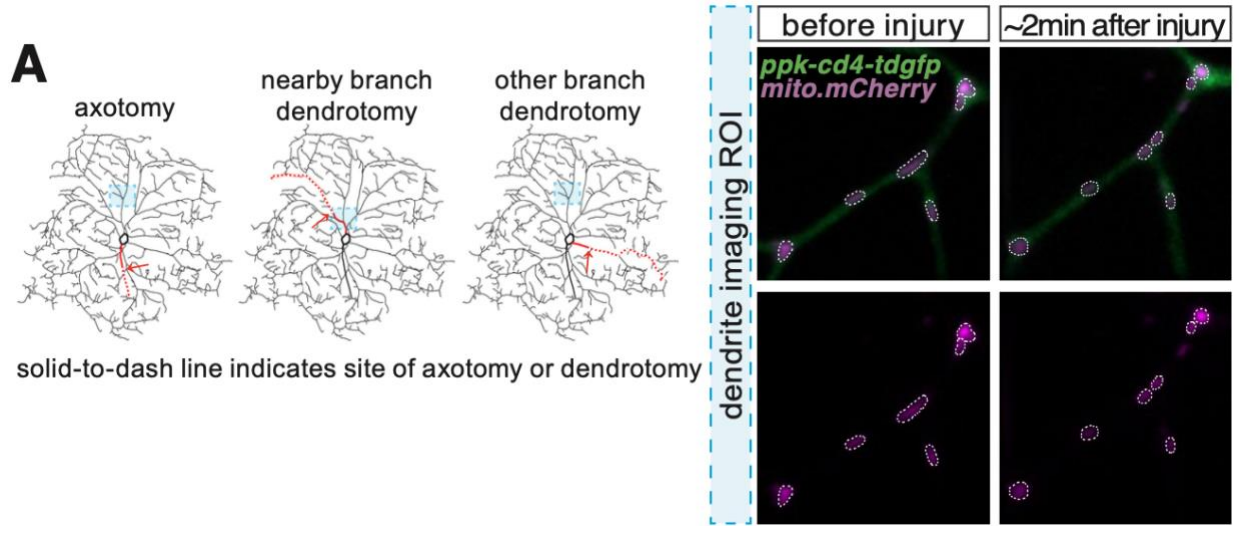

Fig. 1.1 Schematic of injury paradigms. *(A) Left: Schematic of 2-photon laser injury location (red arrow) and imaged mitochondria (blue box). Right: Example of mitochondrial area quantification.*

(**Movie S1**) and alter mitochondrial morphology in the injured axon[26,267]. Based on this, we

hypothesized that axotomy may induce changes in mitochondria morphology in distant, uninjured dendrites.

To test whether axotomy altered mitochondrial morphology in uninjured dendrites, we quantified mitochondrial area dendrites before and after axotomy (**Fig. 1.1A**). Before axotomy, the mitochondria in the uninjured dendrite contained tubular and spherical mitochondria. When we reimaged the same uninjured dendrites, approximately 2 min after axotomy, mitochondria retained their original morphology with no significant change in mitochondrial area (Two-tailed paired t test, p=0.4217) or mitochondrial number (Two-tailed paired t test, p=0.7500) (**Fig. 1.2B and 1.2C,** N=22). From this observation, we conclude that mitochondrial morphology in uninjured dendrites is not altered within 2 min of axotomy.

We next examined whether dendrotomy (dendrite injury) alters the morphology of mitochondria in the injured dendrite and nearby branches. To test this, we imaged dendritic mitochondria just prior to an injury location (nearby branch dendrotomy) and within the dendrite and reimaged the same location approximately 2 min after injury. Notably, when we reimaged the same region after injury, we detected the presence of spherical mitochondria which had initially appeared tubular just prior to injury. This injury-induced change in mitochondrial morphology we observed was supported by a significant decrease in mitochondrial area (Two-tailed paired t test, p<0.0001****) without changing the number of mitochondria (Two-tailed paired t test, p=0.5137) (**Fig. 1.2B and 1.2D,** "nearby branch dendrotomy", N=25). We term this morphological change "mitochondrial contraction" based on the reduction in mitochondrial area without a significant change in the number of mitochondria primarily driven by a reduction in mitochondrial length. Importantly, we counted the number of mitochondria before and after nearby branch dendrotomy and found that the number of mitochondria was consistent following nearby branch dendrotomy.

To determine whether dendrotomy induced changes in mitochondria locally or globally, we

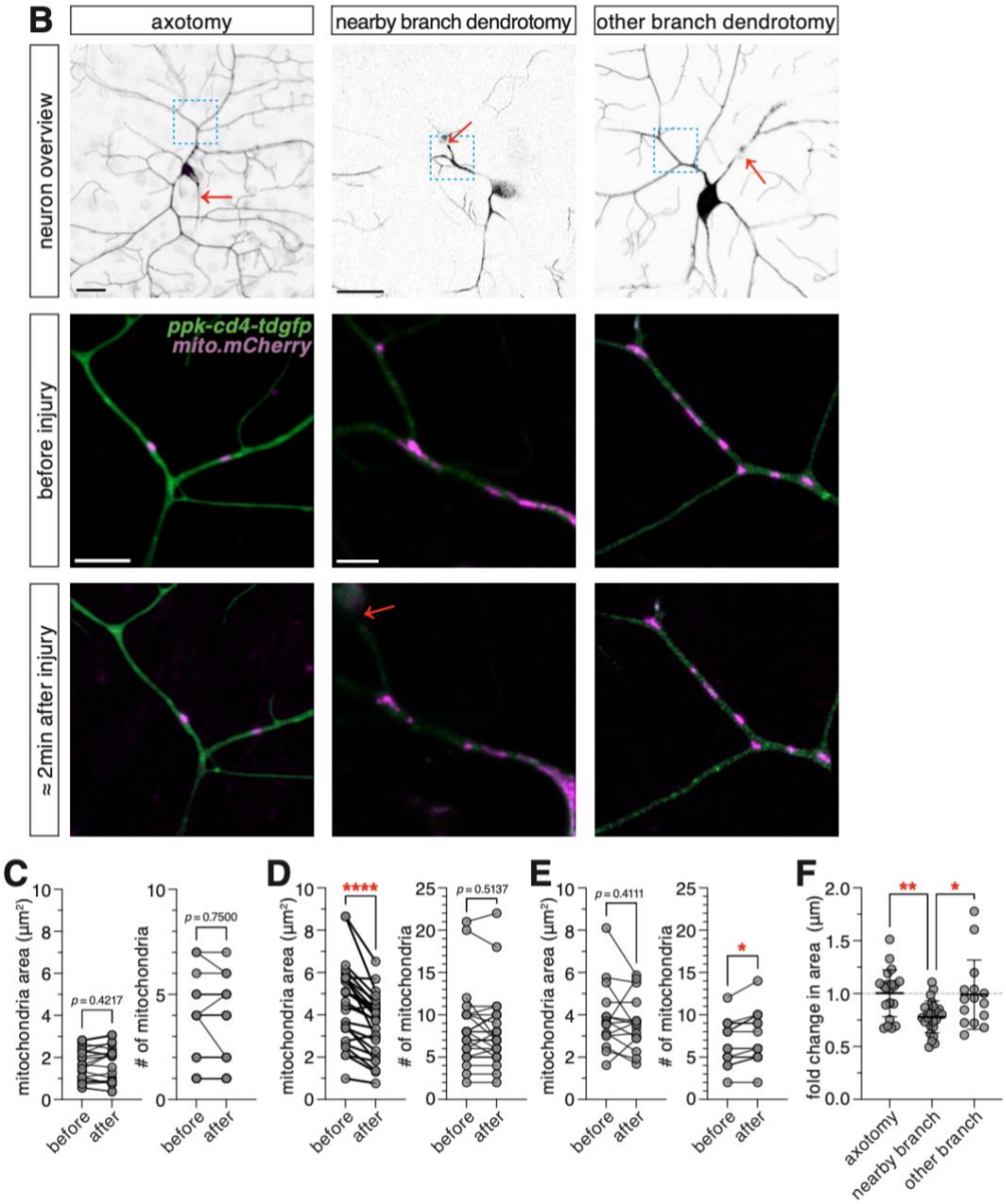

Fig. 1.2 Dendrite injury triggers changes in mitochondrial area. ***(B)*** *Top row: Neuron before axotomy, nearby branch dendrotomy, and other branch dendrotomy (red arrow indicates injury location). Scale bar 40 μm. Center row: representative image of mitochondria labeled with an outer mitochondrial membrane marker (mito.mCherry) (magenta) in neurons (green) before axotomy, before nearby branch dendrotomy, and before other branch dendrotomy. Scale bar 5 μm. Bottom row: representative image of mitochondria approximately 2 mins after axotomy, nearby branch dendrotomy, and other branch dendrotomy.* ***(C-E)*** *Total mitochondrial area and number of mitochondria in the imaged dendrites before and after* ***(C)*** *axotomy (Two-tailed paired t tests, p=0.4217; p=0.7500),* ***(D)*** *nearby branch dendrotomy (Two-tailed paired t tests, p<0.0001****; p=0.5137), and* ***(E)*** *other branch dendrotomy (Two-tailed paired t tests, p=0.4111; p=0.0156*).* ***(F)*** *Fold change in mitochondrial area before versus after: axotomy, nearby branch, and other branch dendrotomy (One-way ANOVA, Bonferroni corrected, axotomy vs. nearby branch p=0.0042**; other branch vs nearby branch p=0.0195*).*

imaged dendritic mitochondria of uninjured dendrites (other branch dendrotomy) separate from the injured dendrite. When reimaging the uninjured dendrites, approximately 2 minutes after other branch dendrotomy, we observed that mitochondria retained their initial tubular morphologies which is supported by unchanged mitochondrial area (Two-tailed paired t test, p=0.4111) (**Fig. 1.2B and 1.2E**, "other branch dendrotomy", N=15). Even though the mitochondrial area remained unchanged in the uninjured branch following dendrotomy, it is worth noting that we observed a significant increase in the number of mitochondria (Two-tailed paired t test, p=0.0156*) (**Fig. 1.2E**). These findings demonstrate that injury-induced mitochondrial morphological changes are spatially restricted to the vicinity of the injury site (**Fig. 1.2F**). In summary, we find that dendrotomy triggers local changes in the mitochondrial area.

Dendrotomy induces distance-dependent mitochondrial contraction

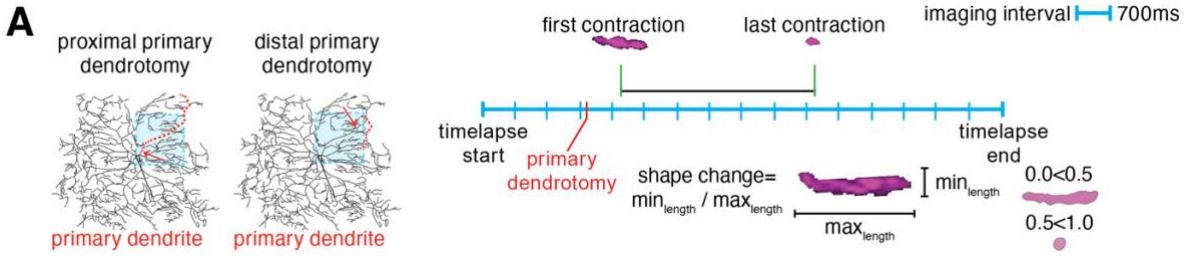

Fig. 2.1 Schematic injury paradigms and time lapse imaging. *(A) Schematic of injury location for proximal primary dendrotomies*

Our observations suggested that dendrotomy induces mitochondrial contraction, a phenomenon similar to that observed in axons after axotomy[230]. We hypothesized that mitochondria respond to laser dendrotomy by contracting, because we primarily observed changes in mitochondrial area but not quantity. To interrogate how dendrotomy induces changes in mitochondrial area we acquired videos of mitochondria during dendrotomy with a more precise spatiotemporal resolution (~700ms) (**Fig. 2.1A**).

First, we wanted to determine if injury-induced changes in mitochondrial morphology

propagated indefinitely in the distal severed dendrite. To test this, we conducted proximal primary dendrotomies and characterized the response governing the change in mitochondrial area in the distal severed dendrite. Before proximal primary dendrotomy, primary dendrites contained tubular mitochondria distributed along their length.

Immediately after dendrotomy, tubular mitochondria in the severed distal segment contracted rapidly and completely, transitioning from tubular to spherical shapes within seconds (**Fig. 2.2B and 2.2C'; Movie S2**), including those most distant to the dendrotomy site (**Fig. 2C''**). We term this morphological change "mitochondrial contraction" based on the morphological change of individual mitochondria. Furthermore, we found that 84 out of 84 of the mitochondria had

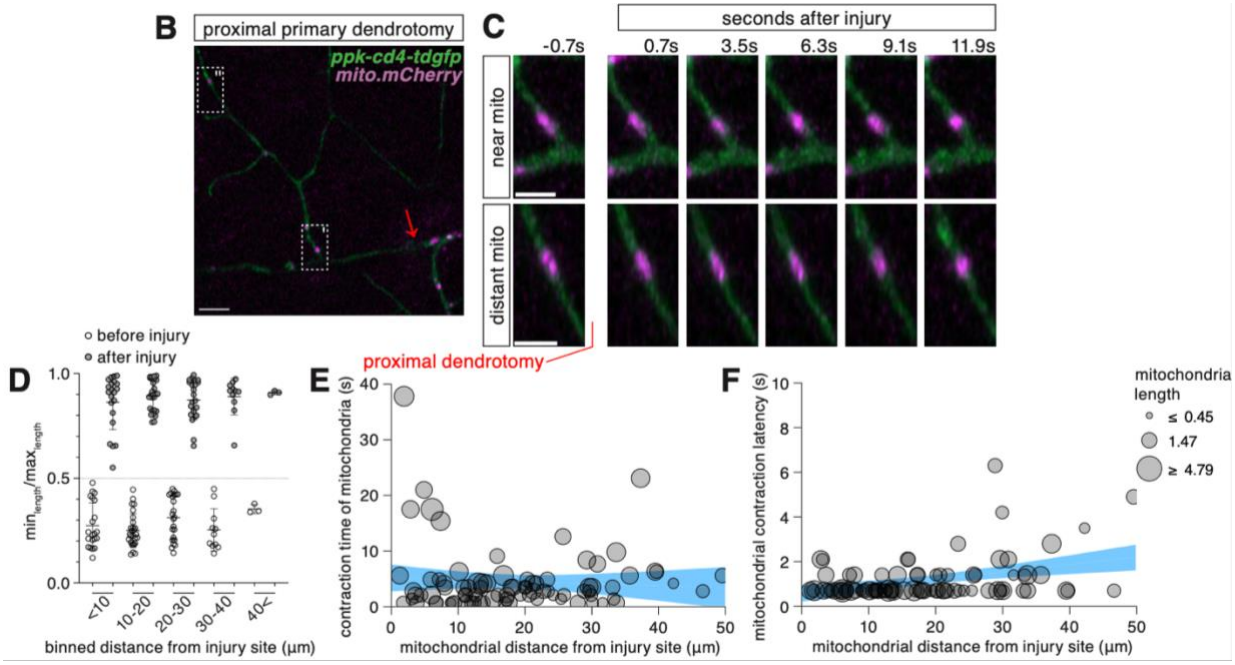

Fig. 2.2 Characterization of mitochondrial contraction after proximal primary dendrotomy. ***(B)*** *Representative snapshot of dendritic mitochondria after proximal primary dendrotomy (red arrow) with mitochondria near (') and far from ('') injury site. Scale bar 5 μm.* ***(C)*** *Magnified view before and after dendrotomy of mitochondria near to (top) and distant from (bottom) the dendrotomy site. Scale bar 2 μm.* ***(D)*** *Mitochondrial shape change binned by distance from injury site.* ***(E)*** *Mitochondrial contraction time in relation to distance from injury site after primary proximal dendrotomy (grey circles = starting mitochondrial length before injury) (linear regression, r=-0.07, p=0.53)* ***(F)*** *Mitochondrial contraction latency in relation to distance from injury site after primary proximal dendrotomy (grey circles = starting mitochondrial length before injury) (linear regression, r=0.38, p=0.0004).*

contracted, regardless of their distance from the site of dendrotomy (**Fig. 2.2D**). To better

understand this contraction response, we quantified the contraction duration time (how long it took for mitochondria to transition from a tubular to a spherical shape) and noted that the contraction time was not correlated with distance from dendrotomy in the distal severed dendrite (**Fig. 2.2E**, linear regression r=-0.07, p=0.5294); however, mitochondrial contraction latency was (**Fig. 2.2F**, linear regression r=0.38, p=0.0004). From these results, we conclude that all mitochondria in the distal severed segment contract after proximal primary dendrotomy.

We next examined mitochondrial responses in the proximal intact dendrite–which remains attached to the cell body–after distal primary dendrotomy. In contrast to the response in the severed segment, not all mitochondria within the injured intact dendrite contracted after dendrotomy (**Fig**

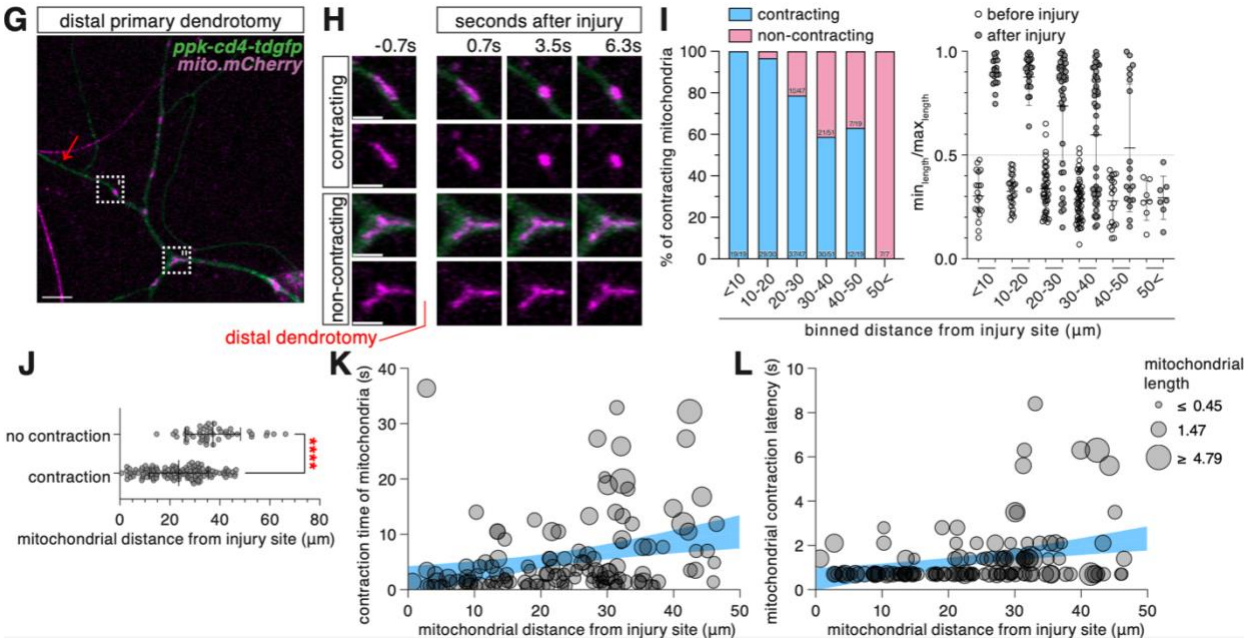

Fig. 2.3 Characterization of mitochondrial contraction after distal primary dendrotomy. ***(G)*** *Representative snapshot of dendritic mitochondria after distal primary dendrotomy (red arrow) with contracting (') and non-contracting (") mitochondria.* ***(H)*** *Magnified view of dendrite before and after dendrotomy containing contracting (top) and non-contracting (bottom) mitochondria. Scale bar is 2 μm.* ***(I)*** *Percentage of contracting/non-contracting mitochondria (left) and the measured change in morphology (right) binned by distance from distal primary dendrotomy site.* ***(J)*** *Mean distance of contracting (n=127) vs non-contracting (n=46) mitochondria after distal primary dendrotomy (Two-tailed Mann-Whitney U test, p<0.0001****) (logistic regression, OR=1.11, 95%CI: 1.07-1.16, p<0.0001).* ***(K)*** *Mitochondrial contraction time in relation to distance from injury site after distal primary dendrotomy (linear regression, r=0.29, p=0.0009).* ***(L)*** *Mitochondrial contraction latency in relation to distance from injury site after distal primary dendrotomy (linear regression, r=0.33, p=0.0002).*

2.3G; Movie S3). This was apparent as mitochondria near the dendrotomy site (**Fig. 2.3H'**)

contracted but mitochondria located farther away failed to contract (**Fig. 2.3H''**). Despite our observations that mitochondria contracted in 100% of the neurons we injured (30), not every mitochondria in each neuron contracted; mitochondria were less likely to contract as the distance between the dendrotomy site and individual mitochondria increased (**Fig. 2.3I**). We observed that mitochondria within <20 μm of the dendrotomy site contracted in the majority of cases (48 out of 49), whereas mitochondria further than 50 μm from the dendrotomy site never contracted (**Fig. 2.3I**). We show this both as a binary representation (contracting or non-contracting, **Fig. 2.3I left**), and as a measurement of the shape change (min/max length, **Fig. 2.3I right**). We noted that the *likelihood* of injury-induced mitochondrial contraction was significantly correlated with distance from dendrotomy site (**Fig. 2.3J,** logistic regression, OR=1.11, 95%CI: 1.07-1.16, p<0.0001). To better understand how distance influenced injury-induced contraction, we plotted how long it took for each mitochondria to contract and uncovered that the distance between mitochondria was significantly correlated with mitochondrial contraction time (**Fig. 2.3K,** linear regression, r=0.29, p=0.0009) and mitochondrial contraction latency (**Fig. 2.3L,** linear regression, r=0.33, p=0.0002). In addition to characterizing the injury induced contraction, we counted the number of mitochondria before and after dendrotomy. The total number of mitochondria remained constant after injury (**Fig. S1A**), supporting our interpretation that the morphological changes we observe represent contraction of existing mitochondria rather than fragmentation into multiple smaller organelles.

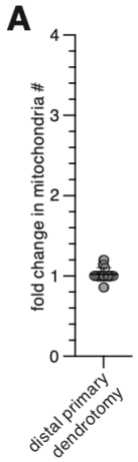

In summary, we conclude that injury induced mitochondrial contraction is dependent on distance from the injury site in the proximal intact dendrite, influencing the likelihood of contraction, how long it takes for mitochondria to contract, and the contraction latency.

To compare how axotomy affects mitochondrial morphology in the injured axons versus what we observed in dendrites, we performed live-imaging of mitochondria in axons during axotomy (**Fig. 3.0A**). Similar to dendrites, axonal mitochondria contain tubular and spherical morphologies before axotomy (**Fig. 3.0B**). Immediately after axotomy, all (78 out of 78) of the mitochondria in the intact axon segment contracted rapidly and completely (**Movie S4**). As observed in dendrites, we noted that the contraction time of mitochondria (**Fig. 3.0C**, linear regression, r=0.59, p<0.0001) and the mitochondrial contraction latency (**Fig. 3.0D**, linear regression, r=0.30, p=0.0079) was correlated with the distance between axotomy site and individual mitochondria. We also observed that the total number of mitochondria remained consistent after injury (**Fig. 3.0E**). From these observations, we conclude that duration and timing of injury-induced mitochondrial contraction is

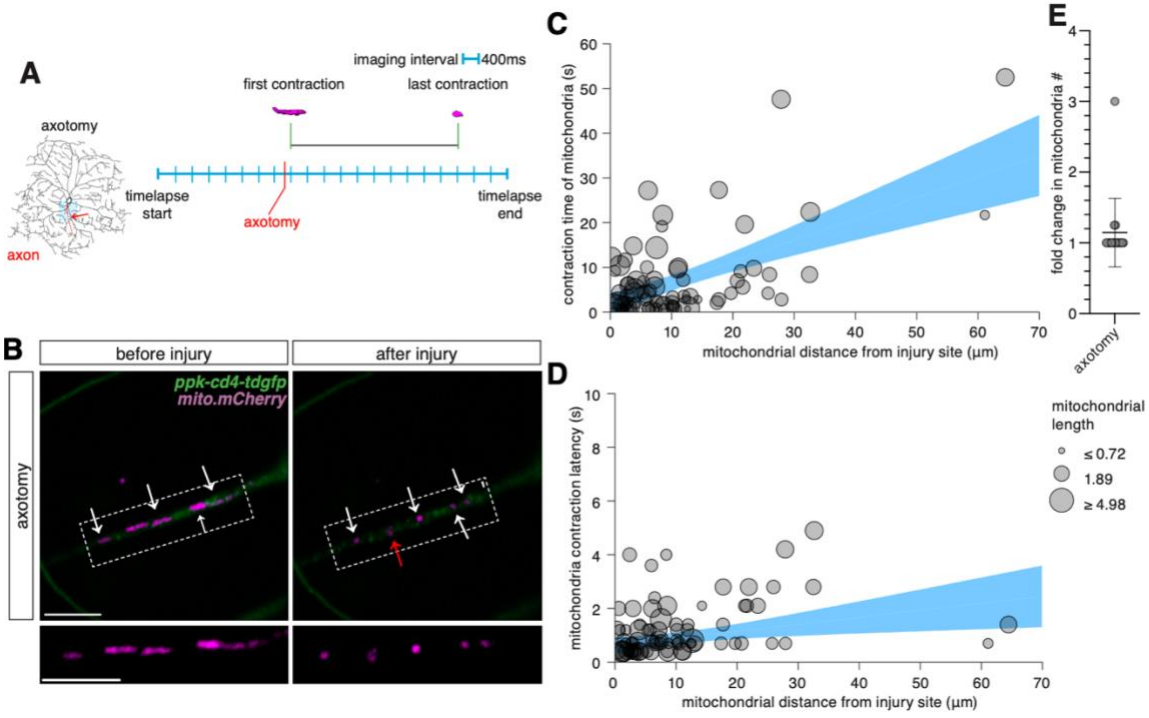

Fig. 3.0 Characterization of mitochondrial contraction axotomy. *(**A**) Schematic of axotomy and imaging location. (**B**) Representative image of axotomy (red arrow) induced mitochondrial contraction (white arrows) before (left) and after (right) axotomy. Scale bar 5 μm. (**C**) Duration of axonal mitochondrial contraction as a function of distance from axotomy site and mitochondrial length after axotomy in wildtype neurons (linear regression, r=0.59, p=0.0001). (**D**) Mitochondrial contraction latency in relation to distance from injury site after axotomy (linear regression, r=0.30, p=0.0079). (**E**) Fold change in mitochondria number after axotomy.*

dependent on distance from the injury site in the proximal intact axon, similar to what we observed in dendrites.

In summary, injury-induced mitochondrial contraction exhibits a clear distance-dependent pattern in both dendrites and axons, with mitochondria closer to the injury site contracting more rapidly and reliably than those located farther away. This spatiotemporal response suggests that injury signals propagate locally through the neuronal process to trigger changes in mitochondrial morphology.

Mitochondria contract independently of changes in microtubules or calcium buffering

Mitochondrial morphology is partly regulated through interactions with microtubules[268]. To determine whether injury-induced changes in microtubules drive mitochondrial contraction, we conducted distal primary dendrotomies live-imaging both microtubules (using the *plus-end binding protein, EB1-GFP*) and mitochondria, simultaneously.

Following dendrotomy, we observed changes in microtubules–evident by the sudden formation of EB1-GFP puncta in dendrites–immediately after injury. EB1-GFP generally forms comets that indicate the direction of microtubule growth, but we observed the appearance of stable EB1-GFP puncta after injury. EB1-GFP puncta represent the plus ends of microtubules, which are sites of microtubule polymerization and growth. In 72% of the cases (21 out of 29 neurons), mitochondrial contraction and EB1-GFP puncta formation occurred simultaneously (**Fig. 4.0A; Movie S5**). However, we observed several instances where these events were temporally uncoupled: EB1-GFP puncta formed prior to mitochondrial contraction (~10.3%), EB1-GFP puncta were present without mitochondrial contraction (~3.4%) (**Movie S6**), mitochondria contracted prior to EB1-GFP puncta forming (~6.9%), and mitochondrial contraction occurred in

the absence of EB1-GFP puncta formation (~6.9%) (**Fig. 4.0B; Movie S7**). These findings suggest that although microtubule alterations and mitochondrial contraction often occur concurrently, they represent independent cellular responses to injury rather than obligate coincident events. We interpret this to mean that microtubule changes often correlate with, but do not drive, mitochondrial contraction.

Both axotomies and dendrotomies trigger cytosolic calcium influx[12,13]. In response to elevated intracellular calcium, mitochondria rapidly buffer calcium to (try to) restore calcium back to

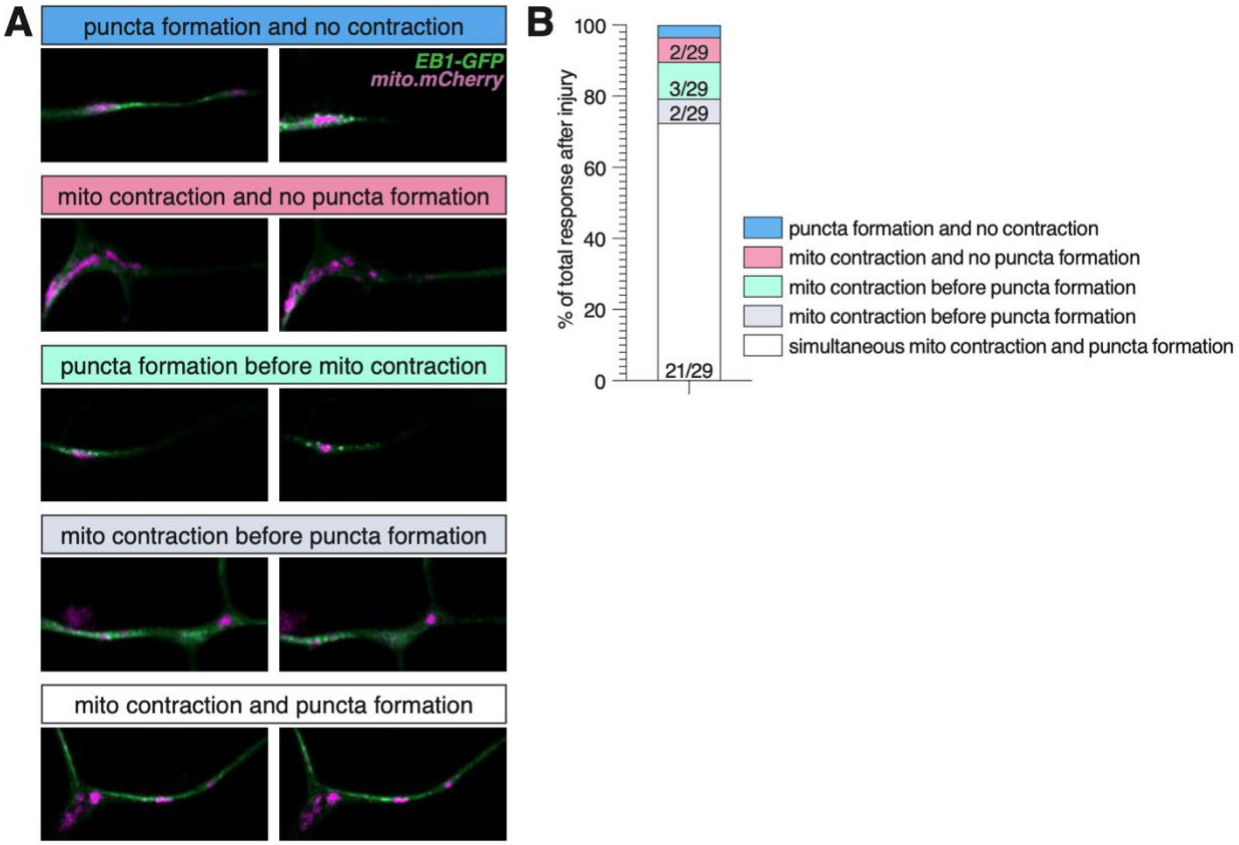

Fig. 4.0 Injury induced mitochondrial contraction can occur independently of the appearance of EB1 puncta. *(**A**) Left columns are before dendrotomy, and right columns are after dendrotomy. Microtubules (green, microtubule plus-end binding protein 1, UAS-EB1-GFP) and mitochondria (magenta, UAS-mCherry.mito.OMM) are imaged. From top to bottom: the formation of EB1-GFP puncta without mitochondrial contraction (1/29). Mitochondrial contraction in the absence of EB1-GFP puncta formation (2/29). The formation of EB1-GFP puncta before mitochondrial contraction (3/29). Mitochondrial contraction before EB1-GFP puncta formation (2/29). Mitochondrial contraction and EB1-GFP puncta formation occurring simultaneously (21/29). (**B**) Percentage of EB1-GFP mitochondrial contraction outcomes after primary distal dendrotomy. Scale bar 5μm.*

baseline levels[269], and mitochondrial calcium buffering is known to affect mitochondrial morphology[181]. We hypothesized that mitochondrial calcium buffering might promote

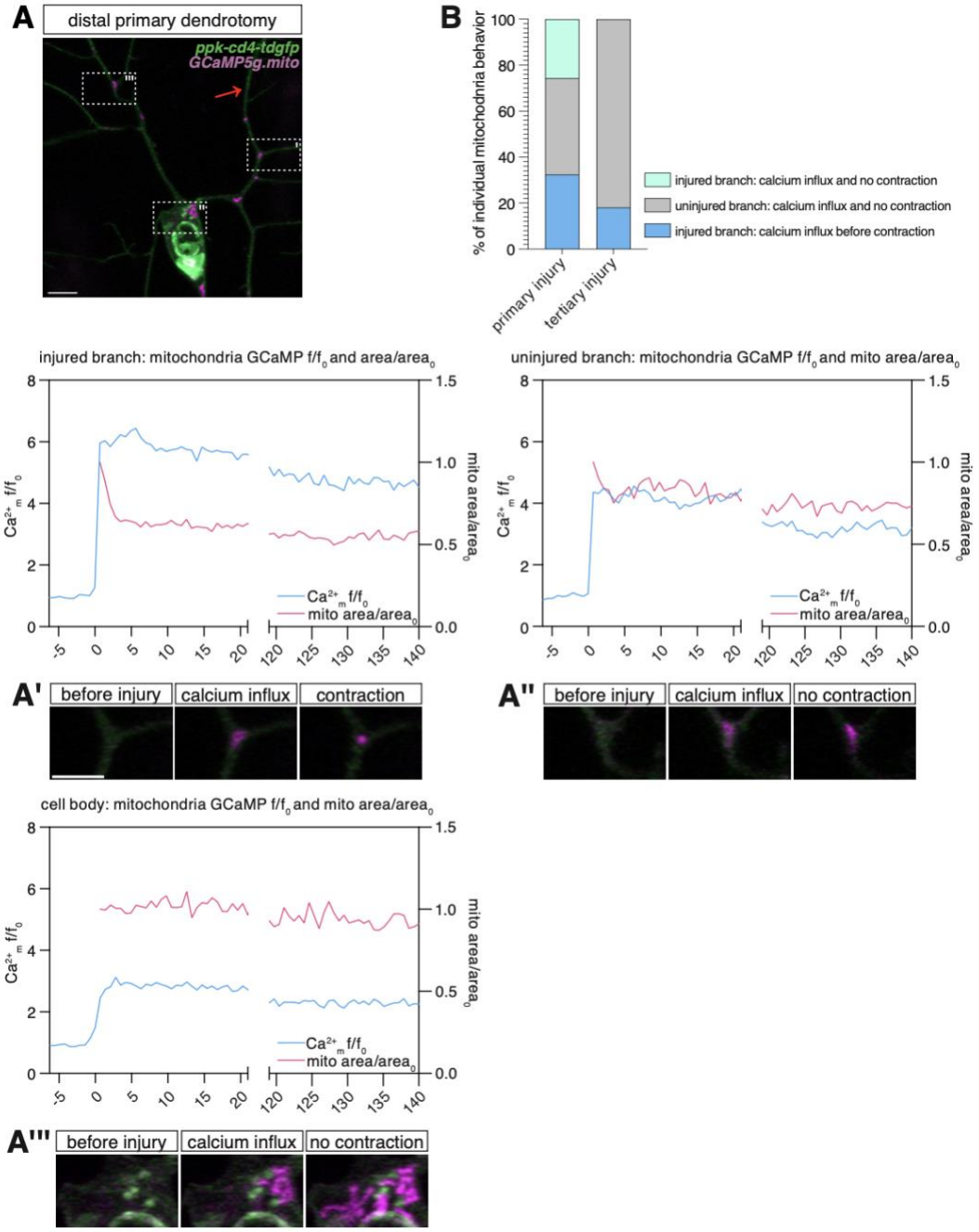

Fig. 5.0. **Dendrotomy induces global mitochondrial calcium buffering**. *(**A**) Mitochondria are not typically visible under baseline conditions with the UAS-GCaMP5g.mito marker, but become detectable following dendrotomy (red arrow). Mitochondrial localization (white boxes) in different neuronal compartments post-dendrotomy. N = 7, n = 50. (**A'**) within the injured dendrite, (**A''**) in an uninjured branch, and (**A'''**) in the cell body. (**B**) Quantification of mitochondrial behavior across injured and uninjured dendrites following primary distal dendrotomy (N = 14) and tertiary dendrotomy (N = 7).*

mitochondrial contraction. To test this, we performed distal primary dendrotomies and tertiary dendrotomies (tertiary dendrite injury) while imaging mitochondrial calcium (Ca^{2+}_m) levels using a mitochondrial GCaMP marker (mitoGCaMP) (**Fig. 5.0A**).

Before injury, mitochondria showed minimal detectable mitoGCaMP signal. Following distal primary dendrotomy, we observed a retroactive wave of Ca^{2+}_m uptake originating from the dendrotomy site that propagated to uninjured dendrites, the cell body, and down the axon (**Fig. 5.0, A and A'; Movie S8)**. Although we observed both increased Ca^{2+}_m levels and mitochondrial contraction in mitochondria near the dendrotomy site we observed contraction only in mitochondria near the injured dendrite. (**Fig. 5.0, A'' and A''', Fig. 5.0B**). This spatial dissociation between calcium uptake and contraction demonstrates that sudden mitochondrial calcium influx is insufficient to trigger injury-induced mitochondrial contraction.

In summary, our correlative analysis suggests that injury-induced mitochondrial contraction occurs independently of microtubule changes and is not solely driven by mitochondrial calcium influx, though we cannot exclude more complex temporal or mechanistic relationships.

Injury-induced mitochondrial contraction scales with dendrite branch order

Injury-induced changes in mitochondrial morphology are known to activate injury signaling

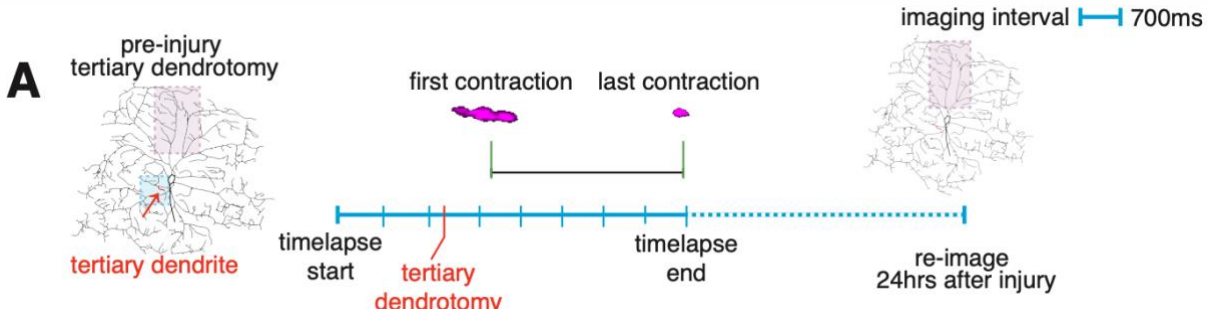

Fig. 6.1 Schematic tertiary injury paradigm and subsequent arbor tracking. ***(A)*** *Schematic of tertiary dendrotomy. An overview of the neuron architecture was taken before dendrotomy. Images of neurons were continuously acquired for 200 frames and dendrites were injured at approximately frame 10. Neurons were imaged 24 hr after.*

cascades[21,97,225]. To evaluate the functional consequences of mitochondrial contraction, we designed a paradigm that allowed us to injure neurons inducing contraction in only a subset of injured neurons, using tertiary dendrite injury to assess the relationship between mitochondrial contraction and repair outcomes.

To investigate the consequence of mitochondrial contraction, we imaged the neuronal architecture before dendrotomy, conducted live-imaging of tertiary dendrotomies (tertiary dendrite injury to small branches), then reimaged the neuronal architecture 24 hr after injury to assess repair responses (**Fig. 6.1A**).

We first established how mitochondria respond to tertiary dendrotomies (**Fig. 6.2B**), which we confirmed by a physically severed branch (**Fig. 6.3A; Movie S9 and Movie S10**). In contrast to primary dendrotomies, which consistently triggered mitochondrial contraction, tertiary dendrotomies produced variable responses, where nearby mitochondria contracted in some neurons (**Fig. 3C'**) but many mitochondria did not (**Fig. 3C''**). In about 30% of the cases (7/23) where there were mitochondria right next to the injury site (within 10 μm), we observed no mitochondrial contraction, which contrasts with primary branch dendrotomies that always induces mitochondrial contraction in that adjacent distance (**Fig. 6.2D**). Furthermore, we failed to observe any instances of injury-induced mitochondrial contraction if the distance between mitochondria and the dendrotomy site exceeded 30 μm (**Fig. 6.2D**). At all distances, tertiary dendrotomies were less likely to induce mitochondrial contraction, as only 38 out of 103 mitochondria contracted overall (37%), compared to 73% of mitochondria contracting after distal primary dendrotomy (**Fig. 6.2E and 6.3B**).

While the likelihood of injury-induced contraction was correlated with the distance from the injury site (**Fig. 6.2E,** logistic regression, OR=1.12, 95%CI [1.07-1.19], p<0.0001), there was no

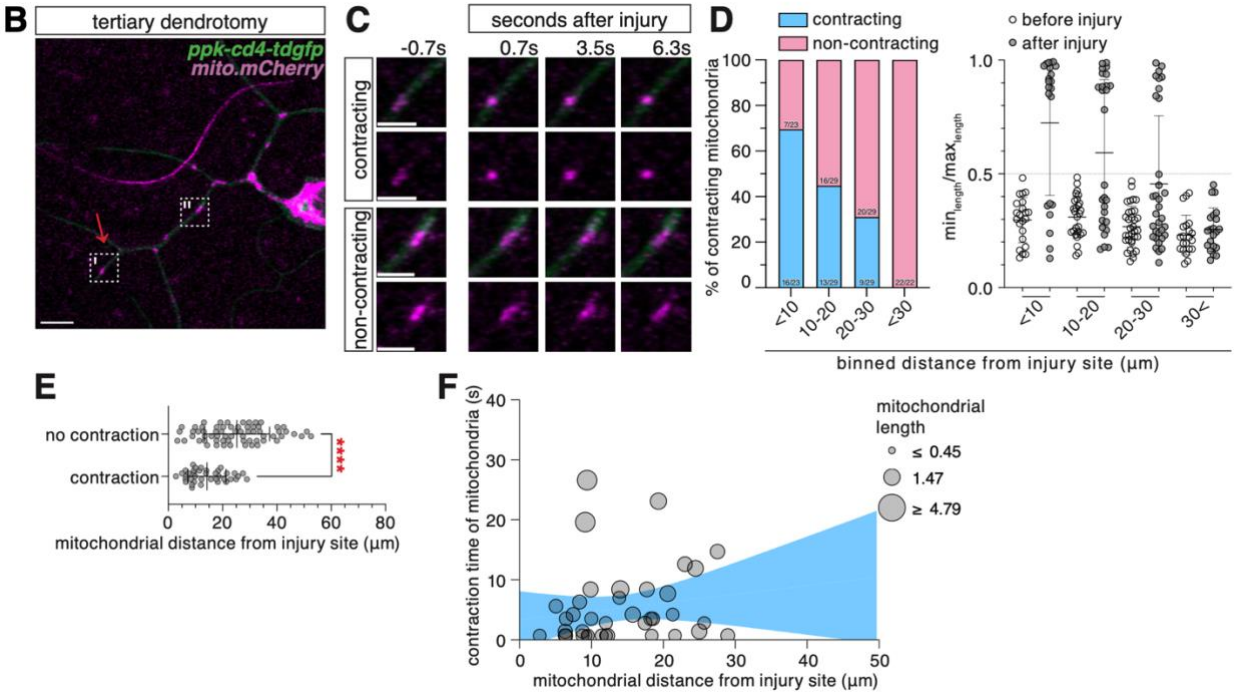

Fig. 6.2 Tertiary dendrotomy induces mitochondrial contraction but to a lesser magnitude. *(**B**) Representative snapshot of dendritic mitochondria after tertiary dendrotomy (red arrow) with contracting (') and non-contracting ('') mitochondria. Scale bar 5 µm. (**C**) Magnified view of dendrite before and after injury containing contracting (top) and non-contracting (bottom) mitochondria. Scale bar 2 um. (**D**) Percent of contracting/non-contracting mitochondria (left) and change in morphology (right) binned by distance from tertiary dendrotomy site. (**E**) Mean distance of contracting mitochondria (n=38) vs non-contracting (n=65) mitochondria after tertiary dendrotomy (Two-tailed Welch's t test, p<0.0001****) (logistic regression, OR=1.12, 95%CI [1.07–1.19], p<0.0001). (**F**) Mitochondrial contraction time in relation to distance from injury site after tertiary dendrotomy (linear regression, r=0.16, p=0.35).*

evident correlation between how long it took mitochondria to contract (**Fig. 6.2F**, linear regression, r=0.16, p=0.35) and distance from the dendrotomy site. When comparing primary versus tertiary dendrotomies we found that at similar distances from the dendrotomy site, mitochondrial contraction after tertiary dendrotomy had a longer duration than distal primary dendrotomies, suggesting that tertiary dendrotomy induces slower mitochondrial contraction (**Fig. 6.3C**).

To test if mitochondrial contraction is correlated with repair responses, we took advantage of the variable contraction responses following tertiary dendrotomies. We imaged the entire architecture of a neuron before injury and an uninjured control, conducted time-lapse imaging of tertiary dendrotomies, reimaged the same neuronal architecture 24 hr after dendrotomy, and

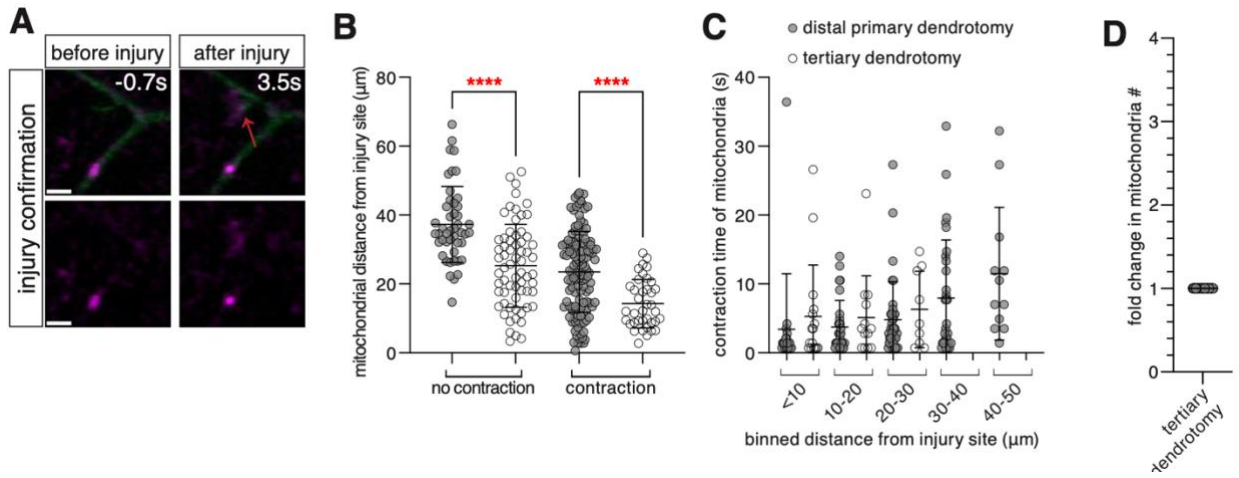

Fig. 6.3 Mitochondrial contraction scales with dendrotomy severity. *(**A**) Screenshot of tertiary dendrotomy (red arrow) and mitochondrial contraction. Scale bar 1.5 µm. (**B**) Comparison between average distances away from dendrotomy site that induced no mitochondrial contraction and mitochondrial contraction after distal primary dendrotomy, and tertiary dendrotomy from the neurons analyzed in Figure 2 and Figure 3. (One-way ANOVA, Bonferroni corrected primary dendrotomy vs. tertiary dendrotomy no contraction, p<0.0001****; primary dendrotomy vs. tertiary dendrotomy contraction, p<0.0001****). (**C**) Binned distance away and duration of mitochondrial contraction for primary dendrotomies vs. tertiary dendrotomies. (**D**) Fold change in mitochondrial number after tertiary dendrotomy.*

quantified the change in dendrite branching to assess repair outcomes (**Fig. 6.2G-I; Movie S11 and Movie S12**).

Because tertiary dendrites are short (<10 μm) and adjacent to the shaft of the primary dendrite, we established strict inclusion criteria for these experiments. To ensure that we were only assessing the consequence of mitochondrial contraction on dendrite growth, we only quantified neurons if the attached primary branch was present before and 24 hr after dendrotomy (**Movie S13**). To account for differences in growth rates between neurons and across animals, we normalized dendrite branching rates of the injured neuron to an uninjured neuron within the same animal.

Following 24 hr after tertiary dendrotomy, we observed that neurons *with* contracting mitochondria displayed significantly increased dendrite branching compared to neurons *without* contracting mitochondria (**Fig. 6.4J,** Two-tailed Welch's t test, p=0.0189*). In contrast, no significant differences were detected in extension of preexisting dendrites (elongation) between these groups (**Fig. 6.4J**, Two-tailed Welch's t test, p=0.2549). This suggests that mitochondrial

contraction specifically correlates with branching regrowth rather than general growth promotion.

In summary, we observe that tertiary dendrotomies induce variable and reduced mitochondrial

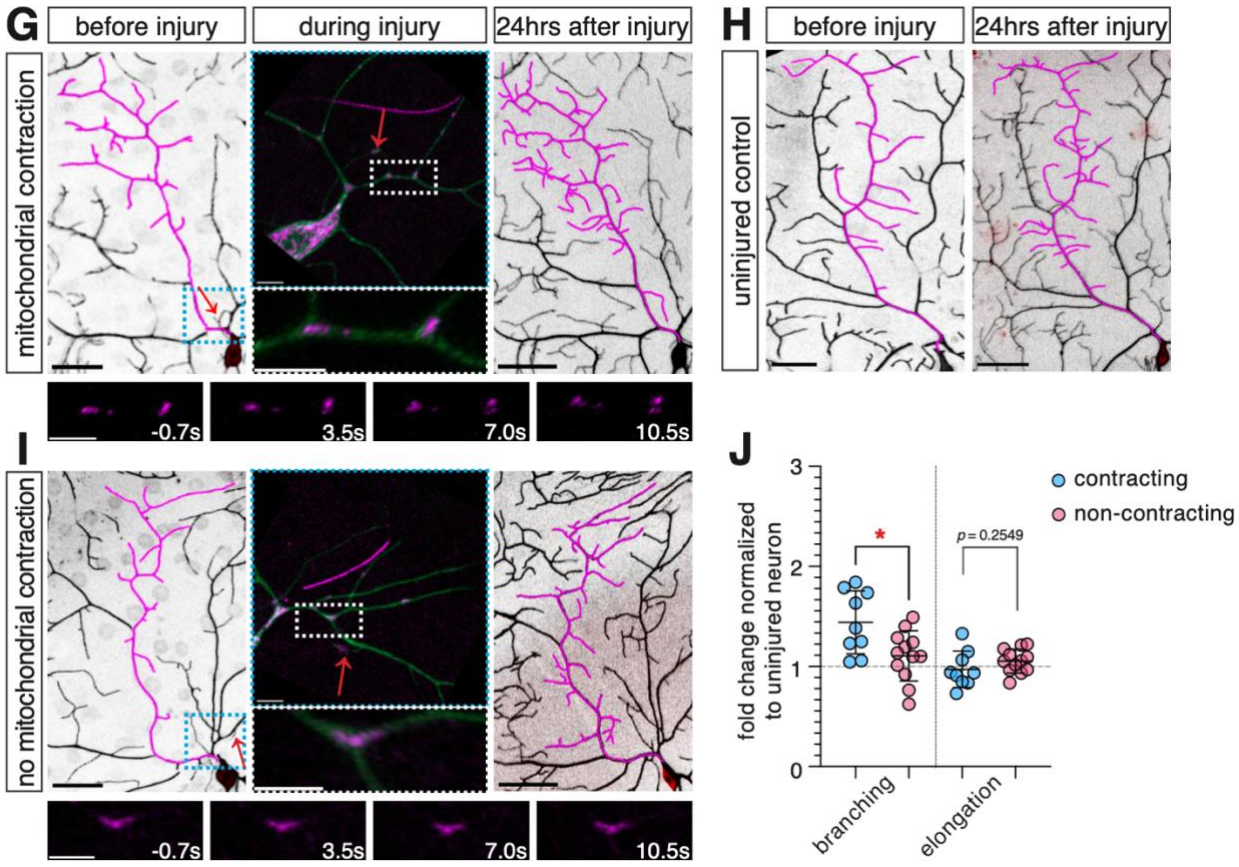

Fig. 6.4 Injury induced mitochondrial contraction is associated with dendrite branching. *(**G**) Representative image of neuron architecture with contracting mitochondria before (left), during (middle), and 24 hr after (right) tertiary dendrotomy. Scale bar 25 µm, 5 µm, 50 µm. (**H**) Uninjured control neuron on the day of dendrotomy and 24 hr after. Scale bar 25 µm, 50 µm. (**I**) Representative image of neuron architecture without contracting mitochondria before (left), during (middle), and 24 hr after (right) tertiary dendrotomy. Scale bar 25 µm, 5 µm, 50 µm. (**J**) Fold change in dendrite branching (Two-tailed Welch's t test, p=0.0189*) and length (Two-tailed Welch's t test, p=0.2549) from before injury to 24 hr after tertiary dendrotomy, in neurons with contracting (N=9) vs non-contracting mitochondria (N=12) normalized to uninjured control.*

contraction compared to primary dendrotomies, and the presence of mitochondrial contraction is correlated with increased dendrite branching during the repair process.

Hyperpolarization via KCNJ2 impairs mitochondrial contraction after primary dendrotomy

Electrical activity is a well-established regulator of dendrite patterning during development[270].

Previous work has shown that hyperpolarizing the resting membrane potential by overexpressing

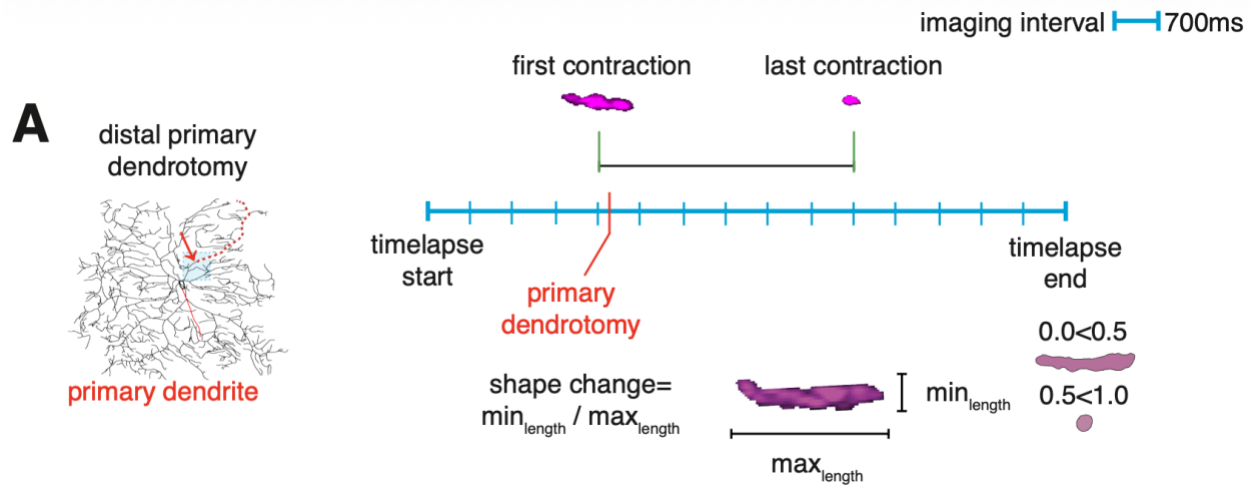

Fig. 7.1 Schematic of injury paradigm for KCNJ2 experiments *(A) Schematic of primary dendrotomy. Live images were acquired for 200 frames and neurons were injured between frame 1 and frame 20.*

KCNJ2 (potassium inwardly rectifying channel subfamily J member 2) inhibits dendrite regeneration[11], partly by blocking calcium-mediated injury detection[12]. Overexpression of *KCNJ2* is a widely used tool to inhibit action potential firing in Drosophila neurons[271–275]. We postulated that injury-induced mitochondrial contraction requires normal neuronal membrane potential.

To test whether membrane hyperpolarization affects mitochondrial contraction, we live-imaged mitochondria during primary dendrotomies in *wildtype* and *KCNJ2*-expressing neurons. We chose primary dendrotomies for this analysis because they elicit more consistent contraction responses than tertiary dendrotomies (**Fig. 7.1A**). We first confirmed that *KCNJ2* expression does not alter baseline mitochondrial morphology, as previous studies have shown that expressing *KCNJ2* can increase mitochondrial length[153]. Prior to dendrotomy, mitochondria in *KCNJ2* neurons showed normal distributions of tubular and spherical morphologies, similar to wildtype controls (**Fig. 7.2B, 7.2C**, Two-tailed Mann-Whitney U test, p=0.4872).

Following primary dendrotomy, *KCNJ2* overexpression significantly inhibited mitochondrial contraction in the intact dendrite compared to wildtype neurons (**Fig. 7.2D; Movie S14**). We

quantified this shape change where higher values indicate more spherical (contracted) mitochondria. *KCNJ2*-expressing neurons showed an insignificant change in mitochondrial morphology before and after injury, compared to *wildtype* controls (**Fig. 7.2E**, One-way ANOVA, Bonferroni Corrected, *wildtype* before vs *wildtype* after, $p<0.0001$****; *KCNJ2* before vs *KCNJ2* after, $p=0.0656$). To directly compare between genotypes, we observed that the fold change in mitochondrial area was significantly more in wildtype neurons compared to *KCNJ2* expressing animals (**Fig. 7.2F,** Two-tailed Mann-Whitney U test, $p<0.0001$****). However, *KCNJ2* expression did not completely abolish contraction responses, as some mitochondria still showed morphological changes.

To better understand how *KCNJ2* affects the spatial pattern of mitochondrial contraction, we

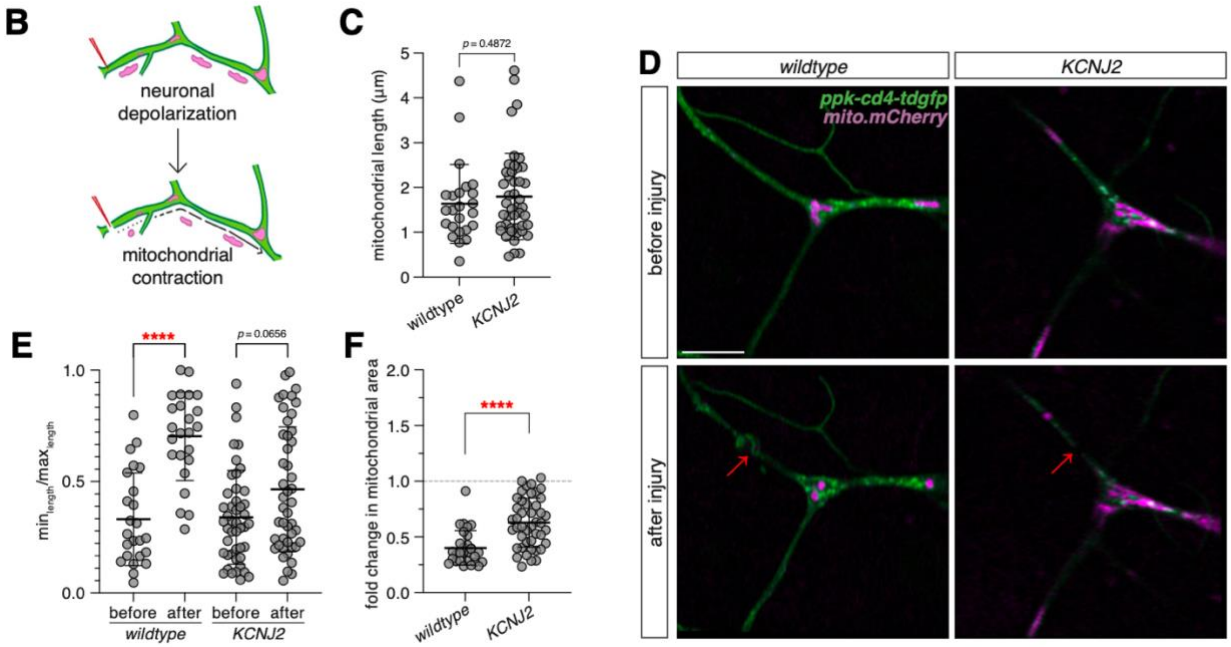

Fig. 7.2 *KCNJ2* inhibits injury induced mitochondrial contraction. ***(B)*** *Schematic of injury-induced mitochondrial contraction associated with neuronal depolarization.* ***(C)*** *Mitochondrial length before dendrotomy in wildtype vs KCNJ2-overexpressing neurons (Two-tailed Mann-Whitney U test, p=0.4872).* ***(D)*** *Representative images of neurons before (top) and after (bottom) dendrotomy (red arrow). Scale bar 5 µm.* ***(E)*** *Mitochondrial shape before and after primary dendrotomy in wildtype and KCNJ2 neurons (One-way ANOVA, Bonferroni corrected, wildtype before vs wildtype after, p<0.0001****; KCNJ2 before vs KCNJ2 after, p=0.0656).* ***(F)*** *Fold change in mitochondria area in wildtype vs KCNJ2 expressing neurons after primary dendrotomy (Two-tailed Mann-Whitney U test, p<0.0001****).*

analyzed contraction responses as a function of distance from the dendrotomy site. Even for

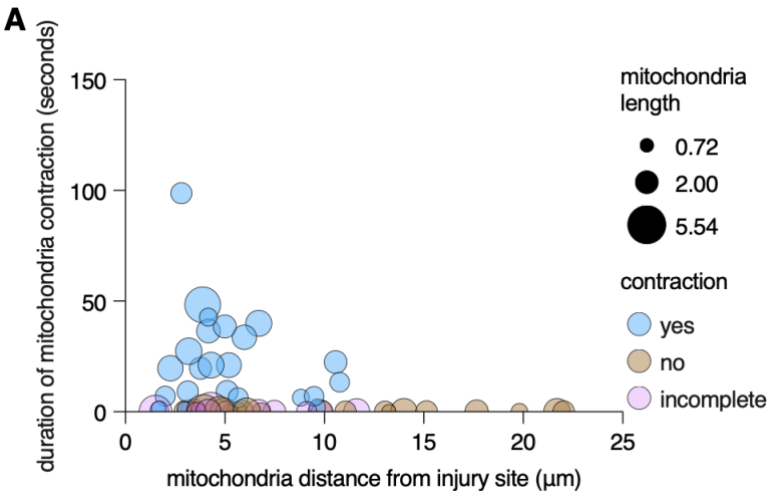

Fig. 7.3. ***KCNJ2* inhibits and prolongs mitochondrial contraction**. *(A) Mitochondrial contraction duration in relation to distance from injury site in KCNJ2 neuron after primary dendrotomy.*

mitochondria immediately adjacent to the dendrotomy site, *KCNJ2* expression increased the duration of mitochondrial contraction, suggesting that membrane hyperpolarization affects the kinetics in addition to the probability of contraction (**Fig. 7.3A; Movie S15**).

We extended our analysis to tertiary dendrotomies, which provide variable contraction responses that allow for the assessment of the relationship between contraction and repair outcomes (**Fig. 4G**). During live imaging, we observed that injury-induced mitochondrial contraction occurred stochastically in both wildtype and *KCNJ2*-expressing neurons.

To determine whether KCNJ2 affects the relationship between mitochondrial contraction and dendrite repair, we tracked the dendrite arbor before and 24 hr after tertiary dendrotomy. In both wildtype and *KCNJ2*-expressing neurons, we observed that neurons *without* contracting mitochondria showed no significant increase in branching rate (**Fig. 7.4H**, Two-tailed Welch's t test, p=0.2103) compared to their uninjured counterparts. In contrast, when mitochondria *contracted* immediately after injury, both wildtype and *KCNJ2*-expressing neurons had increased dendrite branching (**Fig. 7.4H**, Two-tailed Welch's t test, p<0.9225). This suggests that the relationship between mitochondrial contraction and enhanced branching is preserved, even when membrane potential is altered.

Lastly, *KCNJ2* expression significantly reduced the frequency of injury-induced mitochondrial contraction after tertiary dendrotomy. We observed contraction in only 17.9% of the *KCNJ2*-expressing neurons (7/39), compared to 33% of wildtype neurons (12/36) (**Fig. 7.2I; Movie S16 and Movie S17**). This reduction in contraction frequency demonstrates that membrane hyperpolarization impairs the cellular response to injury.

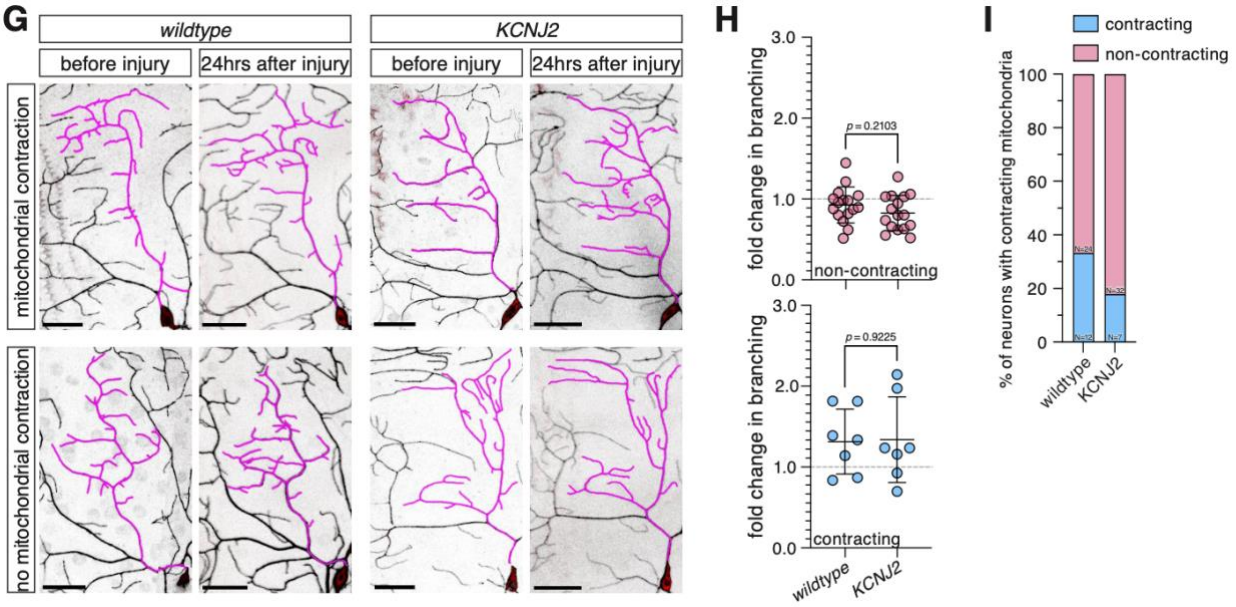

Fig. 7.4 Presence of contraction in *KCNJ2* is sufficient for injury-induced dendrite branching. ***(G)*** *Representative image of neuronal architecture of wildtype vs KCNJ2 expressing neurons before and 24 hr after injury in the presence of mitochondrial contraction (top row) vs absence (bottom row). Scale bar 25 µm, 40 µm.* ***(H)*** *Fold change in dendrite branching for neurons without contracting mitochondria (top; wildtype, N=16 vs KCNJ2, N=16, Two-tailed Welch's t test, p=0.2103) and neurons with contracting mitochondria (bottom; wildtype, N=7 vs KCNJ2, N=7, Two-tailed Welch's t test, p=0.9225) neurons after tertiary dendrotomy.* ***(I)*** *Percent of neurons that exhibited injury-induced mitochondrial contraction in wildtype (N=12 contracting, N=24 non-contracting) vs KCNJ2 (N=7 contracting, N=32 non- contracting) after tertiary dendrotomy.*

In summary, we find that KNCJ2 overexpression significantly impairs both the frequency and kinetics of injury-induced mitochondrial contraction, albeit preserving the correlation between contraction and enhanced dendrite branching. These findings suggest that normal neuronal activity is required for optimal mitochondrial responses to injury.

Previous studies have shown that injury-induced mitochondrial fragmentation is regulated through *Drp1* (*Dynamin related protein 1*)[95,220,221,227,228]. Given that Drp1 is the primary mediator of mitochondrial fission, we hypothesized that injury-induced mitochondrial contraction might also require Drp1 activity, despite the apparent contradiction between the "contraction" we observe and fission-mediated processes.

To test the role of Drp1 in mitochondrial contraction, we conducted distal primary dendrotomies in neurons expressing a GTPase-dead allele of *Drp1* (*Drp1.K38A*), containing a single amino acid residue substitution in the G1 motif in the GTPase domain[63]. As expected, *Drp1.K38A*-expressing neurons displayed dramatically altered baseline mitochondrial morphology, with hyperfused mitochondria forming a single, continuous elongated mitochondria (**Fig. 8.1A and 8.1B**). This contrasts with the mixed tubular and spherical mitochondria observed

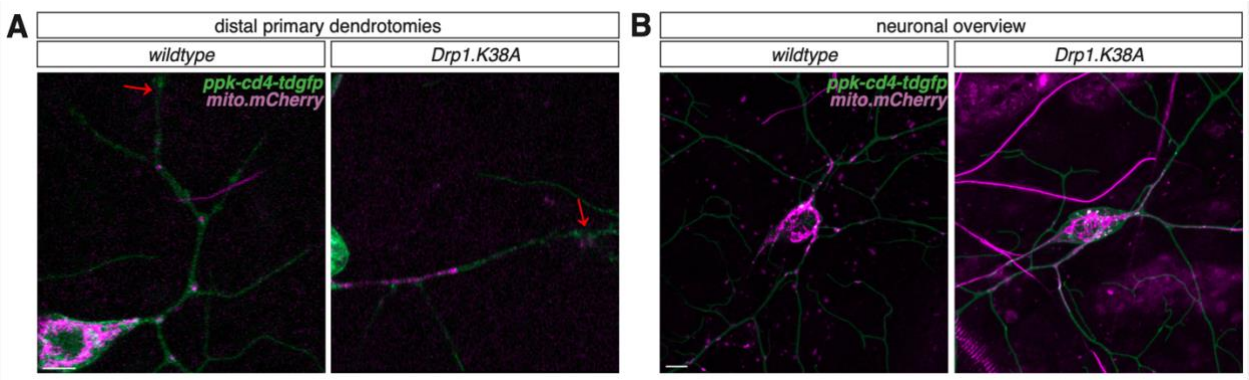

Fig. 8.1 Injury location and hyperfused mitochondria in *Drp1.K38A* neurons. *(**A**) Snapshot of wildtype vs Drp1.K38A neurons after distal primary dendrotomy (red arrow). Scale bar 5 µm. (**B**) Overview of mitochondrial network in wildtype vs Drp1.K38A expressing animals. Scale bar 5 µm.*

in wildtype neurons.

Immediately after distal primary dendrotomy, wildtype neurons showed the characteristic rapid and complete mitochondrial contraction we observed previously. In stark contrast, mitochondria in *Drp1.K38A*-expressing neurons failed to undergo complete morphological changes after injury (**Movie S18**). While some morphological alterations were observed, including

slight retraction, the overall mitochondrial network remained hyperfused retaining their elongated tubular structure rather than contracting to the spherical shapes of which we observed in wildtype neurons.

We quantified this effect by counting the number of tubular and spherical mitochondria before

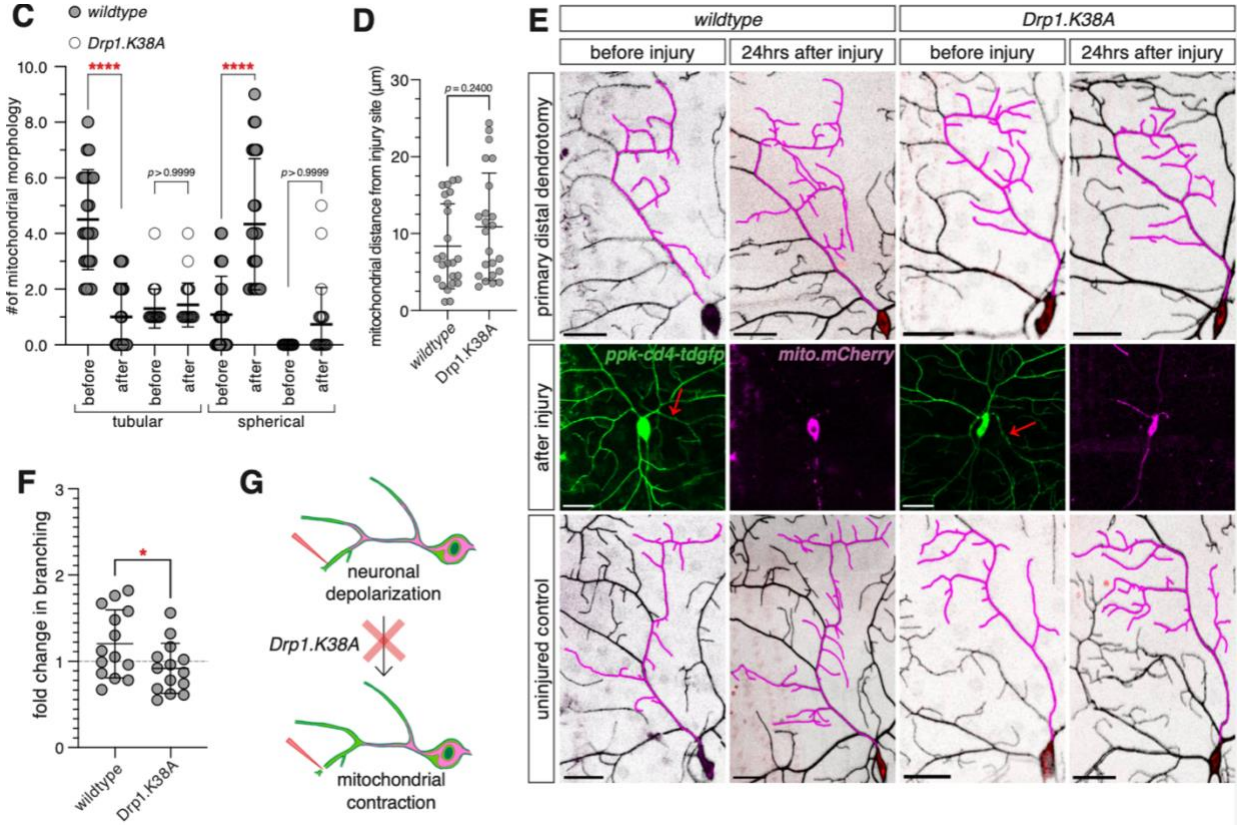

Fig. 8.2 Injury induced mitochondrial contraction and branching requires Drp1. *(**C**) Quantification of total number of tubular and spherical mitochondria before and after dendrotomy (One-way ANOVA, Bonferroni corrected, wildtype before tubular vs wildtype after tubular, p<0.0001****; wildtype before punctate vs wildtype after punctate, p<0.0001****). (**D**) Mitochondrial distance from injury site in wildtype vs Drp1.K38A neurons (Two-tailed Mann-Whitney U test, p=0.2400). (**E**) Overview of neuronal architecture before (top), immediately after (middle), and 24hr after (bottom) primary distal dendrotomy in wildtype vs Drp1.K38A expressing neurons. (**F**) Fold change in dendrite branching in wildtype (N=14) vs Drp1.K38A (N=14) neurons after distal primary dendrotomy (Two-tailed Welch's t test, p=0.0393*) (**G**) Graphical representation of inhibited mitochondrial contraction associated with Drp1.K38A overexpression.*

and after injury. *Drp1.K38A* expression significantly inhibited the injury-induced contraction compared to wildtype controls (**Fig. 8.2C**) even when mitochondria were located within the range of contraction displayed by wildtype neurons (**Fig. 8.2D**, Two-tailed Mann-Whitney U test, *p*=0.2400). This finding suggests that while we term this process "contraction", it mechanistically

requires the fission machinery typically associated with *Drp1*-mediated, injury-induced mitochondrial fragmentation.

Since *Drp1.K38A* expression inhibited injury-induced mitochondrial contraction, we assessed whether this allele would also affect injury-induced branching. We imaged dendrite arbors before injury, conducted primary dendrotomies, and reimaged the injured neuron 24 hr later (**Fig. 8.2E**). Compared to wildtype neurons, which showed increased dendrite branching after primary dendrotomy, *Drp1.K38A*-expressing neurons failed to show enhanced dendrite branching, compared to their uninjured controls (**Fig. 8.2F**, Two-tailed Welch's t test, p=0.0393*). This correlation between impaired mitochondrial morphological changes and reduced branching responses supports a potential functional relationship between these processes.

In summary, injury-induced mitochondrial changes require Drp1 (**Fig. 8.2G**), and impaired mitochondrial responses correlate with reduced dendrite branching after injury.

Previous research has shown that mitochondrial transport facilitates axon regeneration[6–8]. We next asked if there were differences in mitochondrial distribution in the regenerated dendrite architecture. To do this, we positioned the cell body of an uninjured neuron, a neuron with one dendrite removed, and a neuron with all if its dendrites removed. We quantified the mitochondrial area based on the dendrite branching order (**Fig. 9.0A**) at 24, 48, and 72 hr after injury to gain insight into the mitochondrial distribution. In uninjured neurons, mitochondrial area is most abundant in 1˚ order dendrites, followed by 2˚, and lastly 3˚ (**Fig. 9.0B-E**). Despite imaging the same neuron and field of view we never detected mitochondrial positioning identical to their previous imaging time points. Next, we examined the mitochondrial distribution of neurons after we transected a single dendrite. Interestingly, we found that mitochondria were distributed across the dendrite architecture similar to the distribution we observed in the uninjured neuron (**Fig. 9.0F-**

I). This observation was surprising because single branch injury is known to significantly upregulate dendrite branching in the remaining uninjured dendrites. Lastly, we removed all the dendrites of a single neuron. At 24 hr after injury we observed that mitochondrial distribution

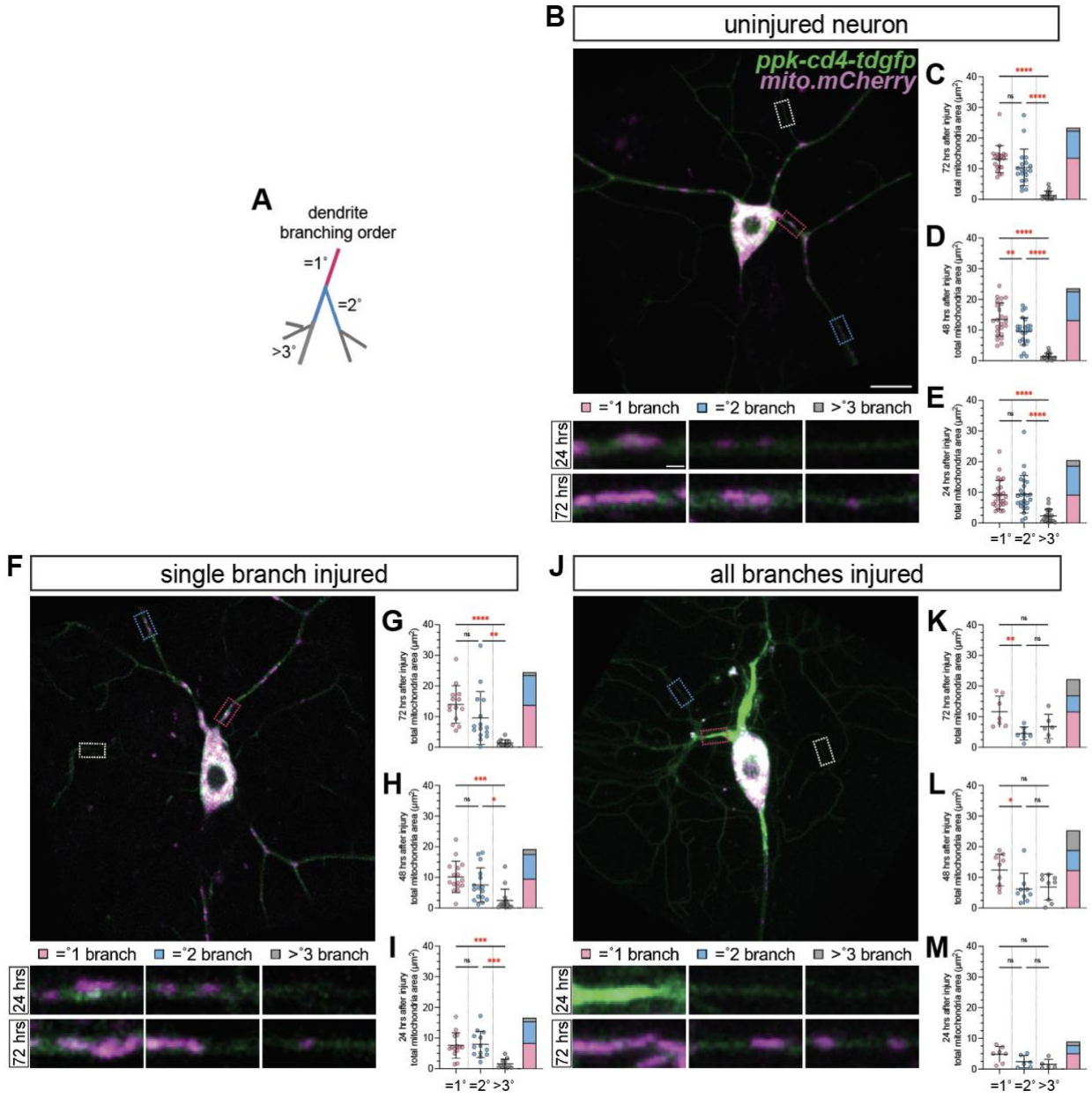

Fig. 9.0 Changes in mitochondrial distribution. *(**A**) diagram of dendrite branching order based on mitochondrial area quantification. (**B-E**) distribution of mitochondria in uninjured neuron across 24, 48, 72hr after. (**F-I**) Distribution of mitochondria area after SBI. (**J-M**) Distribution of mitochondrial area after removal of all dendrites. Uninjured, N=25; single branch injury, N=18; all branches injured N=10. One-way ANOVA Bonferroni corrected.*

remained evenly distributed across 1˚, 2˚, and 3˚ order dendrite branches (**Fig. 9.0J-M**). At 48 and 72hr after regeneration we began observing a shift in dendrite distribution. In the uninjured neuron and after single branch injury, mitochondria are primarily distributed into 1˚ then 2˚ order dendrites. However, we observed that removing all dendrites of a given neuron causes preferential mitochondrial distribution into >3˚ branches (**Fig 9.0K**).

Interestingly, even though single branch dendrotomy is known to induce a significant amount of dendrite branching in preserved dendrites, there was no shift in mitochondrial distribution. These data that mitochondrial distribution is consistent in uninjured and single branch injured neurons suggests that mitochondrial trafficking is not the primary driver of injury induced dendrite branching.

Discussion

While the role of mitochondrial injury signaling and repair is well established across many cell types, their specific function in neuronal injury signaling and repair has yet to be elucidated, specifically in dendrites. Using our model organism's capacity for longitudinal imaging, we monitored how mitochondria respond in real-time during dendrotomy (dendrite injury) and tracked the same neurons through the repair process. Our findings reveal several key insights into the spatiotemporal dynamics of injury-induced changes in mitochondrial morphology and their relationship with dendrite repair following dendrotomy.

First, mitochondrial contraction follows predictable spatial rules that differ between intact and severed dendrite segments. In the proximal intact dendrite, both the timing and duration of mitochondrial contraction depend on distance from the dendrotomy site, with closer mitochondria responding more rapidly and completely. In contrast, within the severed dendrite segment, only

the initiation of contraction is distance dependent. These distinct patterns suggest that different mechanisms may operate in intact versus severed dendrite branches, possibly reflecting differences in calcium dynamics, ATP availability, membrane potential, or other injury-related signals.

We demonstrate that different types of dendrite injuries elicit proportional mitochondrial responses. Primary dendrotomies, which sever major dendrite branches, consistently induce robust and rapid mitochondrial contraction. Tertiary dendrotomies which affect smaller branches produce variable and delayed contraction responses. At equivalent distances from the injury site, a tertiary dendrotomy produces a delayed time to full contraction. Interestingly, injury-induced mitochondrial contraction seemed to be an irreversible response (**Movie S19**), even when we increased the imaging duration (~30mins post injury, although mitochondria bleached at ~15mins of continuous imaging). Since changes in mitochondrial morphology is known to affect mitochondrial distribution (i.e. dense and punctate vs sparse and tubular[113,157,276]), one speculative explanation is that injury-induced mitochondrial contraction preserves mitochondrial integrity, preventing the apoptotic signaling cascade[277].

Our KCNJ2 experiments demonstrate that inhibiting membrane depolarization significantly impairs injury-induced mitochondrial contraction. This finding connects mitochondrial injury responses to membrane potential and suggests that voltage-dependent processes, potentially those involving calcium signaling, are required for robust mitochondrial morphological changes. Even when mitochondrial contraction was suppressed by expression of KCNJ2, the escaper neurons that did show contraction still exhibited enhanced dendritic branching, indicating that the relationship between mitochondrial morphological changes and repair outcomes is preserved. This supports the hypothesis that depolarization is important for mitochondrial contraction, and that mitochondrial contraction then serves as a component of repair activation. Future studies could

test whether reducing KCNJ2 activity enhances mitochondrial contraction and examine how enhanced contraction affects dendrite repair outcomes.

To better understand if the mitochondrial fission machinery was involved in injury induced mitochondrial contraction, we overexpressed a dominant negative version of *Drp1* (*Drp1.K38A*). Surprisingly, we observed that the GTPase dead allele of *Drp1* significantly prevented mitochondria from contracting completely after injury. Moreover, inhibiting injury-induced mitochondrial contraction abrogated the increased dendrite branching observed in wildtype counterparts. Our findings are supported by previous studies demonstrating that injury induces immediate changes in mitochondrial morphology in the epidermis, MEFs, HeLa, HEK293t, c2c12[21,97,225,278,279]. The dramatic baseline alterations in mitochondrial morphology caused by Drp1.K38A expression should be kept in mind when determining specific effects on injury responses versus general mitochondrial dysfunction. The precise relationship between fission and contraction, both of which require Drp1, requires further study. Several mechanisms could mediate injury-induced mitochondrial morphological changes, including loss of mitochondrial membrane potential, opening of the mitochondrial permeability transition pore as suggested by previous studies, inhibition of mitochondrial fusion machinery, or activation of fission machinery through post-translational modifications. Future studies should systematically test these possibilities using targeted pharmacological and genetic approaches, especially inducible or conditional Drp1 inhibition. Together our findings suggest that mitochondrial contraction may act as a critical trigger for dendrites to initiate repair and not a byproduct of injury. Drp1 may be required for the dynamic restructuring of mitochondrial networks that enables morphological plasticity in response to injury signals.

Cellular repair is strongly influenced by the magnitude of injury: severe damage often leads to

cell death, whereas milder injuries can elicit adaptive responses. In this study, we observed that mitochondria undergo immediate contraction following dendrotomy, and the extent of this contraction scales with injury severity (primary vs. tertiary dendrotomy). Our findings are consistent with previous work in live mouse axons, where electrical nerve stimulation and, more severely, axotomy, induced distance-dependent mitochondrial contraction[230]. We built upon this established framework by tracking individual neuronal responses and the consequences of dendrite repair. Future studies could build upon our findings to determine whether mitochondrial contraction serves as a direct trigger for regenerative programs or reflects a broader cellular adaptation to injury.

The terminology used to describe injury-induced mitochondrial morphological changes has varied across studies, reflecting both the complexity of these processes and differences in experimental approaches. We chose the term "mitochondrial contraction" based on our observation of reduced mitochondrial length and increased circularity without an obligate increase in mitochondrial number. This distinguishes our observations from classical mitochondrial fission, which results in an increase in mitochondrial number, or from mitochondrial swelling, which involves increased mitochondrial volume. The requirement for Drp1, a fission protein, in our contraction process suggests that these morphological changes involve more complex remodeling than simple physical contraction. The diversity in terminology, also including fragmentation or rounding, likely reflects the fact that injury-induced mitochondrial responses involve coordinated changes in both fission and fusion machinery, resulting in morphological changes that do not neatly fit into traditional categories. Future studies will be required for a more precise understanding of the relationship between these processes.

Although the structural changes in mitochondrial morphology (i.e. rounding, shortening,

swelling, fragmentation, contraction) following disruptions in cell homeostasis[21,224,228,280–282] are well established, the mechanisms governing these responses are only partially understood. In neurons, the fact that mitochondria contract in both the axon and dendrites highlights the conserved nature of injury-induced mitochondrial remodeling[228]. Our findings that *KCNJ2* or *Drp1.K38A* both suppress injury-induced mitochondrial contraction provides insight into previous literature; previous reports have shown that expressing *KCNJ2*[283] or *Drp1.K38A*[284] prevents cell death after injury. Whether KCNJ2 is involved in regulating injury-induced changes in mitochondrial morphology has yet to be elucidated until now. Future studies should determine whether *KCNJ2* and the *Drp1* converge on a single molecular pathway or diverge.

The correlation between mitochondrial contraction and enhanced dendrite branching across multiple experimental conditions suggests a functional relationship between these processes. Several mechanisms could explain this relationship. Mitochondrial morphological changes may alter local ATP production or calcium buffering, creating metabolic conditions that favor growth. Contracted mitochondria may produce different levels of reactive oxygen species, which can serve as signaling molecules for repair programs. Mitochondrial morphological changes may affect the subcellular distribution of mitochondria, concentrating metabolic resources near repair sites. Even though the function of *Drp1* is well studied, it remains puzzling how its removal can both promote cell survival[228,278,285] and inhibit regeneration[7,21,95]. The process of mitochondrial remodeling itself may activate signaling cascades that promote repair.

Downstream of morphological changes in mitochondria are mtROS (mitochondrial reactive oxygen species). Previous studies have shown that mtROS become upregulated in response to cell injury across various tissues[9,97,98,253,286,287]. Similarly, mtROS is upregulated as a consequence of neuronal activity[153,288] caused by spreading depolarization[230,289]. Lastly, axotomy induced

mitochondrial contraction has been shown to stimulate mtROS production[230]. Whether mtROS functions downstream of mitochondrial contraction after dendrotomy and potentially a primary driver of dendrite repair remains an open question. Whether injury-induced mitochondrial contraction is directly linked to the repair process requires further investigation.

Collectively our findings contribute to a growing understanding of mitochondria as dynamic signaling organelles that respond to and coordinate cellular stress responses. We describe injury-induced changes in mitochondrial morphology which scales with injury severity and proximity, requires normal membrane potential and mitochondrial fission machinery, and correlates with enhanced dendrite branching after injury. These findings highlight an intricate relationship between mitochondrial dynamics and dendrite repair, emphasizing mitochondrial contraction as a potential mediator of injury-induced repair and the need for further investigation into the molecular mechanisms that govern this process.

Chapter 4

Structural and Functional Plasticity

Introduction

Public health organizations estimated that the annual cost of neurological disorders (consisting of 21 brain related disorders) costs approximately ~1.13 trillion dollars globally in 2019 and has since then projected to increase by 3.3-3.5% annually (citation).

Neuronal development, on a structural level, is a tightly regulated process orchestrated by a balance between neurite extension, retraction, and stabilization. Long range neurite guidance is facilitated through robust regulators like chemo-attractant and -repellent cues. These chemotactic cues ensure that neurites can accurately transverse long distances (teneurin, leukokinin, netrins) while simultaneously being repelled from improper partners[290–293]. In addition to these robust regulators, transcription factors and neuronal activity permit the extension and retraction of neurites to further refine the neuron's architecture in development. However, neuronal plasticity is not uniform across the organism's lifespan. In early stages of development, neurons are highly dynamic. For example, in the immature frog optic tectum, dendrites rapidly remodel to refine circuits in development[294]. In the hippocampus of young mice, dendritic filopodia are abundant

and highly dynamic, serving as intermediates before becoming stabilized spines[295]. Structural dynamics shift in aging and the probability of spine stabilization increases, but overall structural remodeling is reduced[296]. Diminished structural dynamics correlates with age-related declines in learning and memory. Intriguingly, age-related memory defects can be rescued in aged mice by knocking out HDAC3 (Histone deacetylase 3), a negative regulator of gene expression[297,298]. These functional changes are accompanied by molecular mechanisms which specify neural fate during progenitor states to functional refinements of postmitotic entities.

One mechanism that regulates neuroplasticity is the ATP-dependent chromatin remodeling complex SWI/SNF (SWI/Sucrose Non-Fermentable), which controls development by regulating nucleosome positioning, DNA accessibility, and transcription. SWI/SNF was first identified in yeast, and its mammalian homolog BAF (BRG1/BRM-associated factor) has been crucial for identifying regulators of neuronal development and function. The mammalian BAF complex is composed of a ~15 submodules encoded by 29 genes consisting of a core base, ATP subunit, and ARP (actin related protein) adaptors[299,300]. Whilst the functions of each subunit have been widely conserved in evolution, many of these subunits have adapted additional functions, crucial for regulating cell homeostasis. For example, *Arp7* and *Arp9* (*actin related proteins 7, -9*) in yeast are homologous to mammalian *Baf53a* and *Baf53b;* however, the mammalian orthologs have likely evolved additional functions, as they are expressed exclusively in neurons and during different developmental stages.

Although Baf53a and Baf53b share nearly identical sequences, the variation in amino acids further confers functional specificity. In neural progenitors, Baf53a is expressed, but is substituted for Baf53b. This switch is mediated by miRNA-9 and -124 binding to the Baf53a transcript, inhibiting its translation, and lifting the repression of Baf53b. This molecular switch is necessary

and sufficient to convert human fibroblasts into neurons[301–303].

The function of Baf53b is critical for activity dependent dendrite outgrowth, and its removal severely impairs dendrite outgrowth after neuronal stimulation[304]. More recently, neuronal activity has shown to stabilize the BAF complex, directly inducing its phosphorylation[305]. This activity-dependent modulation links chromatin remodeling to activity-dependent plasticity, providing a framework for how neurons couple inputs with structural and functional changes at the molecular and cellular level.

Consistent with this epigenetic regulation, Baf53b itself is critical for regulating learning and memory. Loss of subdomain 2 in Baf53b (ΔSB2, one of the domains that is not conserved in Baf53a) impairs long-term potentiation (LTP), a benchmark for learning and memory. Normally, LTP induces phosphorylation of the actin regulator cofilin, but this process is lost in ΔSB2 mutants. Furthermore, expression of a phosphomimetic cofilin restores both LTP and learning and memory in Baf53b mutant mice[306]. Another critical domain of Baf53b is the hydrophobic domain, which enables protein-protein interactions with other nBAF subunits and deletion of this domain acts as a dominant negative [307]. These findings highlight the divergent mechanisms that regulate structural development and neuronal function providing evidence that the molecular switch is crucial for cell function.

The importance of the BAF subunits has been demonstrated across various model organisms. In Drosophila, the ortholog *Bap55* (encodes for Baf53a, and -53b) is required for proper neuronal outgrowth. Loss of Bap55 results in abnormal dendrite patterning in class I multidendritic dendritic arborization (md-da) neurons and improper partner targeting in olfactory glomeruli[308,309]. Interestingly, the routing defects observed in *Bap55* mutants can be rescued by overexpressing wildtype *Bap55*, or mammalian orthologs *Baf53a* or *Baf53b*. Notably, Baf53b provides a more

complete rescue, suggesting that these subunits confer distinct functional capacities in neuronal development. While drosophila only have one homolog of Baf53, one possible explanation is the divergent complexity in lower vs higher eukaryotes.

In Chapter 5, I will review experiments I conducted in an attempt to untangle how structural plasticity (dendrite regeneration, in flies) relates to functional plasticity (learning and memory, in mice). To do this, I overexpressed functional learning and memory genes and assessed dendrite regeneration. The rationale for using this pipeline is based on the premise that neuronal structure and function are highly linked, and functional remodeling of dendrites and synapses is similar to the structural remodeling during dendrite regeneration. I tested how ApoE4 (apolipoprotein E, gene associated with increased risk of developing Alzheimer's disease) overexpression affected dendrite regeneration. The rationale for testing ApoE4 is that Alzheimer's disease is associated structural and functional impairments, and that these structural impairments can be recapitulated during dendrite regeneration in flies. Furthermore, I tracked and characterized dendrite development and regeneration using in vivo time lapse imaging. The rationale for tracking dendrite regeneration and development is based on the fact the fact that dendrites regrow with self-crossing defects and by observing the growth process, we can identify when/which processes become awry. Lastly, I tested dendrite regeneration in flies overexpressing various components of the Baf complex. The rationale for testing Baf is based on the premise that the Baf subunits (specifically Baf53b) is required for learning and memory in mice (functional plasticity), and that its overexpression would increase structural remodeling during dendrite regeneration.

Results

Investigating dendrite regeneration in genes involved in learning and memory in mice

HDACs (known as histone deacetylases) are a group of enzymes that control gene expression on the DNA level, by removing acetyl groups located on histones, causing chromatin compaction, and physically reducing accessibility of pol II to initiate transcription. HDAC3 has been shown to be a negative regulator of learning and memory, and its knockout rescues age-related learning impairments in mice[298]. We tested how overexpression of the dominant negative allele or wildtype

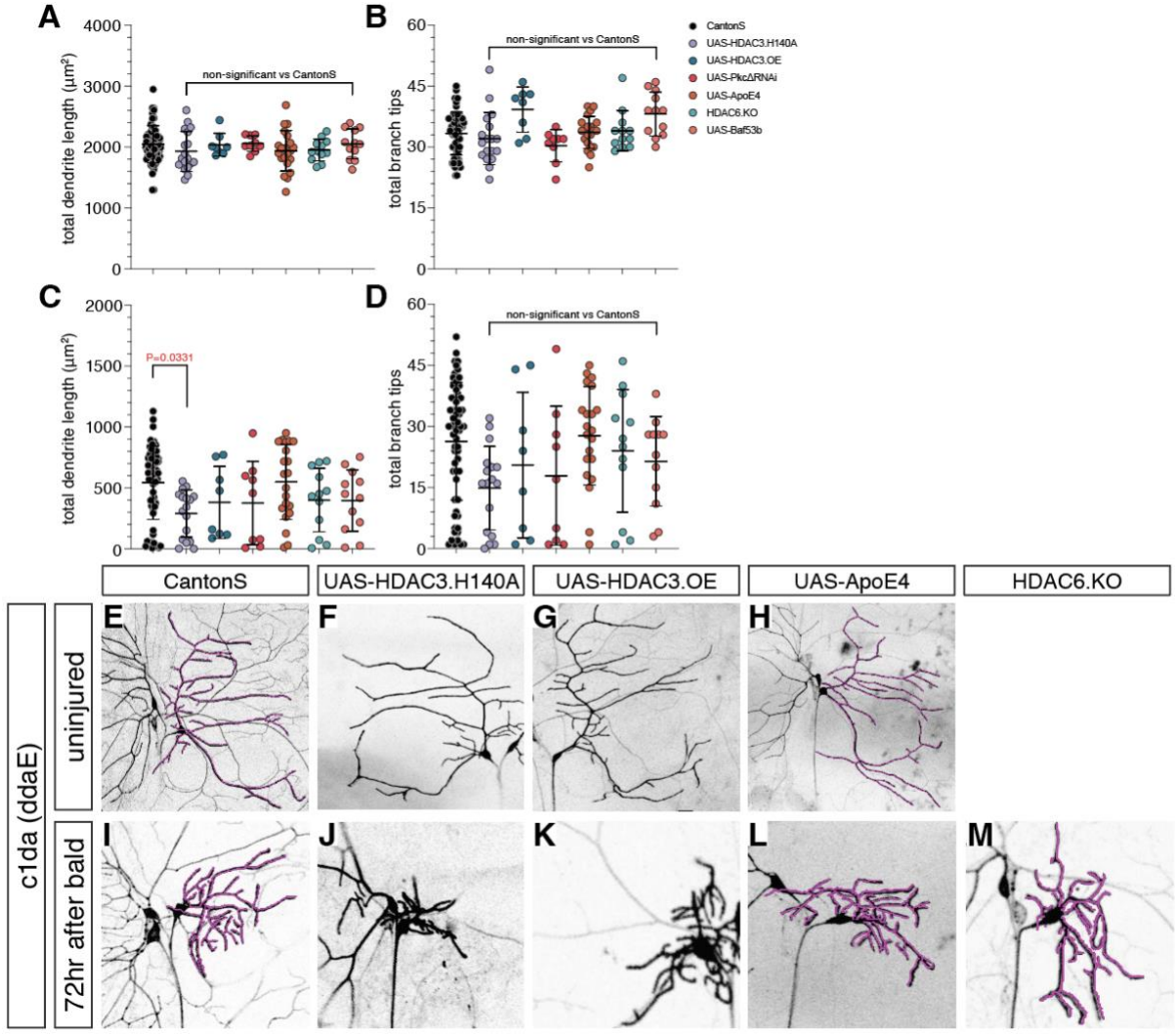

Fig. 10.1 Exploring how genes involved in learning and memory affect dendrite regeneration. ***(A-B)*** *Quantification of total* ***(A)*** *dendrite length and* ***(B)*** *total branch tips uninjured neurons.* ***(C-D)*** *Quantification of total* ***(C)*** *dendrite length (CantonS vs HDAC3.H140A, p=0.0331*) and* ***(D)*** *total branch tips injured neurons. All comparisons above are. One-way ANOVA, Bonferroni corrected.* ***(E-H)*** *Uninjured neurons* ***(E)*** *wildtype* ***(F)*** *UAS-HDAC3.H140A* ***(G)*** *UAS-HDAC3.OE* ***(H)*** *UAS-ApoE4 neurons 72hr after egg lay + 72hr after injury.* ***(I-M)*** *Balded neurons* ***(I)*** *wildtype* ***(J)*** *UAS-HDAC3.H140A* ***(K)*** *UAS-HDAC3.OE* ***(L)*** *UAS-ApoE4* ***(M)*** *HDAC6.KO neurons 72hr after egg lay + 72hr after injury. wildtype N=61, HDAC3.H140A N=18, HDAC3.OE N=8, PKCΔRNAi N=9, ApoE4 N=21, HDAC6.KO N=12, Baf53b N=12*

HDAC3 affected dendrite regeneration (**Fig. 10.1F, J; G, K**). HDAC6 interacts with microtubule proteins and is the main α-tubulin deacetylase. Loss of HDAC6 has been shown to increase acetylated α-tubulin, which creates stable microtubules, and enhances axon[310]. Whether HDAC6 exerts similar effects in dendrite regeneration has not been investigated until our work (**Fig. 10.1M**). Another gene we investigated was *ApoE* (*Apoliprotein ε*), which encodes for the lipid specific transporter important for regulating cholesterol metabolism. Primate specific isoforms of *ApoE* emerged through evolution and is known to decrease (*ApoE2*) and increase (*ApoE4*) the risk of developing Alzheimer's disease. To better understand how *ApoE4*, the disease-risk human specific isoform, affects structural plasticity under stress, we tested dendrite regeneration in animals expressing this isoform (**Fig. 10.1 H, L**). Despite how all the genes we tested were associated with learning and memory, their overexpression did not impact developmental patterning of dendrites measured by total dendrite length and branch tips (**Fig. 10.1A, B**).

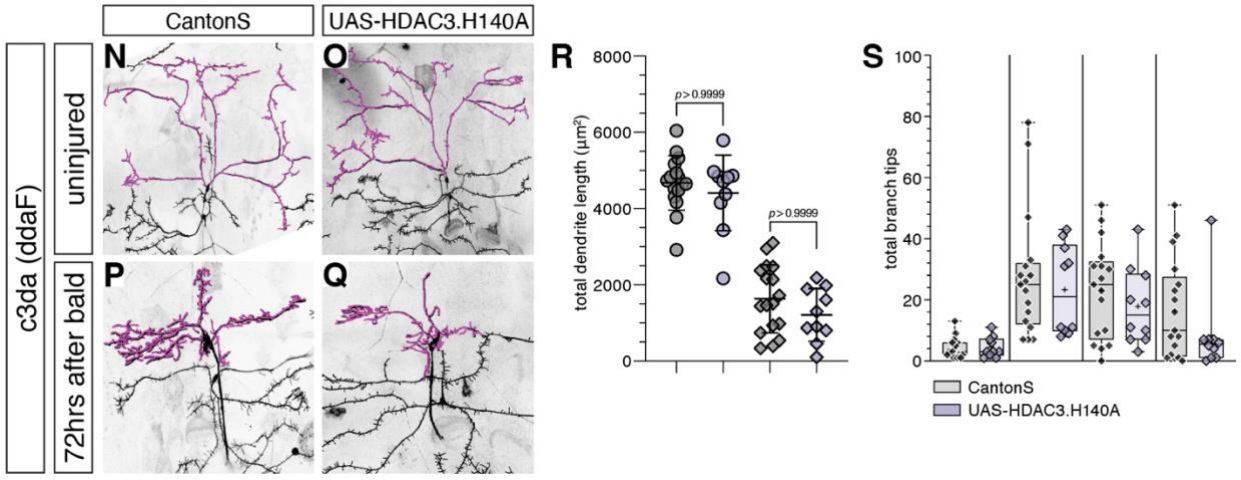

Fig. 10.2 HDAC3.H140 does not inhibit dendrite regeneration in neurons with an actin rich cytoskeleton. *(**N-O**) Uninjured (**N**) Wildtype (**O**) HDAC3.H140A neurons 72hr AEL + 72hr after injury (**P-Q**) Injured (**P**) Wildtype (**Q**) HDAC3.H140A neurons 72hr AEL + 72hr after injury. (**R**) Total dendrite in wildtype vs H140A neurons in development (circles) vs injury (diamonds). One-way ANOVA, Bonferroni corrected. (**S**) Total dendrite branch tips separated by dendrite branching order (1˚–4˚ branching order from left to right). wildtype N=17, HDAC3.H140A N=10*

Unexpectedly, HDAC3.H140A overexpression impaired the total dendrite length regenerated but not branch tips (**Fig. 10.1C, D**).

To determine if HDAC3.H140A impaired dendrite regeneration in a different class of neuron, whose dendrite branches are primarily actin based instead of microtubule based, we overexpressed this allele in class III ddaF neurons (**Fig. 10.2N-Q**). Interestingly, the impaired dendrite regeneration we initially observed in class I neurons was no longer present in class III neurons (**Fig. 10.2R, S**). These results suggest the loss of HDAC3 may inhibit microtubule-based growth mechanisms.

Proof of concept: SWI/SNF subunits Baf53b enhances dendrite regeneration

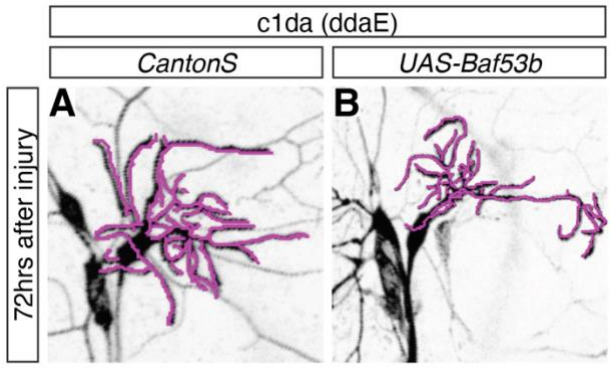

Fig. 10.3 Baf53b overexpression does not enhance dendrite regeneration in highly stable neurons. (**A**) wildtype neurons (**B**) Baf53b expressing neuron 72hr AEL + 72hr after injury

Of the genes we tested, we predicted that overexpression of *Baf53b* would significantly enhance total dendrite length and total branch tips because of its well-established role in learning and memory[306,311]. Surprisingly, *Baf53b* overexpression did not increase total dendrite length or total branch tips in ddaE neurons (**Fig. 10.1C, D; 10.3A, B**). Notably, c1da neurons are highly stable and their dendrite architectures are fully developed by 18hr of AEL. Because of these unexpected results, we reasoned neuronal plasticity cannot be *enabled* per se, but requires neurons to have some degree of innate plasticity. To test this idea, we turned to c4da ddaC neurons, as these dendrite architectures are incredibly dynamic, constantly extending and retracting throughout the entirety of larval development.

Baf53a, Baf53b, and Bap55 attenuate self-crossing defects in dendrite regeneration

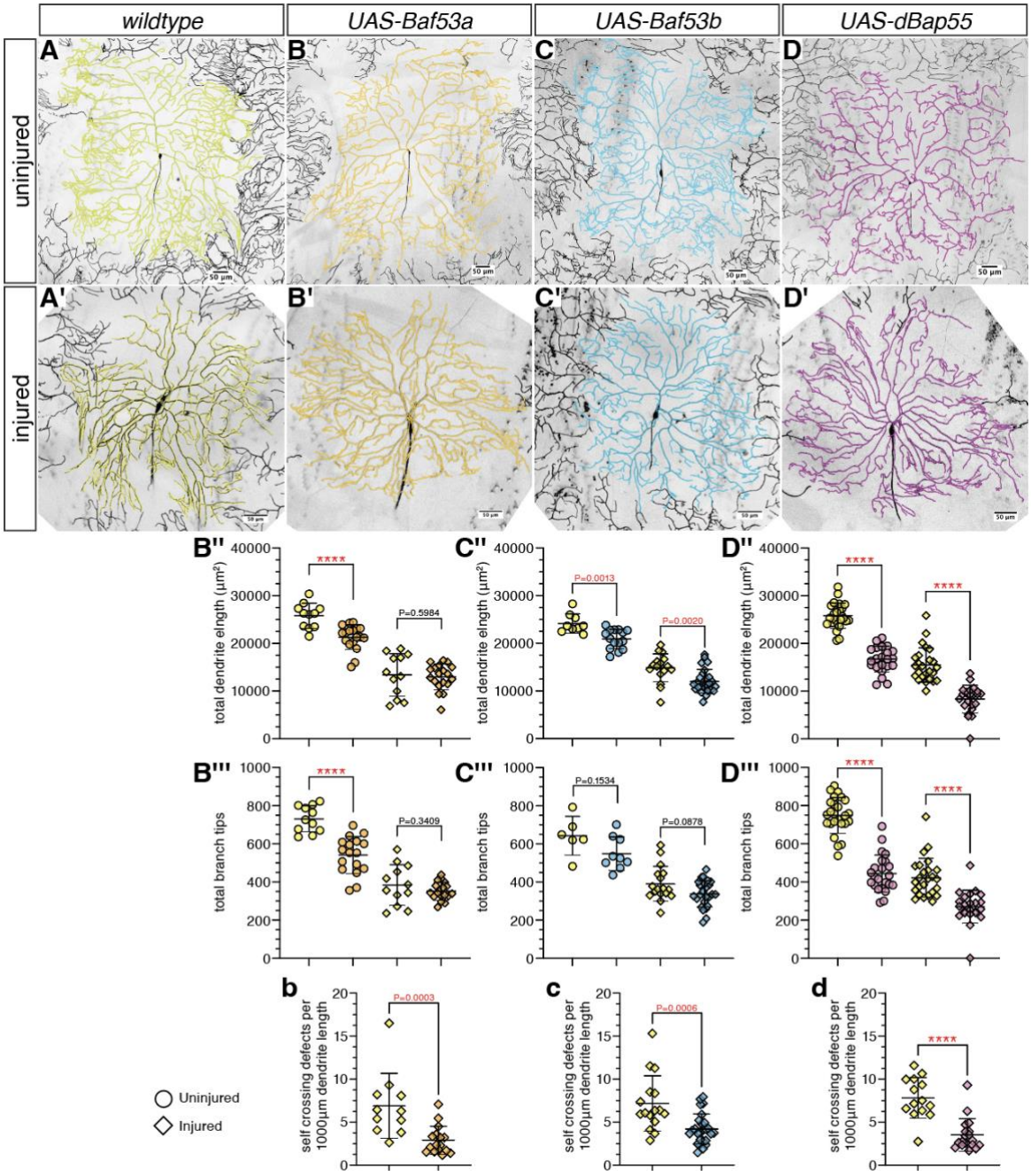

Fig. 11.0 Baf53a, Baf53b, and Bap55 ameliorate self-crossing in ddaC dendrite regeneration. ***(A-D)*** *(**A-D**) Uninjured neurons 72hr AEL + 72hr after injury (**A**) wildtype (**B**)UAS-Baf53a (**C**) UAS-Baf53b (**D**) UAS-dBap55 (**A'-D'**) Injured neurons 72hr AEL + 72hr after injury (**A'**) wildtype (**B'**) UAS-Baf53a (**C'**) UAS-Baf53b (**D'**) UAS-dBap55 (**B''-D''**) Total dendrite length and (**B'''-D'''**) Total branch tips 72hr AEL + 72hr after injury (**B''-B''',b**) Baf53a vs wildtype (**C''-C''',c**) Baf53b vs wildtype (**D''-D''',d**) dBap55 vs wildtype. Quantification of total dendrite length 72hr after injury. One-way ANOVA, Bonferroni corrected. (**b-d**) self-crossing defects per 1000µm. Mann-Whitney U test. Baf53a N=16, WT=11; Baf53b N=26 WT=16, Bap55 N=18, W=14;*

To test the effects of the different *Baf/Bap* orthologs in repair we overexpressed Baf53a, Baf53b, or dBap55 in a cell type specific manner (**Fig 11.0A-D**). To our surprise, all Baf orthologs

decreased total dendrite length during development, but only *Baf53a* and the drosophila ortholog *dBap55* decreased the total branch tips during development. Surprisingly, *dBap55* overexpression decreased the total dendrite length and total branch tips during dendrite regeneration (**Fig. 11.0 D''-D'''**) while *Baf53b* overexpression decreased the total dendrite length (**Fig. 11.0C''-C'''**). Shockingly, *Baf53a* did not affect regenerative capacity compared to wildtype neurons (**Fig. 11.0B''-B'''**). While all overexpression of any of the three orthologs had some effect on dendrite development (either total dendrite length or branch tips) they all ameliorated self-crossing defects that is typically abundant in wildtype regenerating neurons (**Fig. 11.0 b-d**). These findings provide novel insight in nucleosome remodeling during dendrite regeneration. Unsurprisingly, the developmental phenotype we observe in *Baf53a* expressing neurons is consistent with its role in mammalian development, where it is swapped for *Baf53b* in postmitotic neurons. My findings are consistent with *Baf53a*'s role in development, and its function in postmitotic neurons. *Baf53a* overexpression affects development but not regeneration, *Baf53b* overexpression affects development slightly, but exhibits pressure during dendrite regeneration (consistent with its role in postmitotic neurons), and lastly, because drosophila only have one ortholog of *dBap55* (functioning in pre- and postmitotic neurons), overexpression severely affects both development and regeneration.

Dendrite extension and retraction is increased during regeneration

Neurons achieve their final architecture through branching on the dendrite shaft (known as interstitial branching) or by splitting at the tip of the dendrite (known as forking). Extension and retraction of dendrites critically governs the final architecture of the neuron and defects in

morphogens[312–314] and cell adhesion molecules result in abnormal dendrite dynamics. Furthermore, dendrite regeneration is imperfect; when dendrites regrow their architectures, they

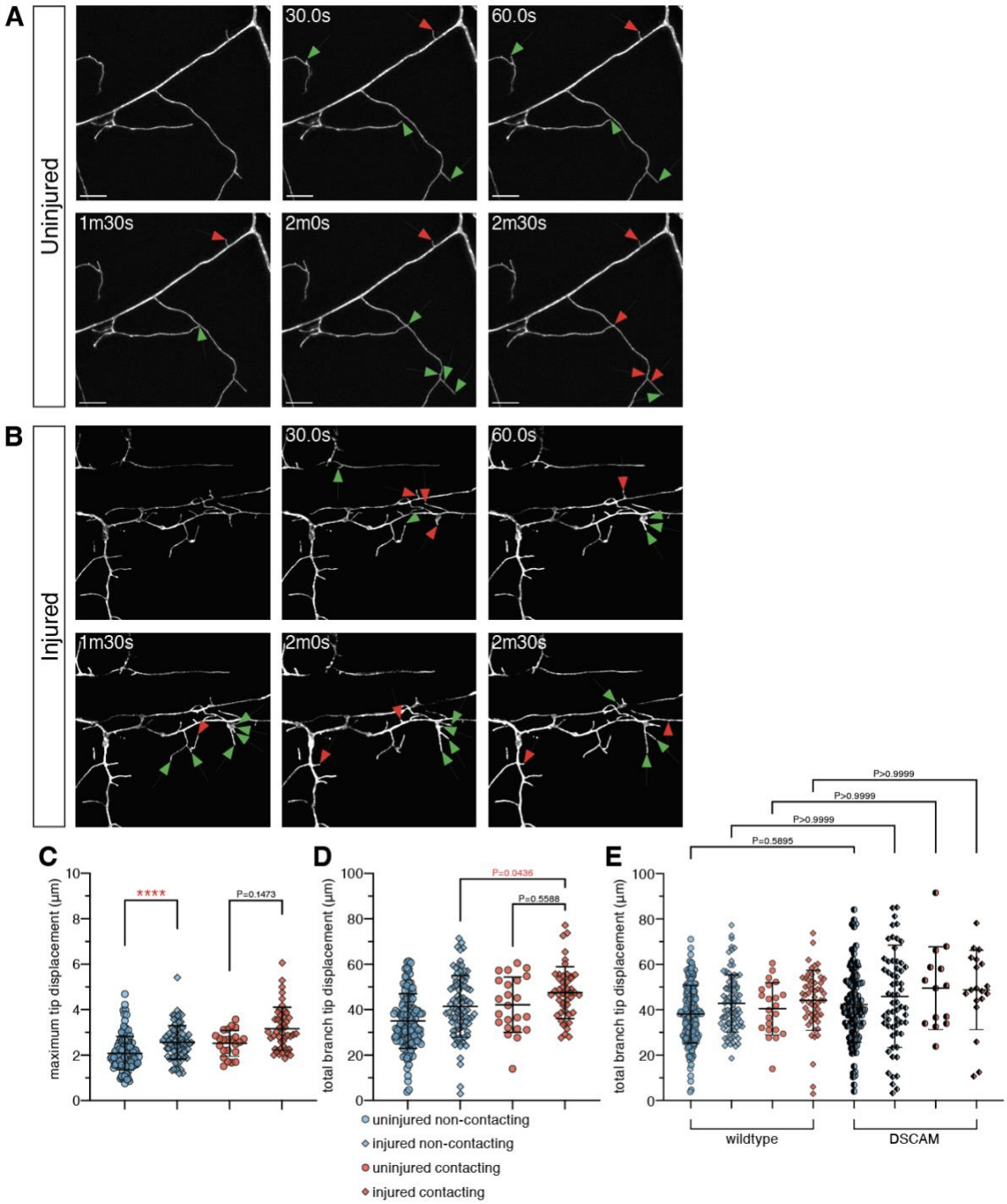

Fig. 12.0 Time lapse imaging of dendrite during development and regeneration. *(**A-B**) Time lapse imaging of 72hr AEL + 24hr after injury of neurons acquired every minute (**A**) Uninjured (**B**) Injured (balded). (**C**) Maximal tip displacement between any given dendrite between each minute. (**D**) Total branch displacement during the imaging interval. (**E**) Total branch displacement in WT vs DSCAM neurons. One-way ANOVA, Bonferroni corrected.*

have a significant amount of self-avoidance defects. Since dendrite patterning is achieved through extension and retraction, we performed time lapse imaging of neurons during development and regeneration (**Fig. 11.0 A, B**). Interestingly, we found that in damaged regenerating neurons, dendrites extend and retract more than uninjured neurons (**Fig 11.0 D**) and transverse greater distances when in motion (**Fig. 11.0 C**). These increased dynamics were especially evident in neurons that were permitted to grow in the absence of self-avoidance cues. Whether the increase in maximum tip displacement in regrowing dendrites resulted in a significant loss or increase in dendrite length begs further characterization of regenerating dendrites. Lastly, we conducted time lapse imaging of developing and regenerating *Dscam1* (*down syndrome cell adhesion molecule 1*) neurons, because *Dscam1* overexpression has been shown to ameliorate self-crossing defects in regenerating dendrites. Interestingly, when we examined the maximum distances moved in dscam1 compared to wildtype neurons, we found that there were no significant differences in how much dendrites moved in total, but we did find a slightly, insignificant decrease in total tip displacement in the injured contacting condition, providing insight into how *dscam1* may ameliorate self-crossing defects in repair (**Fig. 11.0 E**).

Neuronal scaffolding during regeneration

Some of the earliest work by Lugaro[315] demonstrated the importance of extracellular cues in regulating axon repair. In the presence of a synaptic partner, axons have the innate ability to grow towards the severed axon. However, when the axon is physically obstructed from reinnervating its previous synaptic partner, axons are incapable of regeneration. Research in 1980 and 1981 showed that CNS axonal graft into the PNS increased regenerated axon diameter[316] and length of regrowth[317]. An alternative approach to grafting neurons obtained from the CNS into the PNS is

to develop biocompatible implants that can mimic the effects of CNS grafts.

Biocompatible implants are a promising avenue which utilizes polymer meshes to deliver neurotrophic factors or electrically stimulate the endogenous tissue to trigger its release. These trophic factors are known to provide directional cues for cell growth[318] and serve as physical scaffolds[319]. In the 2D surface neurites grow stochastically. However, in 3D nanogrids, neurites extend into the microgrooves and align their protrusions into physical channels[320,321]. Much of the field of biomedical engineering has focused on developing implantable conduits that release growth factors in a controlled manner to facilitate repair, in non-human primates[322]. In addition to secreted factors, biocompatible electrodes are a promising alternative. This alternative approach uses a nano mesh which houses a grid of tiny electrodes, capable of delivery electrical currents controlled by the user. These implantable electrodes stimulate currents which upregulate the release of endogenously expressed growth factors in the intact surrounding tissue microenvironment, thus facilitating repair[323–326]. While these implantable approaches have widely yielded positive results in animal models, a major obstacle is that biomedical implants are highly invasive, and repair is limited due to variability in trauma presented in the clinic.

One outstanding question in the field of neuronal regeneration at the single cell level is whether axon and/or dendrites regenerate independently of other preexisting structures. It has always been assumed that dendrites regenerate independently of one another; however, this question has yet to be addressed. Drosophila c3da and c4da dendrites highly overlap during development (**Fig. 12.0 A**). Furthermore, c4da neurons are known to space fill empty territory in a non-redundant manner, which suggests that c4da neurons can sense dendritic territories occupied by other classes of md-da[265]. To test whether dendrites regenerate independently of one another, we labeled class III and class IV neurons, and conducted various injuries. These conditions included: 1) ablating ddaC

(c4da) and balding (**Fig. 12.0 B**) (removing all dendrites) ddaF (c3da); 2) ablating ddaF and balding ddaC, (**Fig. 12.0 C**) and 3) preserving all dendrites of ddaC while balding ddaF (**Fig. 12.0**

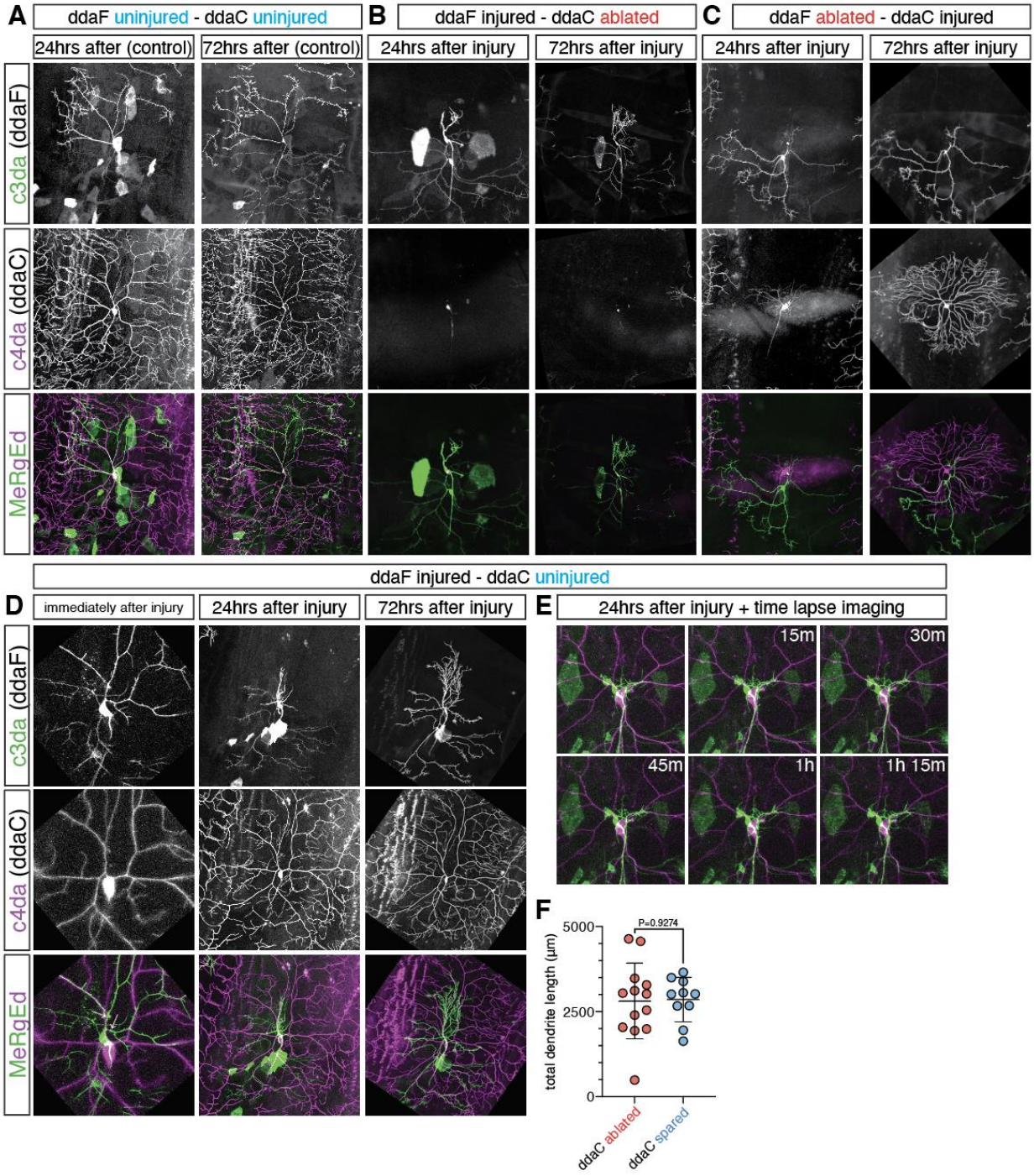

Fig. 13.0 ddaC and ddaF regeneration in the presence or absence of one another. *(**A**) Uninjured ddaF and ddaC at 24 and 72hr after injury, taken at 96 and 144 hr AEL respectively. (**B**) ddaF injury + ddaC ablation. (C) ddaF ablation + ddaC injury. (**D**) ddaF injury + ddaC preservation. (**E**) time lapse imaging of **D**. (**F**) quantification of total ddaF dendrite length regenerated 72hr after injury. ddaC ablated N=13, ddaC spared N= 10*

D). We also conducted time lapse imaging of ddaF regeneration in the presence of ddaC which revealed that ddaF indisputably grow along the path of ddaC dendrites (**Fig. 12.0 E**). However, we quantified ddaF regeneration in the presence or absence of ddaC, to better understand if preexisting ddaC dendrites influenced ddaF dendrite regeneration but failed to find any significant differences (**Fig 12.0 F**). Future studies should further investigate the mechanism governing biased growth of ddaF onto ddaC during regeneration as we were unable to elegantly quantify this phenotype.

Discussion

Dendrites have a remarkable ability to regenerate new dendrites, albeit imperfectly. In an attempt to dissect the mechanism(s) governing imperfect regeneration, pathways and better understand the systems that go awry during repair we conducted in-vivo time lapse imaging of dendrite dynamics during repair, comparing them to dendrite development, finding that regrowing dendrites move more, and transverse larger distances when in motion. My interpretation of this data is that the mechanism(s) that govern dendrite development and regeneration are distinctly different, because of the fact there is/are mechanism(s) that regulate dendrite dynamics differently, distinct from development, because the fact that they are much more dynamic suggests that something else is being activated or accentuated. Secondly, I tested genes involved in learning and memory, expressing critical genes that are required for functional plasticity thinking they would enhance structural plasticitiy which I could measure through measuring dendrite length and dendrite branch tips during regeneration. However, regeneration is much more complex than a binary increase/decrease in repair. It is not necessarily about how much a neuron can regenerate per se, but rather, if the regenerated architecture has the proper structural support to form proper synaptic partners (if the neuron forms pre and post synaptic connections) or if the dendritic territory

covers the proper receptive field. Although expressing *Baf53a*, *Baf53b*, or overexpressing *Bap55* did not increase the total dendrite length or branch tips, the regenerated architecture had a significant decrease in self-crossing defects, resembling an uninjured neuron at an earlier stage in development. Furthermore, we found that expressing *Baf53a* impairs dendrite development, consistent with its role in development. In contrast, we found that expressing *Baf53b* impairs development and significantly impairs dendrite regeneration, consistent with its role in post-mitotic neurons. Moreover, the fact that *Baf53b* affected dendrite development suggests that Baf53b may have likely impaired endogenous Bap55 function. To reconcile these findings, I have a few explanations: 1) Baf53b showed a less severe phenotype than Baf53a in development, and 2) *Bap55* shows more sequence homology to *Baf53b* than to *Baf53a*. Lastly, we found that overexpressing *Bap55* significantly decreased total dendrite length and branch tips during development and regeneration. One potential explanation for this finding is that endogenous Bap55 are titrated to various levels during developmental checkpoints, while overexpression drives bap55 beyond what is typically expressed. These results are consistent with *Baf53a,-b* role in neuronal development and neuronal plasticity.

Lastly, when we tracked dendrite regeneration in the presence of other dendrites, we found that dendrite length was not significantly affected. However, when we monitored dendrite regeneration in the presence of preexisting branches, dendrites indisputably regrew onto preexisting dendrites. These observations that dendrite regeneration no longer seemed stochastic in the presence of other dendrites suggests that dendrites can utilize endogenous signals of other dendrites to guide regrowth (data not quantified). Whether preexisting dendrites regulate the directionality of dendrite regeneration is imperative to determine, because it will further support the principle that neuronal injury must be attenuated immediately, to minimize damage and maximize repair.

This chapter highlights some key findings that I explored throughout my graduate studies. Future studies could build upon this preliminary data by identifying whether expressing the various BAF complexes redirects dendrites as they encounter other dendrites originating from the same neuron through time lapse imaging. Furthermore, it could be informative to identify if BAF and DSCAM converge onto the same molecular pathways, or deviate in function, as both BAF and DSCAM overexpression could ameliorate self-crossing defects during dendrite regeneration. Lastly, whether dendrite regeneration is truly an independent process. Studies have shown enhanced neurite growth in 3D mesh scaffolds[327] and in our studies we observed dendrite directly growing along existing intact dendrites using time lapse imaging, in vivo. Future studies could build upon these results by characterizing how dendrites behave in the presence of other neurons.

Chapter 5

Interpretations, Outlook, and Advice

Interpretations

Many neurological diseases are multifaceted. Our lifestyle choices have a lasting effect on our epigenome and alter the trajectory of disease predisposition. In this chapter I will cover interpretations of the data, my scientific perspectives, outlook for disease therapeutics, and my advice to graduate students.

It is increasingly apparent (to me) that the ambiguity in mitochondrial responses is likely caused by experimental models like various organisms, cell types, and stressors like hypoxia, dietary restriction. For example, injury induced changes in mitochondrial morphology requires Drp1. Preventing injury induced changes in mitochondrial morphology inhibits plasma membrane repair in Drp1.K38A mutants. In a different context, loss of injury induced changes in mitochondrial morphology via K38A increases cell survival. One way to reconcile the duality of Drp1 in repair and cell survival is that loss of Drp1 prevents cells from knowing they were injured, resulting in a delay in apoptosis; furthermore, if cells are unaware of injury, there is nothing to repair.

The overwhelming evidence that mitochondrial morphology is abnormal in NDs (neurodegenerative diseases) suggests that mitochondrial dysfunction may be the underlying cause of neurodegeneration or accentuate disease. Even though mitochondria are primarily hyper fragmented in neurons of NDs their morphology can vary in other cell types[276]. Whether mitochondrial morphology in one tissue type influences the fusion/fission balance in other tissues remains to be directly investigated. Interestingly, stroke has been shown to expel astrocytic mitochondria into the extracellular environment, which is rapidly internalized by neurons[328]. If dysfunctional mitochondria are secreted from astrocytes and internalized by neurons, this may further propagate neuronal dysfunction.

The statement that mitochondrion is the "powerhouse" of the cell significantly undermines the importance of mitochondria in cell homeostasis. While mitochondria are primarily known for their critical role in generating ATP, they are crucial signal transducers; they store Ca^{2+} as a central currency and trade it for other ions to activate ion specific molecular cascades. This exchange is necessary for activating molecular pathways associated with various biological processes. In addition to ion-mediated cell signaling, mtROS further tunes signaling cascades, activating pathways involved in regulating cell survival and cell death. Mitochondria regulate their own organelle integrity, the accumulation of Drp1 (and its scission) ensures that the mitochondrial genome is healthy and dysfunctional mitochondria are targeted for degradation (mitophagy). Thus, when mechanisms regulating mitochondrial homeostasis become awry, cell function is jeopardized.

Outlook for therapeutics

Many new efforts have been focused on mitochondrial transfer as a therapeutic. I too, think

this is a promising approach[329,330]. The idea behind mitochondrial transfer is that mitochondria homogenize with dysfunctional mitochondria through implantation (citation) or through natural occurring mechanisms (like secretion and uptake, or transfer between tunneling nano tubes) to restore mitochondrial homeostasis[99,328]. However, these studies are still in their infant stages and will require more thorough investigation, as mitochondrial transfer yields ambiguous results; sometimes disease pathology is attenuated[331–333] while in others, its exacerbated[334].

Advice for PhD students

During my graduate career I was fortunate to receive amazing scientific and career advice from my mentors. These pieces of advice came from articles which were passed down by their own PhD/Post-doc mentors, from their own graduate experiences, and from my own experiences.

Discipline

Early in your own graduate career, you may feel free to explore whatever you want, you will (should) read familiarize yourself with the literature in the field and begin identifying knowledge gaps and which bridges that need to be formed to move the field forward. If you are like me, you will be eager to conduct experiments to identify novel cool phenotypes. I easily found myself clocking 14-hour days, 7 days a week, and during those hours, I was productive (not performative productivity) doing data quantification, conducting experiments, and thinking critically about the results. The years became months, months became weeks, and before I knew it, I was looking for post-docs. I thought I was "disciplined" because I was a effectively (doing the right thing) efficient (doing things quickly and properly). But being "disciplined" is more than a "good work ethic" but being able to finish projects. To early scientists in the graduate career, if you lack scientific

direction here is my advice to you: every experiment you conduct needs to be proactively built into a figure. This way, you know what pieces of data you have, and you will be able to build your manuscript easily. If the data is not worth thinking about, it is not worth doing. Your graduate career is not about making a groundbreaking discovery, it is a training for you to demonstrate that you can materialize a publication out of data, and rationale.

Experimental design

Being able to apply the scientific method is truly an *art*. Hypothesis are generated curiosities. There must be an obvious phenomenon, it should spark curiosity, form a hypothesis, make predictions, conduct experiments, interpret the data, and form and revise models. Spend time to observe the biology (or whichever discipline you enter), its truly beautiful and will give you an appreciation of academia. None of your committee members or mentors will tell you how to form a proper hypothesis. It took me until the end of my third year to learn state my ideas as a hypothesis, definitively. A proper hypothesis is not "I hypothesize that increasing sugar intake may cause changes in weight gain over 2 weeks", although you have an independent and dependent variable, the results are not definitive and make interpretations hard. Instead, when you generate hypotheses, make a statement that is confident, that can be argued against. For example, "increasing sugar causes weight gain" this statement is disputable and should be supported by the data you present.

Data interpretation

Instead of doing more experiments, spend more time interpreting the data and what it's telling you about the phenomena you are studying. Phenomena are like jigsaw puzzles; they are simple in nature but complex in explanation. If you are proactively plan your experiments, assess

obstacles and limitations, and keep an open mind it will make writing your manuscript much easier. When doing a jigsaw puzzle, separating out pieces by shapes or color (proactively planning experiments), identify the subsection of puzzle that can be completed most efficiently (assessing obstacles) can make things much smoother. As you add in more pieces of the puzzle (collect more pieces of data), the puzzle becomes easier (your results will become more and more predictable). If you don't proactively plan your experiments, your scientific narrative will take a detour, and subsequent experiments may become infested with one-offs.

Good hypothesis will renew every decade. And while hypothesis pass by, facts remain. This is because mechanisms of biology are complete, but our understanding is not. Interpret the data *carefully* and be open to multiple explanations. The data is always unintentional and informative, refine your hypothesis to build a model for your story.

REFERENCES

1. Mitchell, A.J., Cogswell, I.E., Dalos, J., Tsakalos, G., Lei, J., Oros, A., Rafferty, Q., Santoni, S., Steele, X., Dieleman, J.L., et al. (2025). Estimating global direct health-care spending on neurological and mental health between 2000 and 2019: a modelling study. Lancet Public Health *10*, e401–e411.
2. Stone, M.C., Albertson, R.M., Chen, L., and Rolls, M.M. (2014). Dendrite injury triggers DLK-independent regeneration. Cell Rep. *6*, 247–253.
3. Shin, J.E., Cho, Y., Beirowski, B., Milbrandt, J., Cavalli, V., and DiAntonio, A. (2012). Dual leucine zipper kinase is required for retrograde injury signaling and axonal regeneration. Neuron *74*, 1015–1022.
4. Liu, D., Webber, H.C., Bian, F., Xu, Y., Prakash, M., Feng, X., Yang, M., Yang, H., You, I.-J., Li, L., et al. (2025). Optineurin-facilitated axonal mitochondria delivery promotes neuroprotection and axon regeneration. Nat. Commun. *16*, 1789.
5. Lee, S., Wang, W., Hwang, J., Namgung, U., and Min, K.-T. (2019). Increased ER-mitochondria tethering promotes axon regeneration. Proc. Natl. Acad. Sci. U. S. A. *116*, 16074–16079.
6. Cartoni, R., Norsworthy, M.W., Bei, F., Wang, C., Li, S., Zhang, Y., Gabel, C.V., Schwarz, T.L., and He, Z. (2016). The mammalian-specific protein Armcx1 regulates mitochondrial transport during axon regeneration. Neuron *92*, 1294–1307.
7. Han, S.M., Baig, H.S., and Hammarlund, M. (2016). Mitochondria localize to injured axons to support regeneration. Neuron *92*, 1308–1323.
8. Zhou, B., Yu, P., Lin, M.-Y., Sun, T., Chen, Y., and Sheng, Z.-H. (2016). Facilitation of axon regeneration by enhancing mitochondrial transport and rescuing energy deficits. J. Cell

Biol. *214*, 103–119.

9. Rieger, S., and Sagasti, A. (2011). Hydrogen peroxide promotes injury-induced peripheral sensory axon regeneration in the zebrafish skin. PLoS Biol. *9*, e1000621.
10. Ramon y Cajal, S. (1928). Degeneration and regeneration of the nervous system. pp.
11. Thompson-Peer, K.L., DeVault, L., Li, T., Jan, L.Y., and Jan, Y.N. (2016). In vivo dendrite regeneration after injury is different from dendrite development. Genes Dev. *30*, 1776–1789.
12. Duarte, V.N., Lam, V.T., Rimicci, D.S., and Thompson-Peer, K.L. (2024). Calcium plays an essential role in early-stage dendrite injury detection and regeneration. Prog Neurobiol *239*, 102635.
13. Hertzler, J.I., Teng, J., Bernard, A.R., Stone, M.C., Kline, H.L., Mahata, G., Kumar, N., and Rolls, M.M. (2024). Voltage-gated calcium channels act upstream of adenylyl cyclase Ac78C to promote timely initiation of dendrite regeneration. PLoS Genet. *20*, e1011388.
14. Hertzler, J.I., Simonovitch, S.I., Albertson, R.M., Weiner, A.T., Nye, D.M.R., and Rolls, M.M. (2020). Kinetochore proteins suppress neuronal microtubule dynamics and promote dendrite regeneration. Mol. Biol. Cell *31*, 2125–2138.
15. Prange, S.E., Bhakta, I.N., Sysoeva, D., Jean, G.E., Madisetti, A., Le, H.H.N., Duong, L.U., Hwu, P.T., Melton, J.G., and Thompson-Peer, K.L. (2024). Dendrite injury triggers neuroprotection in Drosophila models of neurodegenerative disease. Sci. Rep. *14*, 24766.
16. Nye, D.M.R., Albertson, R.M., Weiner, A.T., Hertzler, J.I., Shorey, M., Goberdhan, D.C.I., Wilson, C., Janes, K.A., and Rolls, M.M. (2020). The receptor tyrosine kinase Ror is required for dendrite regeneration in Drosophila neurons. PLoS Biol. *18*, e3000657.
17. DeVault, L., Li, T., Izabel, S., Thompson-Peer, K.L., Jan, L.Y., and Jan, Y.N. (2018).

Dendrite regeneration of adult Drosophila sensory neurons diminishes with aging and is inhibited by epidermal-derived matrix metalloproteinase 2. Genes Dev. *32*, 402–414.

18. Stone, M.C., Seebold, D.Y., Shorey, M., Kothe, G.O., and Rolls, M.M. (2022). Dendrite regeneration in the vertebrate spinal cord. Dev. Biol. *488*, 114–119.
19. Shorey, M., Stone, M.C., Mandel, J., and Rolls, M.M. (2020). Neurons survive simultaneous injury to axons and dendrites and regrow both types of processes in vivo. Dev. Biol. *465*, 108–118.
20. Liu, C., Mei, M., Li, Q., Roboti, P., Pang, Q., Ying, Z., Gao, F., Lowe, M., and Bao, S. (2017). Loss of the golgin GM130 causes Golgi disruption, Purkinje neuron loss, and ataxia in mice. Proc. Natl. Acad. Sci. U. S. A. *114*, 346–351.
21. Horn, A., Raavicharla, S., Shah, S., Cox, D., and Jaiswal, J.K. (2020). Mitochondrial fragmentation enables localized signaling required for cell repair. J. Cell Biol. *219*. https://doi.org/10.1083/jcb.201909154.
22. Subramanian, K., and Meyer, T. (1997). Calcium-induced restructuring of nuclear envelope and endoplasmic reticulum calcium stores. Cell *89*, 963–971.
23. Weber, J.T., Rzigalinski, B.A., and Ellis, E.F. (2001). Traumatic injury of cortical neurons causes changes in intracellular calcium stores and capacitative calcium influx. J. Biol. Chem. *276*, 1800–1807.
24. Hains, B.C., Klein, J.P., Saab, C.Y., Craner, M.J., Black, J.A., and Waxman, S.G. (2003). Upregulation of sodium channel Nav1.3 and functional involvement in neuronal hyperexcitability associated with central neuropathic pain after spinal cord injury. J. Neurosci. *23*, 8881–8892.
25. Young, W., and Koreh, I. (1986). Potassium and calcium changes in injured spinal cords.

Brain Res. *365*, 42–53.

26. Chen, L., Stone, M.C., Tao, J., and Rolls, M.M. (2012). Axon injury and stress trigger a microtubule-based neuroprotective pathway. Proc. Natl. Acad. Sci. U. S. A. *109*, 11842–11847.

27. Erez, H., Malkinson, G., Prager-Khoutorsky, M., De Zeeuw, C.I., Hoogenraad, C.C., and Spira, M.E. (2007). Formation of microtubule-based traps controls the sorting and concentration of vesicles to restricted sites of regenerating neurons after axotomy. J. Cell Biol. *176*, 497–507.

28. Suleiman, H.Y., Roth, R., Jain, S., Heuser, J.E., Shaw, A.S., and Miner, J.H. (2017). Injury-induced actin cytoskeleton reorganization in podocytes revealed by super-resolution microscopy. JCI Insight *2*. https://doi.org/10.1172/jci.insight.94137.

29. Mukherjee, K., Gu, C., Collins, A., Mettlen, M., Samelko, B., Altintas, M.M., Sudhini, Y.R., Wang, X., Bouley, R., Brown, D., et al. (2022). Simultaneous stabilization of actin cytoskeleton in multiple nephron-specific cells protects the kidney from diverse injury. Nat. Commun. *13*, 2422.

30. Kölliker, A. (1857). Einige Bemerkungen über die Endigungen der Hautnerven und den Bau der Muskeln. Zeitschr f wissensch Zool.

31. Altmann, R. (1894). Die Elementarorganismen und ihre Beziehungen zu den Zellen. https://doi.org/10.1515/9783112366967.

32. Benda, C. (1898). Ueber die spermatogenese der vertebraten und höherer evertebraten, II. Theil: Die histiogenese der spermien. Arch. Anat. Physiol.

33. Keilin, D. (1925). On cytochrome, a respiratory pigment, common to animals, yeast, and higher plants. Proc. R. Soc. Lond. B Biol. Sci. *98*, 312–339.

34. Warburg, O. (1928). Über die Rolle des Eisens in der Atmung des Seeigeleis nebst Bemerkungen über einige durch Eisen beschleunigte Oxydationen. In Über die Katalytischen Wirkungen der Lebendigen Substanz (Springer Berlin Heidelberg), pp. 47–66.

35. Warburg, O. (1910). Über die Oxydationen in lebenden Zellen nach Versuchen am Seeigelei. Hoppe Seylers Z. Physiol. Chem. *66*, 305–340.

36. Warburg, O.H. (1931). The oxygen-transferring ferment of respiration.

37. Banga, I., and Szent-Györgyi, A. (1934). The large scale preparation of ascorbic acid from Hungarian pepper (Capsicum annuum). Biochem. J. *28*, 1625–1628.

38. Szent-Györgyi, A. (1928). Observations on the function of peroxidase systems and the chemistry of the adrenal cortex: Description of a new carbohydrate derivative. Biochem. J. *22*, 1387–1409.

39. Svirbely, J.L., and Szent-Györgyi, A. (1933). XL. The chemical nature of vitamin c. J. biochem, 279–284.

40. Szent-Györgyi, A. (1931). Oxidation, energy transfer, and vitamins.

41. Krebs, H.A., and Johnson, W.A. (1937). Acetopyruvic acid (alphagamma-diketovaleric acid) as an intermediate metabolite in animal tissues. Biochem. J. *31*, 772–779.

42. Krebs, H.A. (1953). The citric acid cycle.

43. Lipmann, F. (1953). Development of the acetylation problem: a personal account.

44. Palade, G.E. (1953). An electron microscope study of the mitochondrial structure. J. Histochem. Cytochem. *1*, 188–211.

45. de Duve, C., Pressman, B.C., Gianetto, R., Wattiaux, R., and Appelmans, F. (1955). Tissue fractionation studies. 6. Intracellular distribution patterns of enzymes in rat-liver tissue.

Biochem. J. *60*, 604–617.

46. De Duve, C., and Baudhuin, P. (1966). Peroxisomes (microbodies and related particles). Physiol. Rev. *46*, 323–357.
47. de Duve, C. (1974). Exploring cells with a centrifuge.
48. Palade, G.E. (1974). Intracellular aspects of the process of protein secretion.
49. Pullman, M.E., Penefsky, H.S., Datta, A., and Racker, E. (1960). Partial resolution of the enzymes catalyzing oxidative phosphorylation. I. Purification and properties of soluble dinitrophenol-stimulated adenosine triphosphatase. J. Biol. Chem. *235*, 3322–3329.
50. Penefsky, H.S., Pullman, M.E., Datta, A., and Racker, E. (1960). Partial resolution of the enzymes catalyzing oxidative phosphorylation. II. Participation of a soluble adenosine tolphosphatase in oxidative phosphorylation. J. Biol. Chem. *235*, 3330–3336.
51. Mitchell, P. (1961). Coupling of phosphorylation to electron and hydrogen transfer by a chemi-osmotic type of mechanism. Nature *191*, 144–148.
52. Mitchell, P. (1978). David Keilin's respiratory chain concept and its chemiosmotic consequences.
53. Nass, M.M., and Nass, S. (1963). Intramitochondrial fibers with DNA characteristics. I. Fixation and electron staining reactions. J. Cell Biol. *19*, 593–611.
54. Wallace, D.C., Singh, G., Lott, M.T., Hodge, J.A., Schurr, T.G., Lezza, A.M., Elsas, L.J., 2nd, and Nikoskelainen, E.K. (1988). Mitochondrial DNA mutation associated with Leber's hereditary optic neuropathy. Science *242*, 1427–1430.
55. Bernardi, P., Vassanelli, S., Veronese, P., Colonna, R., Szabó, I., and Zoratti, M. (1992). Modulation of the mitochondrial permeability transition pore. Effect of protons and divalent cations. J. Biol. Chem. *267*, 2934–2939.

56. Boyer, P.D. (1997). Energy, life, and ATP.

57. Walker, J.E. (1997). Atp synthesis by rotary catalysis.

58. Boyer, P.D. (1993). The binding change mechanism for ATP synthase--some probabilities and possibilities. Biochim. Biophys. Acta *1140*, 215–250.

59. Abrahams, J.P., Leslie, A.G., Lutter, R., and Walker, J.E. (1994). Structure at 2.8 Â resolution of F1-ATPase from bovine heart mitochondria. Nature *370*, 621–628.

60. Skou, J.C. (1997). The identification of the sodium potassium-pump.

61. Skou, J.C. (1957). The influence of some cations on an adenosine triphosphatase from peripheral nerves. Biochim. Biophys. Acta *23*, 394–401.

62. Otsuga, D., Keegan, B.R., Brisch, E., Thatcher, J.W., Hermann, G.J., Bleazard, W., and Shaw, J.M. (1998). The dynamin-related GTPase, Dnm1p, controls mitochondrial morphology in yeast. J. Cell Biol. *143*, 333–349.

63. Smirnova, E., Griparić, L., Shurland, D., and Bliek, A. (2001). Dynamin-related protein Drp1 is required for mitochondrial division in mammalian cells. Mol. Biol. Cell *12*, 2245–2256.

64. Chen, H., Detmer, S.A., Ewald, A.J., Griffin, E.E., Fraser, S.E., and Chan, D.C. (2003). Mitofusins Mfn1 and Mfn2 coordinately regulate mitochondrial fusion and are essential for embryonic development. J. Cell Biol. *160*, 189–200.

65. Mootha, V., Bunkenborg, J., Olsen, J.V., Hjerrild, M., Wiśniewski, J., Stahl, E., Bolouri, M.S., Ray, H.N., Sihag, S., Kamal, M., et al. (2003). Integrated analysis of protein composition, tissue diversity, and gene regulation in mouse mitochondria. Cell *115*, 629–640.

66. Baughman, J.M., Perocchi, F., Girgis, H.S., Plovanich, M., Belcher-Timme, C.A., Sancak, Y., Bao, X.R., Strittmatter, L., Goldberger, O., Bogorad, R.L., et al. (2011). Integrative

genomics identifies MCU as an essential component of the mitochondrial calcium uniporter. Nature *476*, 341–345.

67. De Stefani, D., Raffaello, A., Teardo, E., Szabò, I., and Rizzuto, R. (2011). A forty-kilodalton protein of the inner membrane is the mitochondrial calcium uniporter. Nature *476*, 336–340.

68. Ravitch, E.E., Baltrusaitis, E.E., Perez, T.A., Barrie, K.R., Fenton, A.R., Holzbaur, E.L.F., and Dominguez, R. (2025). Structural-functional characterization of the MIRO1-TRAK1 complex. Nat. Commun. *16*, 6173.

69. Carter, A.P., Cho, C., Jin, L., and Vale, R.D. (2011). Crystal structure of the dynein motor domain. Science *331*, 1159–1165.

70. Rochon, K., Bauer, B.L., Roethler, N.A., Buckley, Y., Su, C.-C., Huang, W., Ramachandran, R., Stoll, M.S.K., Yu, E.W., Taylor, D.J., et al. (2024). Structural basis for regulated assembly of the mitochondrial fission GTPase Drp1. Nat. Commun. *15*, 1328.

71. von der Malsburg, A., Sapp, G.M., Zuccaro, K.E., von Appen, A., Moss, F.R., 3rd, Kalia, R., Bennett, J.A., Abriata, L.A., Dal Peraro, M., van der Laan, M., et al. (2023). Structural mechanism of mitochondrial membrane remodelling by human OPA1. Nature *620*, 1101–1108.

72. Fan, C., Fan, M., Orlando, B.J., Fastman, N.M., Zhang, J., Xu, Y., Chambers, M.G., Xu, X., Perry, K., Liao, M., et al. (2018). X-ray and cryo-EM structures of the mitochondrial calcium uniporter. Nature *559*, 575–579.

73. Lai, L.T.F., Balaraman, J., Zhou, F., and Matthies, D. (2023). Cryo-EM structures of human magnesium channel MRS2 reveal gating and regulatory mechanisms. Nat. Commun. *14*, 7207.

74. He, Z., Tu, Y.-C., Tsai, C.-W., Mount, J., Zhang, J., Tsai, M.-F., and Yuan, P. (2025). Structure and function of the human mitochondrial MRS2 channel. Nat. Struct. Mol. Biol. *32*, 459–468.

75. Yoo, J., Wu, M., Yin, Y., Herzik, M.A., Jr, Lander, G.C., and Lee, S.-Y. (2018). Cryo-EM structure of a mitochondrial calcium uniporter. Science *361*, 506–511.

76. Schubert, A.F., Gladkova, C., Pardon, E., Wagstaff, J.L., Freund, S.M.V., Steyaert, J., Maslen, S.L., and Komander, D. (2017). Structure of PINK1 in complex with its substrate ubiquitin. Nature *552*, 51–56.

77. Riley, B.E., Lougheed, J.C., Callaway, K., Velasquez, M., Brecht, E., Nguyen, L., Shaler, T., Walker, D., Yang, Y., Regnstrom, K., et al. (2013). Structure and function of Parkin E3 ubiquitin ligase reveals aspects of RING and HECT ligases. Nat. Commun. *4*, 1982.

78. Guo, H., Suzuki, T., and Rubinstein, J.L. (2019). Structure of a bacterial ATP synthase. Elife *8*. https://doi.org/10.7554/eLife.43128.

79. Guo, H., and Rubinstein, J.L. (2022). Structure of ATP synthase under strain during catalysis. Nat. Commun. *13*, 2232.

80. Zickermann, V., Wirth, C., Nasiri, H., Siegmund, K., Schwalbe, H., Hunte, C., and Brandt, U. (2015). Structural biology. Mechanistic insight from the crystal structure of mitochondrial complex I. Science *347*, 44–49.

81. Suh, J., Kim, N.-K., Shim, W., Lee, S.-H., Kim, H.-J., Moon, E., Sesaki, H., Jang, J.H., Kim, J.-E., and Lee, Y.-S. (2023). Mitochondrial fragmentation and donut formation enhance mitochondrial secretion to promote osteogenesis. Cell Metab. *35*, 345-360.e7.

82. Donovan, E.J., Agrawal, A., Liberman, N., Kalai, J.I., Adler, A.J., Lamper, A.M., Wang, H.Q., Chua, N.J., Koslover, E.F., and Barnhart, E.L. (2024). Dendrite architecture

determines mitochondrial distribution patterns in vivo. Cell Rep. *43*, 114190.

83. Faits, M.C., Zhang, C., Soto, F., and Kerschensteiner, D. (2016). Dendritic mitochondria reach stable positions during circuit development. Elife *5*, e11583.

84. López-Doménech, G., Higgs, N.F., Vaccaro, V., Roš, H., Arancibia-Cárcamo, I.L., MacAskill, A.F., and Kittler, J.T. (2016). Loss of dendritic complexity precedes neurodegeneration in a mouse model with disrupted mitochondrial distribution in mature dendrites. Cell Rep. *17*, 317–327.

85. Lewis, T.L., Jr, Kwon, S.-K., Lee, A., Shaw, R., and Polleux, F. (2018). MFF-dependent mitochondrial fission regulates presynaptic release and axon branching by limiting axonal mitochondria size. Nat. Commun. *9*, 5008.

86. Fu, H., Zhou, H., Yu, X., Xu, J., Zhou, J., Meng, X., Zhao, J., Zhou, Y., Chisholm, A.D., and Xu, S. (2020). Wounding triggers MIRO-1 dependent mitochondrial fragmentation that accelerates epidermal wound closure through oxidative signaling. Nat. Commun. *11*, 1050.

87. Sridharan, P.S., Koh, Y., Miller, E., Hu, D., Chakraborty, S., Tripathi, S.J., Kee, T.R., Chaubey, K., Vázquez-Rosa, E., Barker, S., et al. (2024). Acutely blocking excessive mitochondrial fission prevents chronic neurodegeneration after traumatic brain injury. Cell Rep. Med. *5*, 101715.

88. Kiryu-Seo, S., Tamada, H., Kato, Y., Yasuda, K., Ishihara, N., Nomura, M., Mihara, K., and Kiyama, H. (2016). Mitochondrial fission is an acute and adaptive response in injured motor neurons. Sci. Rep. *6*, 28331.

89. Luo, J., Khandwala, S., Hu, J., Lee, S.-Y., Hickey, K.L., Levine, Z.G., Harper, J.W., Ting, A.Y., and Weissman, J.S. (2025). Proximity-specific ribosome profiling reveals the logic of localized mitochondrial translation. Cell *188*, 5589-5604.e17.

90. Rangaraju, V., Lauterbach, M., and Schuman, E.M. (2019). Spatially stable mitochondrial compartments fuel local translation during plasticity. Cell *176*, 73-84.e15.

91. Palmer, C.S., Elgass, K.D., Parton, R.G., Osellame, L.D., Stojanovski, D., and Ryan, M.T. (2013). Adaptor proteins MiD49 and MiD51 can act independently of Mff and Fis1 in Drp1 recruitment and are specific for mitochondrial fission. J. Biol. Chem. *288*, 27584–27593.

92. Losón, O.C., Song, Z., Chen, H., and Chan, D.C. (2013). Fis1, Mff, MiD49, and MiD51 mediate Drp1 recruitment in mitochondrial fission. Mol. Biol. Cell *24*, 659–667.

93. Bleazard, W., McCaffery, J.M., King, E.J., Bale, S., Mozdy, A., Tieu, Q., Nunnari, J., and Shaw, J.M. (1999). The dynamin-related GTPase Dnm1 regulates mitochondrial fission in yeast. Nat. Cell Biol. *1*, 298–304.

94. Legros, F., Lombès, A., Frachon, P., and Rojo, M. (2002). Mitochondrial fusion in human cells is efficient, requires the inner membrane potential, and is mediated by mitofusins. Mol. Biol. Cell *13*, 4343–4354.

95. Ponte, S., Carvalho, L., Gagliardi, M., Campos, I., Oliveira, P.J., and Jacinto, A. (2020). Drp1-mediated mitochondrial fission regulates calcium and F-actin dynamics during wound healing. Biol. Open *9*, bio.048629.

96. Han, X.-J., Lu, Y.-F., Li, S.-A., Kaitsuka, T., Sato, Y., Tomizawa, K., Nairn, A.C., Takei, K., Matsui, H., and Matsushita, M. (2008). CaM kinase I alpha-induced phosphorylation of Drp1 regulates mitochondrial morphology. J. Cell Biol. *182*, 573–585.

97. Xu, S., and Chisholm, A.D. (2014). C. elegans epidermal wounding induces a mitochondrial ROS burst that promotes wound repair. Dev. Cell *31*, 48–60.

98. Muliyil, S., and Narasimha, M. (2014). Mitochondrial ROS regulates cytoskeletal and mitochondrial remodeling to tune cell and tissue dynamics in a model for wound healing.

Dev. Cell *28*, 239–252.

99. Levoux, J., Prola, A., Lafuste, P., Gervais, M., Chevallier, N., Koumaiha, Z., Kefi, K., Braud, L., Schmitt, A., Yacia, A., et al. (2021). Platelets facilitate the wound-healing capability of mesenchymal stem cells by mitochondrial transfer and metabolic reprogramming. Cell Metab. *33*, 283-299.e9.

100. Lewis, T.L., Jr, Turi, G.F., Kwon, S.-K., Losonczy, A., and Polleux, F. (2016). Progressive decrease of mitochondrial motility during maturation of cortical axons in vitro and in vivo. Curr. Biol. *26*, 2602–2608.

101. Smith, H.L., Bourne, J.N., Cao, G., Chirillo, M.A., Ostroff, L.E., Watson, D.J., and Harris, K.M. (2016). Mitochondrial support of persistent presynaptic vesicle mobilization with age-dependent synaptic growth after LTP. Elife *5*. https://doi.org/10.7554/eLife.15275.

102. Billups, B., and Forsythe, I.D. (2002). Presynaptic mitochondrial calcium sequestration influences transmission at mammalian central synapses. J. Neurosci. *22*, 5840–5847.

103. Lee, C.W., and Peng, H.B. (2008). The function of mitochondria in presynaptic development at the neuromuscular junction. Mol. Biol. Cell *19*, 150–158.

104. Spillane, M., Ketschek, A., Merianda, T.T., Twiss, J.L., and Gallo, G. (2013). Mitochondria coordinate sites of axon branching through localized intra-axonal protein synthesis. Cell Rep. *5*, 1564–1575.

105. Babic, M., Russo, G.J., Wellington, A.J., Sangston, R.M., Gonzalez, M., and Zinsmaier, K.E. (2015). Miro's N-terminal GTPase domain is required for transport of mitochondria into axons and dendrites. J. Neurosci. *35*, 5754–5771.

106. Silva, C.A., Yalnizyan-Carson, A., Fernández Busch, M.V., van Zwieten, M., Verhage, M., and Lohmann, C. (2021). Activity-dependent regulation of mitochondrial motility in

developing cortical dendrites. Elife *10*. https://doi.org/10.7554/eLife.62091.

107. Li, Z., Okamoto, K.-I., Hayashi, Y., and Sheng, M. (2004). The importance of dendritic mitochondria in the morphogenesis and plasticity of spines and synapses. Cell *119*, 873–887.

108. Russo, G.J., Louie, K., Wellington, A., Macleod, G.T., Hu, F., Panchumarthi, S., and Zinsmaier, K.E. (2009). Drosophila Miro is required for both anterograde and retrograde axonal mitochondrial transport. J. Neurosci. *29*, 5443–5455.

109. López-Doménech, G., Covill-Cooke, C., Ivankovic, D., Halff, E.F., Sheehan, D.F., Norkett, R., Birsa, N., and Kittler, J.T. (2018). Miro proteins coordinate microtubule- and actin-dependent mitochondrial transport and distribution. EMBO J. *37*, 321–336.

110. Wang, X., and Schwarz, T.L. (2009). The mechanism of Ca2+ -dependent regulation of kinesin-mediated mitochondrial motility. Cell *136*, 163–174.

111. Wu, Y., Ding, C., Sharif, B., Weinreb, A., Swaim, G., Hao, H., Yogev, S., Watanabe, S., and Hammarlund, M. (2024). Polarized localization of kinesin-1 and RIC-7 drives axonal mitochondria anterograde transport. J. Cell Biol. *223*. https://doi.org/10.1083/jcb.202305105.

112. MacAskill, A.F., Brickley, K., Stephenson, F.A., and Kittler, J.T. (2009). GTPase dependent recruitment of Grif-1 by Miro1 regulates mitochondrial trafficking in hippocampal neurons. Mol. Cell. Neurosci. *40*, 301–312.

113. Smith, G.A., Lin, T.-H., Sheehan, A.E., Van der Goes van Naters, W., Neukomm, L.J., Graves, H.K., Bis-Brewer, D.M., Züchner, S., and Freeman, M.R. (2019). Glutathione S-transferase regulates mitochondrial populations in axons through increased glutathione oxidation. Neuron *103*, 52-65.e6.

114. Stowers, R., Megeath, L.J., Górska-Andrzejak, J., Meinertzhagen, I., and Schwarz, T. (2002). Axonal transport of mitochondria to synapses depends on Milton, a novel Drosophila protein. Neuron *36*, 1063–1077.

115. van Spronsen, M., Mikhaylova, M., Lipka, J., Schlager, M.A., van den Heuvel, D.J., Kuijpers, M., Wulf, P.S., Keijzer, N., Demmers, J., Kapitein, L.C., et al. (2013). TRAK/Milton motor-adaptor proteins steer mitochondrial trafficking to axons and dendrites. Neuron *77*, 485–502.

116. Pathak, D., Sepp, K.J., and Hollenbeck, P.J. (2010). Evidence that myosin activity opposes microtubule-based axonal transport of mitochondria. J. Neurosci. *30*, 8984–8992.

117. Quintero, O.A., DiVito, M.M., Adikes, R.C., Kortan, M.B., Case, L.B., Lier, A.J., Panaretos, N.S., Slater, S.Q., Rengarajan, M., Feliu, M., et al. (2009). Human Myo19 is a novel myosin that associates with mitochondria. Curr. Biol. *19*, 2008–2013.

118. Trevisan, T., Pendin, D., Montagna, A., Bova, S., Ghelli, A.M., and Daga, A. (2018). Manipulation of mitochondria dynamics reveals separate roles for form and function in mitochondria distribution. Cell Rep. *23*, 1742–1753.

119. O'Donnell, K.C., Vargas, M.E., and Sagasti, A. (2013). WldS and PGC-1α regulate mitochondrial transport and oxidation state after axonal injury. J. Neurosci. *33*, 14778–14790.

120. Wang, X., Winter, D., Ashrafi, G., Schlehe, J., Wong, Y.L., Selkoe, D., Rice, S., Steen, J., LaVoie, M.J., and Schwarz, T.L. (2011). PINK1 and Parkin target Miro for phosphorylation and degradation to arrest mitochondrial motility. Cell *147*, 893–906.

121. Wang, J., Fröhlich, H., Torres, F.B., Silva, R.L., Poschet, G., Agarwal, A.R., and Rappold, G. (2021). Mitochondrial dysfunction and oxidative stress contribute to cognitive and

motor impairment in FOXP1 syndrome. Proc. Natl. Acad. Sci. U. S. A. *119*. https://doi.org/10.1073/pnas.2112852119.

122. Smirnova, E., Shurland, D., Ryazantsev, S., and van der Bliek, A.M. (1998). A human dynamin-related protein controls the distribution of mitochondria. J. Cell Biol. *143*, 351–358.

123. Misko, A.L., Sasaki, Y., Tuck, E., Milbrandt, J., and Baloh, R.H. (2012). Mitofusin2 mutations disrupt axonal mitochondrial positioning and promote axon degeneration. J. Neurosci. *32*, 4145–4155.

124. Sandoval, H., Yao, C.-K., Chen, K., Jaiswal, M., Donti, T., Lin, Y.Q., Bayat, V., Xiong, B., Zhang, K., David, G., et al. (2014). Mitochondrial fusion but not fission regulates larval growth and synaptic development through steroid hormone production. Elife *3*, e03558.

125. Kang, J.-S., Tian, J.-H., Pan, P.-Y., Zald, P., Li, C., Deng, C., and Sheng, Z.-H. (2008). Docking of axonal mitochondria by syntaphilin controls their mobility and affects short-term facilitation. Cell *132*, 137–148.

126. Chen, Y., and Sheng, Z.-H. (2013). Kinesin-1-syntaphilin coupling mediates activity-dependent regulation of axonal mitochondrial transport. J. Cell Biol. *202*, 351–364.

127. Bapat, O., Purimetla, T., Kruessel, S., Shah, M., Fan, R., Thum, C., Rupprecht, F., Langer, J.D., and Rangaraju, V. (2024). VAP spatially stabilizes dendritic mitochondria to locally support synaptic plasticity. Nat. Commun. *15*, 205.

128. Kornmann, B., Osman, C., and Walter, P. (2011). The conserved GTPase Gem1 regulates endoplasmic reticulum-mitochondria connections. Proc. Natl. Acad. Sci. U. S. A. *108*, 14151–14156.

129. Hirabayashi, Y., Kwon, S.-K., Paek, H., Pernice, W.M., Paul, M.A., Lee, J., Erfani, P.,

Raczkowski, A., Petrey, D.S., Pon, L.A., et al. (2017). ER-mitochondria tethering by PDZD8 regulates Ca2+ dynamics in mammalian neurons. Science *358*, 623–630.

130. López-Doménech, G., Serrat, R., Mirra, S., D'Aniello, S., Somorjai, I., Abad, A., Vitureira, N., García-Arumí, E., Alonso, M.T., Rodriguez-Prados, M., et al. (2012). The Eutherian Armcx genes regulate mitochondrial trafficking in neurons and interact with Miro and Trak2. Nat. Commun. *3*, 814.

131. Stoica, R., De Vos, K.J., Paillusson, S., Mueller, S., Sancho, R.M., Lau, K.-F., Vizcay-Barrena, G., Lin, W.-L., Xu, Y.-F., Lewis, J., et al. (2014). ER-mitochondria associations are regulated by the VAPB-PTPIP51 interaction and are disrupted by ALS/FTD-associated TDP-43. Nat. Commun. *5*, 3996.

132. Murley, A., Lackner, L.L., Osman, C., West, M., Voeltz, G.K., Walter, P., and Nunnari, J. (2013). ER-associated mitochondrial division links the distribution of mitochondria and mitochondrial DNA in yeast. Elife *2*, e00422.

133. Singh, G., Vengayil, V., Khanna, A., Adhikary, S., and Laxman, S. (2025). Active control of mitochondrial network morphology by metabolism-driven redox state. Proc. Natl. Acad. Sci. U. S. A. *122*, e2421953122.

134. Youle, R.J., and van der Bliek, A.M. (2012). Mitochondrial fission, fusion, and stress. Science *337*, 1062–1065.

135. Garcia, G.C., Bartol, T.M., Phan, S., Bushong, E.A., Perkins, G., Sejnowski, T.J., Ellisman, M.H., and Skupin, A. (2019). Mitochondrial morphology provides a mechanism for energy buffering at synapses. Sci. Rep. *9*, 18306.

136. Shen, Q., Yamano, K., Head, B.P., Kawajiri, S., Cheung, J.T.M., Wang, C., Cho, J.-H., Hattori, N., Youle, R.J., and van der Bliek, A.M. (2014). Mutations in Fis1 disrupt orderly

disposal of defective mitochondria. Mol. Biol. Cell *25*, 145–159.

137. Obinata, H., Watanabe, T., Takahashi, H., Shimo, S., Oda, T., Sugimoto, A., and Niwa, S. (2025). SLC-25A46 regulates mitochondrial fusion through the mitofusin protein FZO-1 and is essential for maintaining neuronal morphology. J. Cell Sci. *138*. https://doi.org/10.1242/jcs.263571.

138. Tsubouchi, A., Tsuyama, T., Fujioka, M., Kohda, H., Okamoto-Furuta, K., Aigaki, T., and Uemura, T. (2009). Mitochondrial protein Preli-like is required for development of dendritic arbors and prevents their regression in the Drosophila sensory nervous system. Development *136*, 3757–3766.

139. Song, Z., Chen, H., Fiket, M., Alexander, C., and Chan, D.C. (2007). OPA1 processing controls mitochondrial fusion and is regulated by mRNA splicing, membrane potential, and Yme1L. J. Cell Biol. *178*, 749–755.

140. Olichon, A., Elachouri, G., Baricault, L., Delettre, C., Belenguer, P., and Lenaers, G. (2007). OPA1 alternate splicing uncouples an evolutionary conserved function in mitochondrial fusion from a vertebrate restricted function in apoptosis. Cell Death Differ. *14*, 682–692.

141. Wang, R., Mishra, P., Garbis, S.D., Moradian, A., Sweredoski, M.J., and Chan, D.C. (2021). Identification of new OPA1 cleavage site reveals that short isoforms regulate mitochondrial fusion. Mol. Biol. Cell *32*, 157–168.

142. Ge, Y., Shi, X., Boopathy, S., McDonald, J., Smith, A.W., and Chao, L.H. (2020). Two forms of Opa1 cooperate to complete fusion of the mitochondrial inner-membrane. Elife *9*. https://doi.org/10.7554/eLife.50973.

143. Ishihara, N., Fujita, Y., Oka, T., and Mihara, K. (2006). Regulation of mitochondrial morphology through proteolytic cleavage of OPA1. EMBO J. *25*, 2966–2977.

144. Anand, R., Wai, T., Baker, M.J., Kladt, N., Schauss, A.C., Rugarli, E., and Langer, T. (2014). The i-AAA protease YME1L and OMA1 cleave OPA1 to balance mitochondrial fusion and fission. J. Cell Biol. *204*, 919–929.

145. Ehses, S., Raschke, I., Mancuso, G., Bernacchia, A., Geimer, S., Tondera, D., Martinou, J.-C., Westermann, B., Rugarli, E.I., and Langer, T. (2009). Regulation of OPA1 processing and mitochondrial fusion by m-AAA protease isoenzymes and OMA1. J. Cell Biol. *187*, 1023–1036.

146. Yamada, T., Ikeda, A., Murata, D., Wang, H., Zhang, C., Khare, P., Adachi, Y., Ito, F., Quirós, P.M., Blackshaw, S., et al. (2025). Dual regulation of mitochondrial fusion by Parkin-PINK1 and OMA1. Nature *639*, 776–783.

147. Mahajan, M., Bharambe, N., Shang, Y., Lu, B., Mandal, A., Madan Mohan, P., Wang, R., Boatz, J.C., Manuel Martinez Galvez, J., Shnyrova, A.V., et al. (2021). NMR identification of a conserved Drp1 cardiolipin-binding motif essential for stress-induced mitochondrial fission. Proc. Natl. Acad. Sci. U. S. A. *118*, e2023079118.

148. Koirala, S., Guo, Q., Kalia, R., Bui, H.T., Eckert, D.M., Frost, A., and Shaw, J.M. (2013). Interchangeable adaptors regulate mitochondrial dynamin assembly for membrane scission. Proc. Natl. Acad. Sci. U. S. A. *110*, E1342-51.

149. Liu, R., and Chan, D.C. (2015). The mitochondrial fission receptor Mff selectively recruits oligomerized Drp1. Mol. Biol. Cell *26*, 4466–4477.

150. Kamerkar, S.C., Kraus, F., Sharpe, A.J., Pucadyil, T.J., and Ryan, M.T. (2018). Dynamin-related protein 1 has membrane constricting and severing abilities sufficient for mitochondrial and peroxisomal fission. Nat. Commun. *9*, 5239.

151. Gomes, L.C., Di Benedetto, G., and Scorrano, L. (2011). During autophagy mitochondria

elongate, are spared from degradation and sustain cell viability. Nat. Cell Biol. *13*, 589–598.

152. Faitg, J., Lacefield, C., Davey, T., White, K., Laws, R., Kosmidis, S., Reeve, A.K., Kandel, E.R., Vincent, A.E., and Picard, M. (2021). 3D neuronal mitochondrial morphology in axons, dendrites, and somata of the aging mouse hippocampus. Cell Rep. *36*, 109509.

153. Virga, D.M., Hamilton, S., Osei, B., Morgan, A., Kneis, P., Zamponi, E., Park, N.J., Hewitt, V.L., Zhang, D., Gonzalez, K.C., et al. (2024). Activity-dependent compartmentalization of dendritic mitochondria morphology through local regulation of fusion-fission balance in neurons in vivo. Nat. Commun. *15*, 2142.

154. Fung, T.S., Ji, W.-K., Higgs, H.N., and Chakrabarti, R. (2019). Two distinct actin filament populations have effects on mitochondria, with differences in stimuli and assembly factors. J. Cell Sci. *132*, jcs234435.

155. Liu, X., Weaver, D., Shirihai, O., and Hajnóczky, G. (2009). Mitochondrial "kiss-and-run": interplay between mitochondrial motility and fusion-fission dynamics. EMBO J. *28*, 3074–3089.

156. Lee, H., and Yoon, Y. (2014). Transient contraction of mitochondria induces depolarization through the inner membrane dynamin OPA1 protein. J. Biol. Chem. *289*, 11862–11872.

157. Mehta, K., Chacko, L.A., Chug, M.K., Jhunjhunwala, S., and Ananthanarayanan, V. (2019). Association of mitochondria with microtubules inhibits mitochondrial fission by precluding assembly of the fission protein Dnm1. J. Biol. Chem. *294*, 3385–3396.

158. DuBoff, B., Götz, J., and Feany, M.B. (2012). Tau promotes neurodegeneration via DRP1 mislocalization in vivo. Neuron *75*, 618–632.

159. Cereghetti, G.M., Costa, V., and Scorrano, L. (2010). Inhibition of Drp1-dependent

mitochondrial fragmentation and apoptosis by a polypeptide antagonist of calcineurin. Cell Death Differ. *17*, 1785–1794.

160. Schwarz, L., Sharma, K., Dodi, L.D., Rieder, L.-S., Fallier-Becker, P., Casadei, N., and Fitzgerald, J.C. (2022). Miro1 R272Q disrupts mitochondrial calcium handling and neurotransmitter uptake in dopaminergic neurons. Front. Mol. Neurosci. *15*, 966209.

161. Nemani, N., Carvalho, E., Tomar, D., Dong, Z., Ketschek, A., Breves, S.L., Jaña, F., Worth, A.M., Heffler, J., Palaniappan, P., et al. (2018). MIRO-1 determines mitochondrial shape transition upon GPCR activation and Ca2+ stress. Cell Rep. *23*, 1005–1019.

162. Ding, L., Lei, Y., Han, Y., Li, Y., Ji, X., and Liu, L. (2016). Vimar is a novel regulator of mitochondrial fission through Miro. PLoS Genet. *12*, e1006359.

163. Nakamura, K., Aoyama-Ishiwatari, S., Nagao, T., Paaran, M., Obara, C.J., Sakurai-Saito, Y., Johnston, J., Du, Y., Suga, S., Tsuboi, M., et al. (2025). Mitochondrial complexity is regulated at ER-mitochondria contact sites via PDZD8-FKBP8 tethering. Nat. Commun. *16*, 3401.

164. Fowler, P.C., Byrne, D.J., Blackstone, C., and O'Sullivan, N.C. (2020). Loss of the mitochondrial fission GTPase Drp1 contributes to neurodegeneration in a Drosophila model of hereditary spastic paraplegia. Brain Sci. *10*, 646.

165. Wong, Y.C., Ysselstein, D., and Krainc, D. (2018). Mitochondria-lysosome contacts regulate mitochondrial fission via RAB7 GTP hydrolysis. Nature *554*, 382–386.

166. Nag, S., Szederkenyi, K., Gorbenko, O., Tyrrell, H., Yip, C.M., and McQuibban, G.A. (2023). PGAM5 is an MFN2 phosphatase that plays an essential role in the regulation of mitochondrial dynamics. Cell Rep. *42*, 112895.

167. Tanaka, H., Okazaki, T., Aoyama, S., Yokota, M., Koike, M., Okada, Y., Fujiki, Y., and

Gotoh, Y. (2019). Peroxisomes control mitochondrial dynamics and the mitochondrion-dependent apoptosis pathway. J. Cell Sci. *132*, jcs224766.

168. DiGiovanni, L.F., Khroud, P.K., Carmichael, R.E., Schrader, T.A., Gill, S.K., Germain, K., Jomphe, R.Y., Wiesinger, C., Boutry, M., Kamoshita, M., et al. (2025). ROS transfer at peroxisome-mitochondria contact regulates mitochondrial redox. Science *389*, 157–162.

169. Shi, P., Ren, X., Meng, J., Kang, C., Wu, Y., Rong, Y., Zhao, S., Jiang, Z., Liang, L., He, W., et al. (2022). Mechanical instability generated by Myosin 19 contributes to mitochondria cristae architecture and OXPHOS. Nat. Commun. *13*, 2673.

170. Simpson, C.L., Tokito, M.K., Uppala, R., Sarkar, M.K., Gudjonsson, J.E., and Holzbaur, E.L.F. (2021). NIX initiates mitochondrial fragmentation via DRP1 to drive epidermal differentiation. Cell Rep. *34*, 108689.

171. Jouaville, L.S., Pinton, P., Bastianutto, C., Rutter, G.A., and Rizzuto, R. (1999). Regulation of mitochondrial ATP synthesis by calcium: evidence for a long-term metabolic priming. Proc. Natl. Acad. Sci. U. S. A. *96*, 13807–13812.

172. Llorente-Folch, I., Rueda, C.B., Amigo, I., del Arco, A., Saheki, T., Pardo, B., and Satrústegui, J. (2013). Calcium-regulation of mitochondrial respiration maintains ATP homeostasis and requires ARALAR/AGC1-malate aspartate shuttle in intact cortical neurons. J. Neurosci. *33*, 13957–13971, 13971a.

173. Gherardi, G., Monticelli, H., Rizzuto, R., and Mammucari, C. (2020). The mitochondrial Ca2+ uptake and the fine-tuning of aerobic metabolism. Front. Physiol. *11*, 554904.

174. Pivovarova, N., Hongpaisan, J., Andrews, S., and Friel, D. (1999). Depolarization-induced mitochondrial Ca accumulation in sympathetic neurons: Spatial and temporal characteristics. J. Neurosci. *19*, 6372–6384.

175. Deluca, H.F., and Engstrom, G.W. (1961). Calcium uptake by rat kidney mitochondria. Proc. Natl. Acad. Sci. U. S. A. *47*, 1744–1750.

176. Vasington, F.D., and Murphy, J.V. (1962). Ca ion uptake by rat kidney mitochondria and its dependence on respiration and phosphorylation. J. Biol. Chem. *237*, 2670–2677.

177. Kirichok, Y., Krapivinsky, G., and Clapham, D.E. (2004). The mitochondrial calcium uniporter is a highly selective ion channel. Nature *427*, 360–364.

178. Sancak, Y., Markhard, A.L., Kitami, T., Kovács-Bogdán, E., Kamer, K.J., Udeshi, N.D., Carr, S.A., Chaudhuri, D., Clapham, D.E., Li, A.A., et al. (2013). EMRE is an essential component of the mitochondrial calcium uniporter complex. Science *342*, 1379–1382.

179. Perocchi, F., Gohil, V.M., Girgis, H.S., Bao, X.R., McCombs, J.E., Palmer, A.E., and Mootha, V.K. (2010). MICU1 encodes a mitochondrial EF hand protein required for Ca(2+) uptake. Nature *467*, 291–296.

180. Choi, S., Quan, X., Bang, S., Yoo, H., Kim, J., Park, J., Park, K.-S., and Chung, J. (2017). Mitochondrial calcium uniporter in Drosophila transfers calcium between the endoplasmic reticulum and mitochondria in oxidative stress-induced cell death. J. Biol. Chem. *292*, 14473–14485.

181. Lee, K.-S., Huh, S., Lee, S., Wu, Z., Kim, A.-K., Kang, H.-Y., and Lu, B. (2018). Altered ER-mitochondria contact impacts mitochondria calcium homeostasis and contributes to neurodegeneration in vivo in disease models. Proc. Natl. Acad. Sci. U. S. A. *115*, E8844–E8853.

182. Favaro, G., Romanello, V., Varanita, T., Andrea Desbats, M., Morbidoni, V., Tezze, C., Albiero, M., Canato, M., Gherardi, G., De Stefani, D., et al. (2019). DRP1-mediated mitochondrial shape controls calcium homeostasis and muscle mass. Nat. Commun. *10*,

2576.

183. Wang, J.-Q., Chen, Q., Wang, X., Wang, Q.-C., Wang, Y., Cheng, H.-P., Guo, C., Sun, Q., Chen, Q., and Tang, T.-S. (2013). Dysregulation of mitochondrial calcium signaling and superoxide flashes cause mitochondrial genomic DNA damage in Huntington disease. J. Biol. Chem. *288*, 3070–3084.

184. Twyning, M.J., Tufi, R., Gleeson, T.P., Kolodziej, K.M., Campesan, S., Terriente-Felix, A., Collins, L., De Lazzari, F., Giorgini, F., and Whitworth, A.J. (2024). Partial loss of MCU mitigates pathology in vivo across a diverse range of neurodegenerative disease models. Cell Rep. *43*, 113681.

185. Ferreira, I.L., Ferreiro, E., Schmidt, J., Cardoso, J.M., Pereira, C.M.F., Carvalho, A.L., Oliveira, C.R., and Rego, A.C. (2015). Aβ and NMDAR activation cause mitochondrial dysfunction involving ER calcium release. Neurobiol. Aging *36*, 680–692.

186. Jadiya, P., Kolmetzky, D.W., Tomar, D., Thomas, M., Cohen, H.M., Khaledi, S., Garbincius, J.F., Hildebrand, A.N., and Elrod, J.W. (2023). Genetic ablation of neuronal mitochondrial calcium uptake halts Alzheimer's disease progression. bioRxivorg, 2023.10.11.561889. https://doi.org/10.1101/2023.10.11.561889.

187. Begley, J.G., Duan, W., Chan, S., Duff, K., and Mattson, M.P. (1999). Altered calcium homeostasis and mitochondrial dysfunction in cortical synaptic compartments of presenilin-1 mutant mice. J. Neurochem. *72*, 1030–1039.

188. Jadiya, P., Cohen, H.M., Kolmetzky, D.W., Kadam, A.A., Tomar, D., and Elrod, J.W. (2023). Neuronal loss of NCLX-dependent mitochondrial calcium efflux mediates age-associated cognitive decline. iScience *26*, 106296.

189. Kowaltowski, A.J., Menezes-Filho, S.L., Assali, E.A., Gonçalves, I.G., Cabral-Costa, J.V.,

Abreu, P., Miller, N., Nolasco, P., Laurindo, F.R.M., Bruni-Cardoso, A., et al. (2019). Mitochondrial morphology regulates organellar Ca^{2+} uptake and changes cellular Ca^{2+} homeostasis. FASEB J. *33*, 13176–13188.

190. Kolisek, M., Zsurka, G., Samaj, J., Weghuber, J., Schweyen, R.J., and Schweigel, M. (2003). Mrs2p is an essential component of the major electrophoretic Mg2+ influx system in mitochondria. EMBO J. *22*, 1235–1244.

191. Li, M., Li, Y., Lu, Y., Li, J., Lu, X., Ren, Y., Wen, T., Wang, Y., Chang, S., Zhang, X., et al. (2023). Molecular basis of Mg2+ permeation through the human mitochondrial Mrs2 channel. Nat. Commun. *14*, 4713.

192. Hou, H., Wang, L., Fu, T., Papasergi, M., Yule, D.I., and Xia, H. (2020). Magnesium acts as a second messenger in the regulation of NMDA receptor-mediated CREB signaling in neurons. Mol. Neurobiol. *57*, 2539–2550.

193. Sun, Y., Sukumaran, P., and Singh, B.B. (2020). Magnesium-induced cell survival is dependent on TRPM7 expression and function. Mol. Neurobiol. *57*, 528–538.

194. Strom, A., Strassburger, K., Schmuck, M., Shevalye, H., Davidson, E., Zivehe, F., Bönhof, G., Reimer, R., Belgardt, B.-F., Fleming, T., et al. (2021). Interaction between magnesium and methylglyoxal in diabetic polyneuropathy and neuronal models. Mol. Metab. *43*, 101114.

195. Inoue, I., Nagase, H., Kishi, K., and Higuti, T. (1991). ATP-sensitive K+ channel in the mitochondrial inner membrane. Nature *352*, 244–247.

196. Paggio, A., Checchetto, V., Campo, A., Menabò, R., Di Marco, G., Di Lisa, F., Szabo, I., Rizzuto, R., and De Stefani, D. (2019). Identification of an ATP-sensitive potassium channel in mitochondria. Nature *572*, 609–613.

197. Lange, H., Kispal, G., and Lill, R. (1999). Mechanism of iron transport to the site of heme synthesis inside yeast mitochondria. J. Biol. Chem. *274*, 18989–18996.

198. Foury, F., and Roganti, T. (2002). Deletion of the mitochondrial carrier genes MRS3 and MRS4 suppresses mitochondrial iron accumulation in a yeast frataxin-deficient strain. J. Biol. Chem. *277*, 24475–24483.

199. Shaw, G.C., Cope, J.J., Li, L., Corson, K., Hersey, C., Ackermann, G.E., Gwynn, B., Lambert, A.J., Wingert, R.A., Traver, D., et al. (2006). Mitoferrin is essential for erythroid iron assimilation. Nature *440*, 96–100.

200. Paradkar, P.N., Zumbrennen, K.B., Paw, B.H., Ward, D.M., and Kaplan, J. (2009). Regulation of mitochondrial iron import through differential turnover of mitoferrin 1 and mitoferrin 2. Mol. Cell. Biol. *29*, 1007–1016.

201. Chen, W., Paradkar, P.N., Li, L., Pierce, E.L., Langer, N.B., Takahashi-Makise, N., Hyde, B.B., Shirihai, O.S., Ward, D.M., Kaplan, J., et al. (2009). Abcb10 physically interacts with mitoferrin-1 (Slc25a37) to enhance its stability and function in the erythroid mitochondria. Proc. Natl. Acad. Sci. U. S. A. *106*, 16263–16268.

202. Muñoz, P., Humeres, A., Elgueta, C., Kirkwood, A., Hidalgo, C., and Núñez, M.T. (2011). Iron mediates N-methyl-D-aspartate receptor-dependent stimulation of calcium-induced pathways and hippocampal synaptic plasticity. J. Biol. Chem. *286*, 13382–13392.

203. Carafoli, E., Tiozzo, R., Lugli, G., Crovetti, F., and Kratzing, C. (1974). The release of calcium from heart mitochondria by sodium. J. Mol. Cell. Cardiol. *6*, 361–371.

204. Palty, R., Silverman, W.F., Hershfinkel, M., Caporale, T., Sensi, S.L., Parnis, J., Nolte, C., Fishman, D., Shoshan-Barmatz, V., Herrmann, S., et al. (2010). NCLX is an essential component of mitochondrial Na+/Ca2+ exchange. Proc. Natl. Acad. Sci. U. S. A. *107*, 436–

441.

205. Stavsky, A., Stoler, O., Kostic, M., Katoshevsky, T., Assali, E.A., Savic, I., Amitai, Y., Prokisch, H., Leiz, S., Daumer-Haas, C., et al. (2021). Aberrant activity of mitochondrial NCLX is linked to impaired synaptic transmission and is associated with mental retardation. Commun. Biol. *4*, 666.

206. Fan, M., Tsai, C.-W., Zhang, J., Zhang, J., Krishnan, A.R., Liu, T.-Y., Huang, Y.-L., Aydin, D., Du, S., Sobecks, B.L., et al. (2025). Structure and mechanism of the mitochondrial calcium transporter NCLX. Nature, 1–9.

207. Douglas, M.G., and Cockrell, R.S. (1974). Mitochondrial cation-hydrogen ion exchange. J. Biol. Chem. *249*, 5464–5471.

208. Numata, M., Petrecca, K., Lake, N., and Orlowski, J. (1998). Identification of a mitochondrial Na+/H+ exchanger. J. Biol. Chem. *273*, 6951–6959.

209. Hernansanz-Agustín, P., Morales-Vidal, C., Calvo, E., Natale, P., Martí-Mateos, Y., Jaroszewicz, S.N., Cabrera-Alarcón, J.L., Acín-Pérez, R., López-Montero, I., Vázquez, J., et al. (2024). A transmitochondrial sodium gradient controls membrane potential in mammalian mitochondria. Cell *187*, 6599-6613.e21.

210. Denton, R.M., Randle, P.J., and Martin, B.R. (1972). Stimulation by calcium ions of pyruvate dehydrogenase phosphate phosphatase. Biochem. J. *128*, 161–163.

211. McCormack, J.G., and Denton, R.M. (1990). The role of mitochondrial Ca2+ transport and matrix Ca2+ in signal transduction in mammalian tissues. Biochim. Biophys. Acta *1018*, 287–291.

212. Denton, R.M., and McCormack, J.G. (1990). Ca2+ as a second messenger within mitochondria of the heart and other tissues. Annu. Rev. Physiol. *52*, 451–466.

213. Zhu, L.P., Yu, X.D., Ling, S., Brown, R.A., and Kuo, T.H. (2000). Mitochondrial Ca(2+)homeostasis in the regulation of apoptotic and necrotic cell deaths. Cell Calcium *28*, 107–117.

214. Kirova, D.G., Judasova, K., Vorhauser, J., Zerjatke, T., Leung, J.K., Glauche, I., and Mansfeld, J. (2022). A ROS-dependent mechanism promotes CDK2 phosphorylation to drive progression through S phase. Dev. Cell *57*, 1712-1727.e9.

215. Byrne, D.P., Shrestha, S., Galler, M., Cao, M., Daly, L.A., Campbell, A.E., Eyers, C.E., Veal, E.A., Kannan, N., and Eyers, P.A. (2020). Aurora A regulation by reversible cysteine oxidation reveals evolutionarily conserved redox control of Ser/Thr protein kinase activity. Sci. Signal. *13*, eaax2713.

216. Khacho, M., Clark, A., Svoboda, D.S., Azzi, J., MacLaurin, J.G., Meghaizel, C., Sesaki, H., Lagace, D.C., Germain, M., Harper, M.-E., et al. (2016). Mitochondrial dynamics impacts stem cell identity and fate decisions by regulating a nuclear transcriptional program. Cell Stem Cell *19*, 232–247.

217. Oswald, M.C., Brooks, P.S., Zwart, M.F., Mukherjee, A., West, R.J., Giachello, C.N., Morarach, K., Baines, R.A., Sweeney, S.T., and Landgraf, M. (2018). Reactive oxygen species regulate activity-dependent neuronal plasticity in Drosophila. Elife *7*, e39393.

218. Perier, C., Tieu, K., Guégan, C., Caspersen, C., Jackson-Lewis, V., Carelli, V., Martinuzzi, A., Hirano, M., Przedborski, S., and Vila, M. (2005). Complex I deficiency primes Bax-dependent neuronal apoptosis through mitochondrial oxidative damage. Proc. Natl. Acad. Sci. U. S. A. *102*, 19126–19131.

219. Liao, P.-C., Tandarich, L.C., and Hollenbeck, P.J. (2017). ROS regulation of axonal mitochondrial transport is mediated by Ca2+ and JNK in Drosophila. PLoS One *12*,

e0178105.

220. Frank, S.D., Gaume, B., Bergmann-Leitner, E., Leitner, W., Robert, E., Catez, F., Smith, C.L., and Youle, R. (2001). The role of dynamin-related protein 1, a mediator of mitochondrial fission, in apoptosis. Dev. Cell *1*, 515–525.

221. Milani, M., Beckett, A.J., Al-Zebeeby, A., Luo, X., Prior, I.A., Cohen, G.M., and Varadarajan, S. (2019). DRP-1 functions independently of mitochondrial structural perturbations to facilitate BH3 mimetic-mediated apoptosis. Cell Death Discov. *5*, 117.

222. Oltvai, Z.N., Milliman, C.L., and Korsmeyer, S.J. (1993). Bcl-2 heterodimerizes in vivo with a conserved homolog, Bax, that accelerates programmed cell death. Cell *74*, 609–619.

223. Karbowski, M., and Youle, R.J. (2003). Dynamics of mitochondrial morphology in healthy cells and during apoptosis. Cell Death Differ. *10*, 870–880.

224. Cho, D.-H., Nakamura, T., Fang, J., Cieplak, P., Godzik, A., Gu, Z., and Lipton, S.A. (2009). S-nitrosylation of Drp1 mediates beta-amyloid-related mitochondrial fission and neuronal injury. Science *324*, 102–105.

225. Horn, A., Van der Meulen, J.H., Defour, A., Hogarth, M., Sreetama, S., Reed, A., Scheffer, L., Chandel, N., and Jaiswal, J. (2017). Mitochondrial redox signaling enables repair of injured skeletal muscle cells. Sci. Signal. *10*. https://doi.org/10.1126/scisignal.aaj1978.

226. Hongpaisan, J., Winters, C.A., and Andrews, S.B. (2004). Strong calcium entry activates mitochondrial superoxide generation, upregulating kinase signaling in hippocampal neurons. J. Neurosci. *24*, 10878–10887.

227. Kedra, J., Lin, S., Pacheco, A., Gallo, G., and Smith, G.M. (2021). Axotomy induces Drp1-dependent fragmentation of axonal mitochondria. Front. Mol. Neurosci. *14*, 668670.

228. Gómez-Deza, J., Nebiyou, M., Alkaslasi, M.R., Nadal-Nicolás, F.M., Somasundaram, P.,

Slavutsky, A.L., Li, W., Ward, M.E., Watkins, T.A., and Le Pichon, C.E. (2024). DLK-dependent axonal mitochondrial fission drives degeneration after axotomy. Nat. Commun. *15*, 10806.

229. Gomez-Deza, J., Slavutsky, A.L., Nebiyou, M., and Le Pichon, C.E. (2023). Local production of reactive oxygen species drives vincristine-induced axon degeneration. Cell Death Dis. *14*, 807.

230. Breckwoldt, M.O., Pfister, F.M.J., Bradley, P.M., Marinković, P., Williams, P.R., Brill, M.S., Plomer, B., Schmalz, A., St Clair, D.K., Naumann, R., et al. (2014). Multiparametric optical analysis of mitochondrial redox signals during neuronal physiology and pathology in vivo. Nat. Med. *20*, 555–560.

231. Di Pietro, V., Lazzarino, G., Amorini, A.M., Signoretti, S., Hill, L.J., Porto, E., Tavazzi, B., Lazzarino, G., and Belli, A. (2017). Fusion or fission: The Destiny of mitochondria in traumatic brain injury of different severities. Sci. Rep. *7*, 9189.

232. Hunter, D.R., and Haworth, R.A. (1979). The Ca2+-induced membrane transition in mitochondria. I. The protective mechanisms. Arch. Biochem. Biophys. *195*, 453–459.

233. Karch, J., Kwong, J.Q., Burr, A.R., Sargent, M.A., Elrod, J.W., Peixoto, P.M., Martinez-Caballero, S., Osinska, H., Cheng, E.H.-Y., Robbins, J., et al. (2013). Bax and Bak function as the outer membrane component of the mitochondrial permeability pore in regulating necrotic cell death in mice. Elife *2*, e00772.

234. Schinzel, A.C., Takeuchi, O., Huang, Z., Fisher, J.K., Zhou, Z., Rubens, J., Hetz, C., Danial, N.N., Moskowitz, M.A., and Korsmeyer, S.J. (2005). Cyclophilin D is a component of mitochondrial permeability transition and mediates neuronal cell death after focal cerebral ischemia. Proc. Natl. Acad. Sci. U. S. A. *102*, 12005–12010.

235. Barrientos, S.A., Martinez, N.W., Yoo, S., Jara, J.S., Zamorano, S., Hetz, C., Twiss, J.L., Alvarez, J., and Court, F.A. (2011). Axonal degeneration is mediated by the mitochondrial permeability transition pore. J. Neurosci. *31*, 966–978.

236. Park, J.Y., Jang, S.Y., Shin, Y.K., Koh, H., Suh, D.J., Shinji, T., Araki, T., and Park, H.T. (2013). Mitochondrial swelling and microtubule depolymerization are associated with energy depletion in axon degeneration. Neuroscience *238*, 258–269.

237. Ashrafi, G., Schlehe, J.S., LaVoie, M.J., and Schwarz, T.L. (2014). Mitophagy of damaged mitochondria occurs locally in distal neuronal axons and requires PINK1 and Parkin. J. Cell Biol. *206*, 655–670.

238. Poirazi, P., and Mel, B.W. (2001). Impact of active dendrites and structural plasticity on the memory capacity of neural tissue. Neuron *29*, 779–796.

239. Šišková, Z., Justus, D., Kaneko, H., Friedrichs, D., Henneberg, N., Beutel, T., Pitsch, J., Schoch, S., Becker, A., von der Kammer, H., et al. (2014). Dendritic structural degeneration is functionally linked to cellular hyperexcitability in a mouse model of Alzheimer's disease. Neuron *84*, 1023–1033.

240. Luo, P., Li, X., Wu, X., Dai, S., Yang, Y., Xu, H., Jing, D., Rao, W., Xu, H., Gao, X., et al. (2019). Preso regulates NMDA receptor-mediated excitotoxicity via modulating nitric oxide and calcium responses after traumatic brain injury. Cell Death Dis. *10*, 496.

241. Kupina, N.C., Detloff, M.R., Bobrowski, W.F., Snyder, B.J., and Hall, E.D. (2003). Cytoskeletal protein degradation and neurodegeneration evolves differently in males and females following experimental head injury. Exp. Neurol. *180*, 55–73.

242. Geddes, J.F., Vowles, G.H., Nicoll, J.A., and Révész, T. (1999). Neuronal cytoskeletal changes are an early consequence of repetitive head injury. Acta Neuropathol. *98*, 171–

178.

243. Butler, M.L.M.D., Pervaiz, N., Breen, K., Calderazzo, S., Ypsilantis, P., Wang, Y., Breda, J.C., Mazzilli, S., Nicks, R., Spurlock, E., et al. (2025). Repeated head trauma causes neuron loss and inflammation in young athletes. Nature, 1–10.

244. Dash, U.C., Bhol, N.K., Swain, S.K., Samal, R.R., Nayak, P.K., Raina, V., Panda, S.K., Kerry, R.G., Duttaroy, A.K., and Jena, A.B. (2025). Oxidative stress and inflammation in the pathogenesis of neurological disorders: Mechanisms and implications. Acta Pharm. Sin. B. *15*, 15–34.

245. Xu, W., Chi, L., Xu, R., Ke, Y., Luo, C., Cai, J., Qiu, M., Gozal, D., and Liu, R. (2005). Increased production of reactive oxygen species contributes to motor neuron death in a compression mouse model of spinal cord injury. Spinal Cord *43*, 204–213.

246. Bodmer, R., and Jan, Y.N. (1987). Morphological differentiation of the embryonic peripheral neurons in Drosophila. Rouxs. Arch. Dev. Biol. *196*, 69–77.

247. Berdan, R.C., Easaw, J.C., and Wang, R. (1993). Alterations in membrane potential after axotomy at different distances from the soma of an identified neuron and the effect of depolarization on neurite outgrowth and calcium channel expression. J. Neurophysiol. *69*, 151–164.

248. Wolf, J.A., Stys, P.K., Lusardi, T., Meaney, D., and Smith, D.H. (2001). Traumatic axonal injury induces calcium influx modulated by tetrodotoxin-sensitive sodium channels. J. Neurosci. *21*, 1923–1930.

249. Kucharz, K., Wieloch, T., and Toresson, H. (2011). Rapid fragmentation of the endoplasmic reticulum in cortical neurons of the mouse brain in situ following cardiac arrest. J. Cereb. Blood Flow Metab. *31*, 1663–1667.

250. Mortimer, A.E., Reid, A.J., and Das, R.M. (2024). Golgi compaction facilitates microtubule nucleation to drive adult vertebrate peripheral neuron regeneration. bioRxiv, 2024.08.12.607597. https://doi.org/10.1101/2024.08.12.607597.

251. Alam, S.R., Wallrabe, H., Christopher, K.G., Siller, K.H., and Periasamy, A. (2022). Characterization of mitochondrial dysfunction due to laser damage by 2-photon FLIM microscopy. Sci. Rep. *12*, 11938.

252. Ji, H., and Han, C. (2020). LarvaSPA, A Method for Mounting Drosophila Larva for Long-Term Time-Lapse Imaging. J Vis Exp. https://doi.org/10.3791/60792.

253. Bai, H., Fang, C.-W., Shi, Y., Zhai, S., Jiang, A., Li, Y.-N., Wang, L., Liu, Q.-L., Zhou, G.-Y., Cao, J.-H., et al. (2023). Mitochondria-derived H2O2 triggers liver regeneration via FoxO3a signaling pathway after partial hepatectomy in mice. Cell Death Dis. *14*, 216.

254. Shimura, D., Nuebel, E., Baum, R., Valdez, S.E., Xiao, S., Warren, J.S., Palatinus, J.A., Hong, T., Rutter, J., and Shaw, R.M. (2021). Protective mitochondrial fission induced by stress-responsive protein GJA1-20k. Elife *10*. https://doi.org/10.7554/eLife.69207.

255. Winkelman, J.D., Anderson, C.A., Suarez, C., Kovar, D.R., and Gardel, M.L. (2020). Evolutionarily diverse LIM domain-containing proteins bind stressed actin filaments through a conserved mechanism. Proc. Natl. Acad. Sci. U. S. A. *117*, 25532–25542.

256. Zerihun, M., Sukumaran, S., and Qvit, N. (2023). The Drp1-mediated mitochondrial fission protein interactome as an emerging core player in mitochondrial dynamics and cardiovascular disease therapy. Int. J. Mol. Sci. *24*. https://doi.org/10.3390/ijms24065785.

257. Sturm, G., Karan, K.R., Monzel, A.S., Santhanam, B., Taivassalo, T., Bris, C., Ware, S.A., Cross, M., Towheed, A., Higgins-Chen, A., et al. (2023). OxPhos defects cause hypermetabolism and reduce lifespan in cells and in patients with mitochondrial diseases.

Commun. Biol. *6*, 22.

258. Bretheau, F., Castellanos-Molina, A., Bélanger, D., Kusik, M., Mailhot, B., Boisvert, A., Vallières, N., Lessard, M., Gunzer, M., Liu, X., et al. (2022). The alarmin interleukin-1α triggers secondary degeneration through reactive astrocytes and endothelium after spinal cord injury. Nat. Commun. *13*, 5786.

259. Faden, A.I., Demediuk, P., Panter, S.S., and Vink, R. (1989). The role of excitatory amino acids and NMDA receptors in traumatic brain injury. Science *244*, 798–800.

260. Norat, P., Soldozy, S., Sokolowski, J.D., Gorick, C.M., Kumar, J.S., Chae, Y., Yağmurlu, K., Prada, F., Walker, M., Levitt, M.R., et al. (2020). Mitochondrial dysfunction in neurological disorders: Exploring mitochondrial transplantation. NPJ Regen. Med. *5*, 22.

261. Rangaraju, V., Calloway, N., and Ryan, T.A. (2014). Activity-driven local ATP synthesis is required for synaptic function. Cell *156*, 825–835.

262. Rizzuto, R., Pinton, P., Carrington, W., Fay, F.S., Fogarty, K.E., Lifshitz, L.M., Tuft, R.A., and Pozzan, T. (1998). Close contacts with the endoplasmic reticulum as determinants of mitochondrial Ca2+ responses. Science *280*, 1763–1766.

263. Cereghetti, G.M., Stangherlin, A., Martins de Brito, O., Chang, C.R., Blackstone, C., Bernardi, P., and Scorrano, L. (2008). Dephosphorylation by calcineurin regulates translocation of Drp1 to mitochondria. Proc. Natl. Acad. Sci. U. S. A. *105*, 15803–15808.

264. Ziv, N.E., and Spira, M.E. (1993). Spatiotemporal distribution of Ca2+ following axotomy and throughout the recovery process of cultured Aplysia neurons. Eur. J. Neurosci. *5*, 657–668.

265. Grueber, W.B., Jan, L.Y., and Jan, Y.N. (2002). Tiling of the Drosophila epidermis by multidendritic sensory neurons. Development *129*, 2867–2878.

266. Kim, S.Y., Strucinska, K., Osei, B., Han, K., Kwon, S.-K., and Lewis, T.L., Jr (2022). Neuronal mitochondrial morphology is significantly affected by both fixative and oxygen level during perfusion. Front. Mol. Neurosci. *15*, 1042616.

267. Allegra Mascaro, A.L., Cesare, P., Sacconi, L., Grasselli, G., Mandolesi, G., Maco, B., Knott, G., Huang, L., De Paola, V., Strata, P., et al. (2013). In vivo single branch axotomy induces GAP-43–dependent sprouting and synaptic remodeling in cerebellar cortex. Proc. Natl. Acad. Sci. U. S. A. *110*, 10824–10829.

268. Fernández Casafuz, A.B., De Rossi, M.C., and Bruno, L. (2023). Mitochondrial cellular organization and shape fluctuations are differentially modulated by cytoskeletal networks. Sci. Rep. *13*, 4065.

269. Calvo-Rodriguez, M., Hou, S.S., Snyder, A.C., Kharitonova, E.K., Russ, A.N., Das, S., Fan, Z., Muzikansky, A., Garcia-Alloza, M., Serrano-Pozo, A., et al. (2020). Increased mitochondrial calcium levels associated with neuronal death in a mouse model of Alzheimer's disease. Nat. Commun. *11*, 2146.

270. McAllister, A.K., Katz, L.C., and Lo, D.C. (1996). Neurotrophin regulation of cortical dendritic growth requires activity. Neuron *17*, 1057–1064.

271. Nakamizo-Dojo, M., Ishii, K., Yoshino, J., Tsuji, M., and Emoto, K. (2023). Descending GABAergic pathway links brain sugar-sensing to peripheral nociceptive gating in Drosophila. Nat. Commun. *14*, 6515.

272. Yang, C.-H., Rumpf, S., Xiang, Y., Gordon, M.D., Song, W., Jan, L.Y., and Jan, Y.-N. (2009). Control of the postmating behavioral switch in Drosophila females by internal sensory neurons. Neuron *61*, 519–526.

273. Song, W., Onishi, M., Jan, L.Y., and Jan, Y.N. (2007). Peripheral multidendritic sensory

neurons are necessary for rhythmic locomotion behavior in Drosophila larvae. Proc. Natl. Acad. Sci. U. S. A. *104*, 5199–5204.

274. Liu, G., Seiler, H., Wen, A., Zars, T., Ito, K., Wolf, R., Heisenberg, M., and Liu, L. (2006). Distinct memory traces for two visual features in the Drosophila brain. Nature *439*, 551–556.

275. Baines, R.A., Uhler, J.P., Thompson, A., Sweeney, S.T., and Bate, M. (2001). Altered electrical properties in Drosophila neurons developing without synaptic transmission. J. Neurosci. *21*, 1523–1531.

276. Wang, X., Su, B., Fujioka, H., and Zhu, X. (2008). Dynamin-like protein 1 reduction underlies mitochondrial morphology and distribution abnormalities in fibroblasts from sporadic Alzheimer's disease patients. Am. J. Pathol. *173*, 470–482.

277. Jürgensmeier, J.M., Xie, Z., Deveraux, Q., Ellerby, L., Bredesen, D., and Reed, J.C. (1998). Bax directly induces release of cytochrome c from isolated mitochondria. Proc. Natl. Acad. Sci. U. S. A. *95*, 4997–5002.

278. Pedrera, L., Prieto Clemente, L., Dahlhaus, A., Lotfipour Nasudivar, S., Tishina, S., Olmo González, D., Stroh, J., Yapici, F.I., Singh, R.P., Grotehans, N., et al. (2025). Ferroptosis triggers mitochondrial fragmentation via Drp1 activation. Cell Death Dis. *16*, 40.

279. Seager, R., Ramesh, N.S., Cross, S., Guo, C., Wilkinson, K.A., and Henley, J.M. (2024). SUMOylation of MFF coordinates fission complexes to promote stress-induced mitochondrial fragmentation. Sci. Adv. *10*, eadq6223.

280. Miyazono, Y., Hirashima, S., Ishihara, N., Kusukawa, J., Nakamura, K.-I., and Ohta, K. (2018). Uncoupled mitochondria quickly shorten along their long axis to form indented spheroids, instead of rings, in a fission-independent manner. Sci. Rep. *8*, 350.

281. Knott, A.B., Perkins, G., Schwarzenbacher, R., and Bossy-Wetzel, E. (2008). Mitochondrial fragmentation in neurodegeneration. Nat. Rev. Neurosci. *9*, 505–518.

282. Wang, C., Taki, M., Sato, Y., Tamura, Y., Yaginuma, H., Okada, Y., and Yamaguchi, S. (2019). A photostable fluorescent marker for the superresolution live imaging of the dynamic structure of the mitochondrial cristae. Proc. Natl. Acad. Sci. U. S. A. *116*, 15817–15822.

283. Lai, J.D., Berlind, J.E., Fricklas, G., Lie, C., Urenda, J.-P., Lam, K., Sta Maria, N., Jacobs, R., Yu, V., Zhao, Z., et al. (2024). KCNJ2 inhibition mitigates mechanical injury in a human brain organoid model of traumatic brain injury. Cell Stem Cell *31*, 519-536.e8.

284. Song, W., Chen, J., Petrilli, A., Liot, G., Klinglmayr, E., Zhou, Y., Poquiz, P., Tjong, J., Pouladi, M.A., Hayden, M.R., et al. (2011). Mutant huntingtin binds the mitochondrial fission GTPase dynamin-related protein-1 and increases its enzymatic activity. Nat. Med. *17*, 377–382.

285. Tang, S., Fuß, A., Fattahi, Z., and Culmsee, C. (2024). Drp1 depletion protects against ferroptotic cell death by preserving mitochondrial integrity and redox homeostasis. Cell Death Dis. *15*, 626.

286. Jia, Q., and Sieburth, D. (2021). Mitochondrial hydrogen peroxide positively regulates neuropeptide secretion during diet-induced activation of the oxidative stress response. Nat. Commun. *12*, 2304.

287. Santabárbara-Ruiz, P., López-Santillán, M., Martínez-Rodríguez, I., Binagui-Casas, A., Pérez, L., Milán, M., Corominas, M., and Serras, F. (2015). ROS-induced JNK and p38 signaling is required for Unpaired cytokine activation during Drosophila regeneration. PLoS Genet. *11*, e1005595.

288. Sword, J., Fomitcheva, I.V., and Kirov, S.A. (2024). Spreading depolarization causes reversible neuronal mitochondria fragmentation and swelling in healthy, normally perfused neocortex. J. Cereb. Blood Flow Metab. *44*, 1561–1579.

289. Ackermann, M.A., Buchholz, S.M., Dietrich, K., and Müller, M. (2024). Quantitative, real-time imaging of spreading depolarization-associated neuronal ROS production. Front. Cell. Neurosci. *18*, 1465531.

290. Kidd, T., Brose, K., Mitchell, K.J., Fetter, R.D., Tessier-Lavigne, M., Goodman, C.S., and Tear, G. (1998). Roundabout controls axon crossing of the CNS midline and defines a novel subfamily of evolutionarily conserved guidance receptors. Cell *92*, 205–215.

291. Xu, C., Li, Z., Lyu, C., Hu, Y., McLaughlin, C.N., Wong, K.K.L., Xie, Q., Luginbuhl, D.J., Li, H., Udeshi, N.D., et al. (2024). Molecular and cellular mechanisms of teneurin signaling in synaptic partner matching. Cell *187*, 5081-5101.e19.

292. Berns, D.S., DeNardo, L.A., Pederick, D.T., and Luo, L. (2018). Teneurin-3 controls topographic circuit assembly in the hippocampus. Nature *554*, 328–333.

293. Pederick, D.T., Lui, J.H., Gingrich, E.C., Xu, C., Wagner, M.J., Liu, Y., He, Z., Quake, S.R., and Luo, L. (2021). Reciprocal repulsions instruct the precise assembly of parallel hippocampal networks. Science *372*, 1068–1073.

294. Wu, G.Y., Zou, D.J., Rajan, I., and Cline, H. (1999). Dendritic dynamics in vivo change during neuronal maturation. J. Neurosci. *19*, 4472–4483.

295. Zuo, Y., Lin, A., Chang, P., and Gan, W.-B. (2005). Development of long-term dendritic spine stability in diverse regions of cerebral cortex. Neuron *46*, 181–189.

296. Mostany, R., Anstey, J.E., Crump, K.L., Maco, B., Knott, G., and Portera-Cailliau, C. (2013). Altered synaptic dynamics during normal brain aging. J. Neurosci. *33*, 4094–4104.

297. McQuown, S.C., Barrett, R.M., Matheos, D.P., Post, R.J., Rogge, G.A., Alenghat, T., Mullican, S.E., Jones, S., Rusche, J.R., Lazar, M.A., et al. (2011). HDAC3 is a critical negative regulator of long-term memory formation. J. Neurosci. *31*, 764–774.

298. Kwapis, J.L., Alaghband, Y., Kramár, E.A., López, A.J., Vogel Ciernia, A., White, A.O., Shu, G., Rhee, D., Michael, C.M., Montellier, E., et al. (2018). Epigenetic regulation of the circadian gene Per1 contributes to age-related changes in hippocampal memory. Nat. Commun. *9*, 3323.

299. He, S., Wu, Z., Tian, Y., Yu, Z., Yu, J., Wang, X., Li, J., Liu, B., and Xu, Y. (2020). Structure of nucleosome-bound human BAF complex. Science *367*, 875–881.

300. Centore, R.C., Sandoval, G.J., Soares, L.M.M., Kadoch, C., and Chan, H.M. (2020). Mammalian SWI/SNF chromatin remodeling complexes: Emerging mechanisms and therapeutic strategies. Trends Genet. *36*, 936–950.

301. Yoo, A.S., Staahl, B.T., Chen, L., and Crabtree, G.R. (2009). MicroRNA-mediated switching of chromatin-remodelling complexes in neural development. Nature *460*, 642–646.

302. Yoo, A.S., Sun, A.X., Li, L., Shcheglovitov, A., Portmann, T., Li, Y., Lee-Messer, C., Dolmetsch, R.E., Tsien, R.W., and Crabtree, G.R. (2011). MicroRNA-mediated conversion of human fibroblasts to neurons. Nature *476*, 228–231.

303. Lessard, J., Wu, J.I., Ranish, J.A., Wan, M., Winslow, M.M., Staahl, B.T., Wu, H., Aebersold, R., Graef, I.A., and Crabtree, G.R. (2007). An essential switch in subunit composition of a chromatin remodeling complex during neural development. Neuron *55*, 201–215.

304. Wu, J.I., Lessard, J., Olave, I.A., Qiu, Z., Ghosh, A., Graef, I.A., and Crabtree, G.R. (2007). Regulation of dendritic development by neuron-specific chromatin remodeling complexes. Neuron *56*, 94–108.

305. Gourisankar, S., Nettles, S.A., Wenderski, W., Paulo, J.A., Kim, S.H., Roepke, K.C., Ellis, C., Abuzaid, H.Z., Gygi, S.P., and Crabtree, G.R. (2025). Synaptic activity causes minute-scale changes in BAF complex composition and function. Mol. Cell *85*, 2374-2389.e11.

306. Vogel Ciernia, A., Kramár, E.A., Matheos, D.P., Havekes, R., Hemstedt, T.J., Magnan, C.N., Sakata, K., Tran, A., Azzawi, S., Lopez, A., et al. (2017). Mutation of neuron-specific chromatin remodeling subunit BAF53b: rescue of plasticity and memory by manipulating actin remodeling. Learn. Mem. *24*, 199–209.

307. Vogel-Ciernia, A., Matheos, D.P., Barrett, R.M., Kramár, E.A., Azzawi, S., Chen, Y., Magnan, C.N., Zeller, M., Sylvain, A., Haettig, J., et al. (2013). The neuron-specific chromatin regulatory subunit BAF53b is necessary for synaptic plasticity and memory. Nat. Neurosci. *16*, 552–561.

308. Parrish, J.Z., Kim, M.D., Jan, L.Y., and Jan, Y.N. (2006). Genome-wide analyses identify transcription factors required for proper morphogenesis of Drosophila sensory neuron dendrites. Genes Dev. *20*, 820–835.

309. Tea, J.S., and Luo, L. (2011). The chromatin remodeling factor Bap55 functions through the TIP60 complex to regulate olfactory projection neuron dendrite targeting. Neural Dev. *6*, 5.

310. Vargas, E.J.M., Matamoros, A.J., Qiu, J., Jan, C.H., Wang, Q., Gorczyca, D., Han, T.W., Weissman, J.S., Jan, Y.N., Banerjee, S., et al. (2020). The microtubule regulator ringer functions downstream from the RNA repair/splicing pathway to promote axon regeneration. Genes Dev. *34*, 194–208.

311. White, A.O., Kramár, E.A., López, A.J., Kwapis, J.L., Doan, J., Saldana, D., Davatolhagh, M.F., Alaghband, Y., Blurton-Jones, M., Matheos, D.P., et al. (2016). BDNF rescues

BAF53b-dependent synaptic plasticity and cocaine-associated memory in the nucleus accumbens. Nat. Commun. *7*, 11725.

312. Poe, A.R., Tang, L., Wang, B., Li, Y., Sapar, M.L., and Han, C. (2017). Dendritic space-filling requires a neuronal type-specific extracellular permissive signal in Drosophila. Proc. Natl. Acad. Sci. U. S. A. *114*, E8062–E8071.

313. Meltzer, S., Yadav, S., Lee, J., Soba, P., Younger, S.H., Jin, P., Zhang, W., Parrish, J., Jan, L.Y., and Jan, Y.-N. (2016). Epidermis-derived semaphorin promotes dendrite self-avoidance by regulating dendrite-substrate adhesion in Drosophila sensory neurons. Neuron *89*, 741–755.

314. Gao, F.B., Kohwi, M., Brenman, J.E., Jan, L.Y., and Jan, Y.N. (2000). Control of dendritic field formation in Drosophila: the roles of flamingo and competition between homologous neurons. Neuron *28*, 91–101.

315. Lugaro, E. (1906). Sul neurotropismo e sui trapianti dei nervi. Riv. Patol. Nerv. Ment.

316. Richardson, P.M., McGuinness, U.M., and Aguayo, A.J. (1980). Axons from CNS neurons regenerate into PNS grafts. Nature *284*, 264–265.

317. David, S., and Aguayo, A.J. (1981). Axonal elongation into peripheral nervous system "bridges" after central nervous system injury in adult rats. Science *214*, 931–933.

318. Wilson, K.L., Pérez, S.C.L., Naffaa, M.M., Kelly, S.H., and Segura, T. (2022). Stoichiometric post-modification of hydrogel microparticles dictates neural stem cell fate in microporous annealed particle scaffolds. Adv. Mater. *34*, e2201921.

319. Yeh, J.-Z., Wang, D.-H., Cherng, J.-H., Wang, Y.-W., Fan, G.-Y., Liou, N.-H., Liu, J.-C., and Chou, C.-H. (2020). A collagen-based scaffold for promoting neural plasticity in a rat model of spinal cord injury. Polymers (Basel) *12*, 2245.

320. Agrawal, L., Saidani, M., Guillaud, L., and Terenzio, M. (2021). Development of 3D culture scaffolds for directional neuronal growth using 2-photon lithography. Mater. Sci. Eng. C Mater. Biol. Appl. *131*, 112502.

321. Ranjan, V.D., Qiu, L., Lee, J.W.-L., Chen, X., Jang, S.E., Chai, C., Lim, K.-L., Tan, E.-K., Zhang, Y., Huang, W.M., et al. (2020). A microfiber scaffold-based 3D in vitro human neuronal culture model of Alzheimer's disease. Biomater. Sci. *8*, 4861–4874.

322. Fadia, N.B., Bliley, J.M., DiBernardo, G.A., Crammond, D.J., Schilling, B.K., Sivak, W.N., Spiess, A.M., Washington, K.M., Waldner, M., Liao, H.-T., et al. (2020). Long-gap peripheral nerve repair through sustained release of a neurotrophic factor in nonhuman primates. Sci. Transl. Med. *12*, eaav7753.

323. Ahn, H.-Y., Walters, J.B., Avila, R., Oh, S., Seo, S.G., Kim, J.U., Park, J., Yoo, S., Choi, Y.S., Kim, T.Y., et al. (2025). Bioresorbable, wireless dual stimulator for peripheral nerve regeneration. Nat. Commun. *16*, 4752.

324. Al-Majed, A.A., Tam, S.L., and Gordon, T. (2004). Electrical stimulation accelerates and enhances expression of regeneration-associated genes in regenerating rat femoral motoneurons. Cell. Mol. Neurobiol. *24*, 379–402.

325. Al-Majed, A.A., Neumann, C.M., Brushart, T.M., and Gordon, T. (2000). Brief electrical stimulation promotes the speed and accuracy of motor axonal regeneration. J. Neurosci. *20*, 2602–2608.

326. Xu, C., Kou, Y., Zhang, P., Han, N., Yin, X., Deng, J., Chen, B., and Jiang, B. (2014). Electrical stimulation promotes regeneration of defective peripheral nerves after delayed repair intervals lasting under one month. PLoS One *9*, e105045.

327. Yoo, S.J., Kim, J., Lee, C.-S., and Nam, Y. (2011). Simple and novel three dimensional

neuronal cell culture using a micro mesh scaffold. Exp. Neurobiol. *20*, 110–115.

328. Hayakawa, K., Esposito, E., Wang, X., Terasaki, Y., Liu, Y., Xing, C., Ji, X., and Lo, E.H. (2016). Transfer of mitochondria from astrocytes to neurons after stroke. Nature *535*, 551–555.

329. Tiash, S., Brestoff, J.R., and Crewe, C. (2023). A guide to studying mitochondria transfer. Nat. Cell Biol. *25*, 1551–1553.

330. Brestoff, J.R., Singh, K.K., Aquilano, K., Becker, L.B., Berridge, M.V., Boilard, E., Caicedo, A., Crewe, C., Enríquez, J.A., Gao, J., et al. (2025). Recommendations for mitochondria transfer and transplantation nomenclature and characterization. Nat. Metab. *7*, 53–67.

331. Baldwin, J.G., Heuser-Loy, C., Saha, T., Schelker, R.C., Slavkovic-Lukic, D., Strieder, N., Hernandez-Lopez, I., Rana, N., Barden, M., Mastrogiovanni, F., et al. (2024). Intercellular nanotube-mediated mitochondrial transfer enhances T cell metabolic fitness and antitumor efficacy. Cell *187*, 6614-6630.e21.

332. Zhou, J., Zhang, L., Peng, J., Zhang, X., Zhang, F., Wu, Y., Huang, A., Du, F., Liao, Y., He, Y., et al. (2024). Astrocytic LRP1 enables mitochondria transfer to neurons and mitigates brain ischemic stroke by suppressing ARF1 lactylation. Cell Metab. *36*, 2054-2068.e14.

333. Gao, L., Liu, F., Hou, P.-P., Manaenko, A., Xiao, Z.-P., Wang, F., Xu, T.-L., and Hu, Q. (2022). Neurons release injured mitochondria as “help-me” signaling after ischemic stroke. Front. Aging Neurosci. *14*, 785761.

334. Kidwell, C.U., Casalini, J.R., Pradeep, S., Scherer, S.D., Greiner, D., Bayik, D., Watson, D.C., Olson, G.S., Lathia, J.D., Johnson, J.S., et al. (2023). Transferred mitochondria accumulate reactive oxygen species, promoting proliferation. Elife *12*. https://doi.org/10.7554/eLife.85494.

APPENDIX A: 2-Photon-induced Neurodegeneration

One serendipitous discovery I came across while doing experiments was the ability to induce neurodegeneration in wildtype animals using the 2-Photon laser. I called this the 2PiND (2P-induced neurodegeneration) which resulted in gradual neurodegeneration of the dendrite arbor. I was hoping to optimize this as a tool for screening, because it would have been a powerful tool to screen if genes could ameliorate 2PiND in the context of wildtype cells.

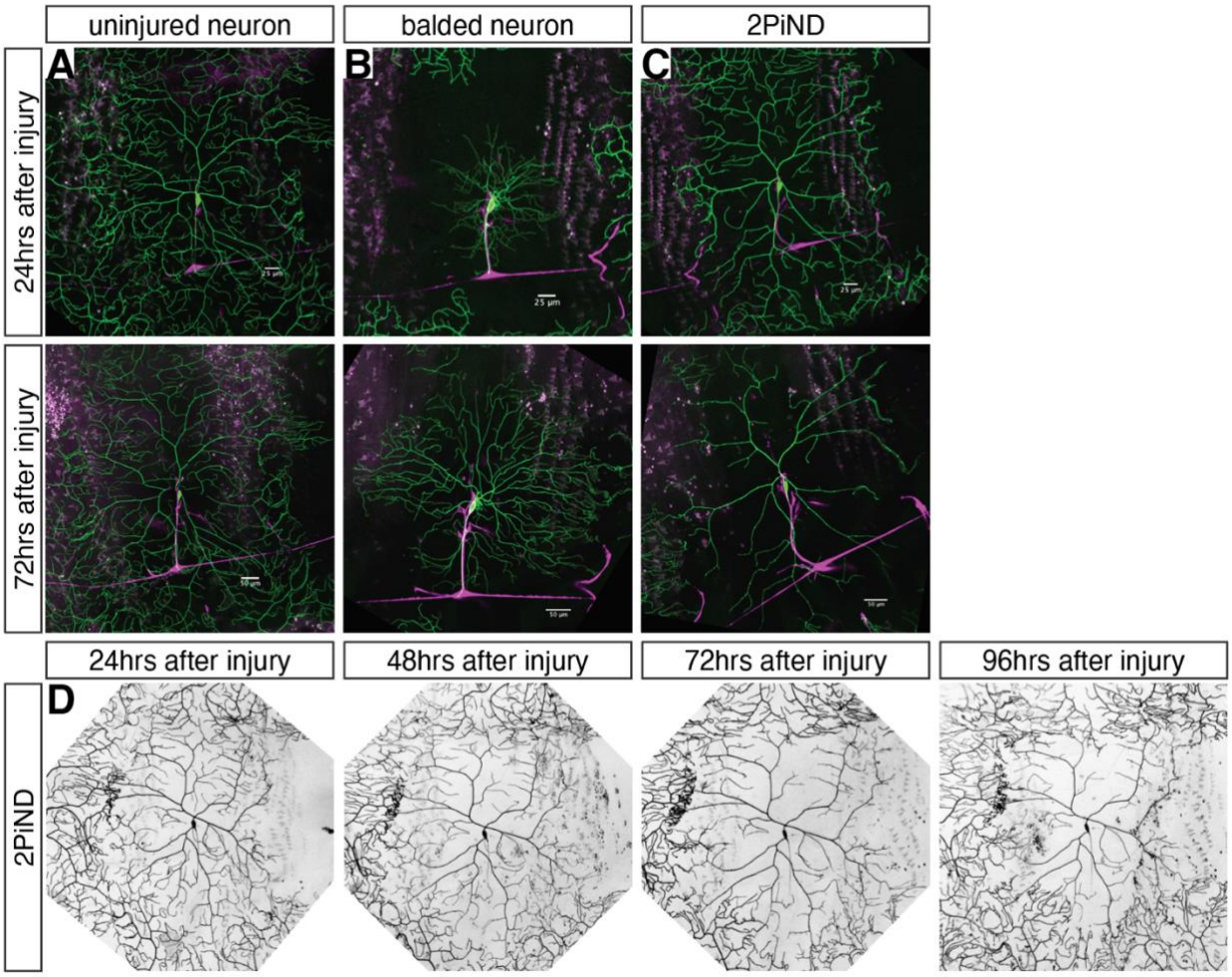

Fig. 14.0 2PiND (2-Photon induced Neurodegeneration)

APPENDIX B: LCM tissue isolation for downstream genome sequencing

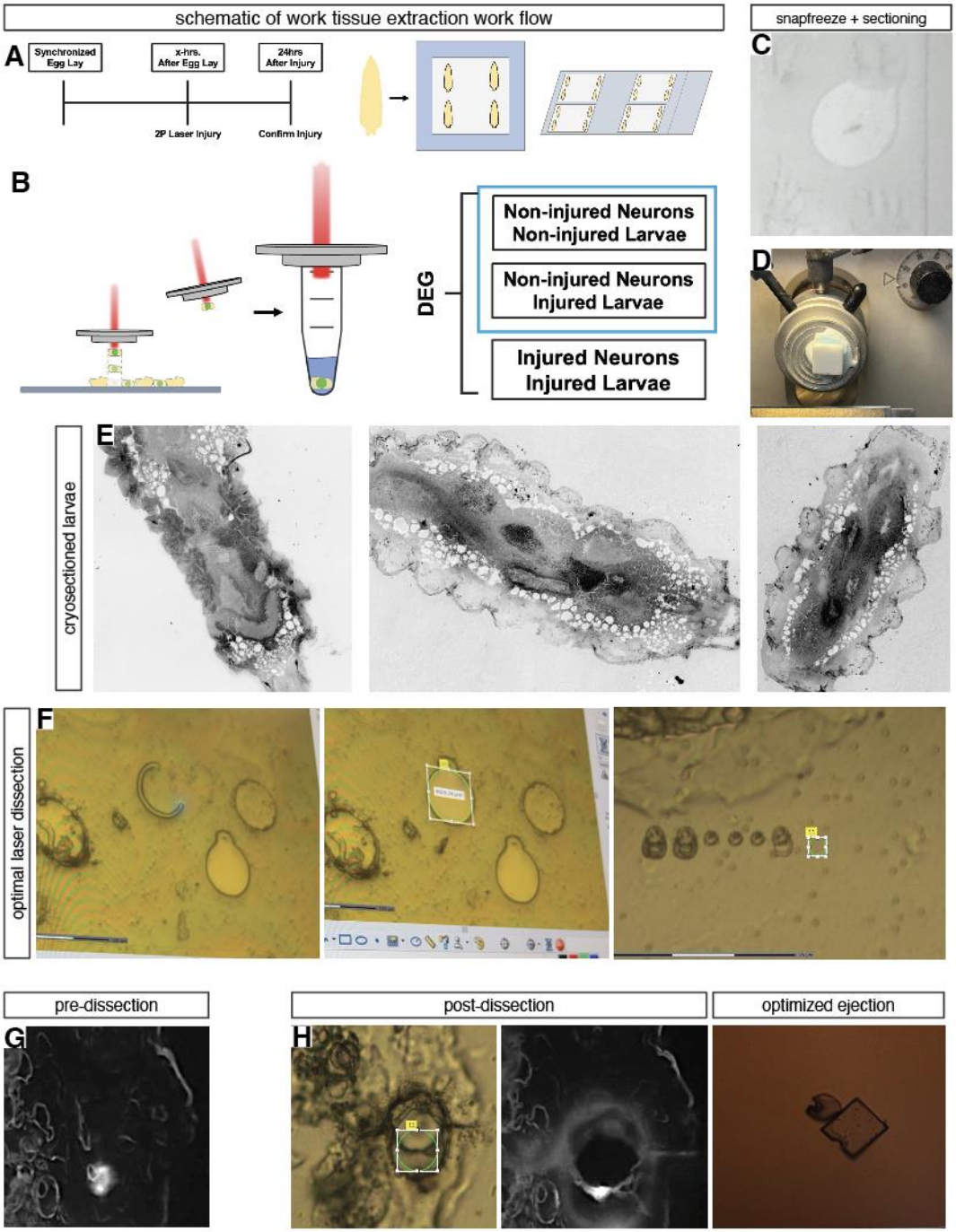

Fig. 15.0 Zeiss PALM microbeam LCM (Laser Capture Microdissection) for RNA-sequencing

During my graduate career, I optimized tissue extraction for RNA sequencing. The flow of the experiments are described in (**A-B**) The big picture of this project was to injure neurons, extract

neurons as they were regrowing (24hr after injury), and conduct RNA sequencing on them. This involved first sandwiching larvae between a cover slip and slide embedded in Tissue-Tek O.C.T. (**C**), immediately snap freezing animals on dry ice (the animals between a coverslip and a slide (**C**), cryosectioning the samples (**D-E**). One of the largest obstacles of these experiments is being able to cryosection animals in the correct plane and identifying which neurons to extract. Regardless, I was able to optimize laser dissection parameters on the Zeiss PALM microbeam (**F**), and successful dissect (**G-H**) tissue out. I spent time optimizing turret ejection of the dissected cap (**H**, last panel). All that remained was the RNA extraction. Realistically, this method had many obstacles and although tissue extraction was feasible, RNA extraction was not (primarily because the duration to extract tissue took too much time.

APPENDIX C: Miro N-terminal GTPase domain and EF hands are required for dendrite development

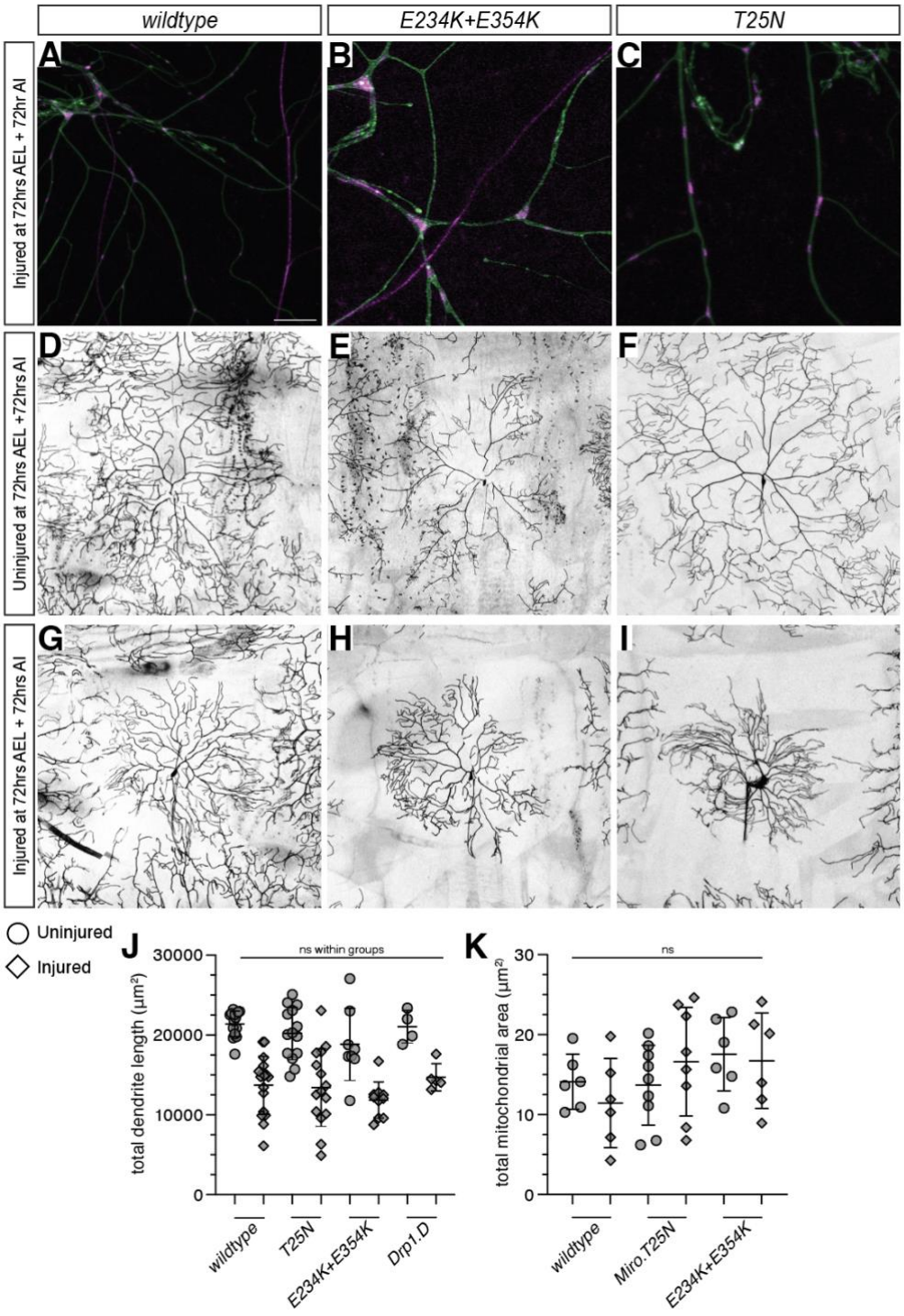

Fig. 16.0 Dendrite regeneration in T25N (N-terminal GTPase) or E234K + E354K miro overexpression

One of the experiments I performed involved overexpressing various Miro SNP mutants. Miro, a key mitochondrial motor adaptor localized to the outer mitochondrial membrane (OMM), recruits TRAK proteins to mediate both dynein- and kinesin-dependent transport. We examined how loss of the N-terminal GTPase activity and disruption of the EF-hand calcium-binding domains affected dendrite development and regeneration. Interestingly, dendrite development was impaired in the EF-hand double mutants and the N-terminal GTPase mutants. Notably, the representative images shown were obtained using the genotype ppk-CD4-tdGFP; ppk >miro.SNP, which consistently exhibited this phenotype. However, when mitochondria were directly visualized in these mutants, the developmental defect was suppressed. I suspect this suppression occurred because the fluorescent tag was fused to the C-terminus of wildtype Miro, effectively resulting in co-overexpression of WT miro.mCherry alongside the Miro SNP mutants. Therefore, these experiments may have functionally overexpressed wildtype Miro in trans, thereby mitigating the mutant phenotype. Regardless, across control or regenerated, conditions across the various genotypes we failed to observe any effects. However, future studies should elucidate how these various mutants affected dendrite branching without the confounding variable.

APPENDIX D: Mitochondrial recovery after dendrotomy

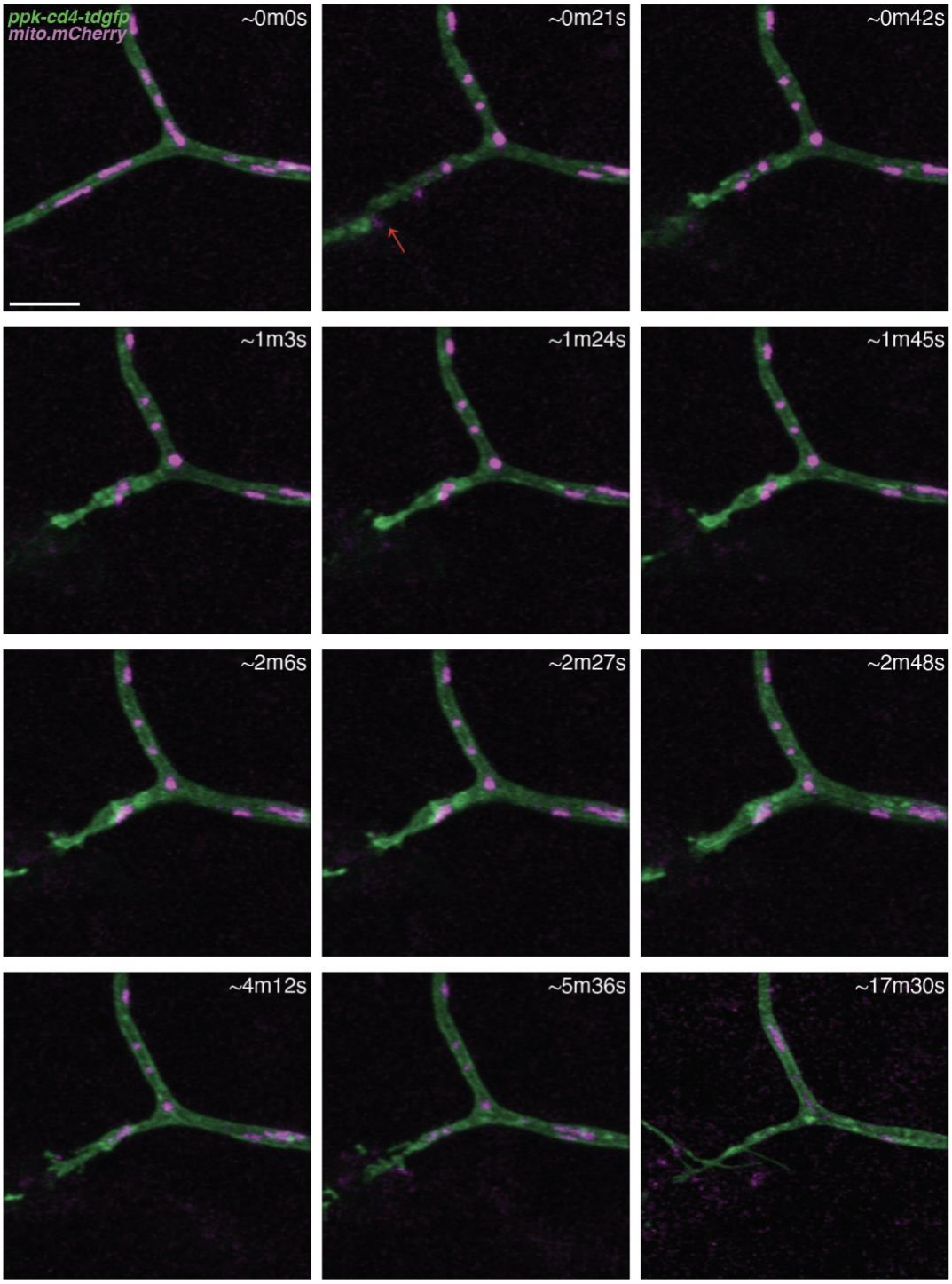

Fig. 17.0 Mitochondrial dynamics + recovery 30mins after dendrotomy

One thing that we also tested was whether mitochondria recovered back to tubular structures

after injury-induced contraction. To test this, we conducted larvaSPA and imaged mitochondria up to 30mins after injury. Interestingly, we never observed mitochondria recovering back to their baseline morphologies, even when they were still obviously visible (data not quantified). While mitochondria have been shown to recover their tubular morphologies following injury-induced contraction and transient contraction, we failed to observe this recovery.

APPENDIX E: Characterization of ddaE and ddaD branching order for computational simulations

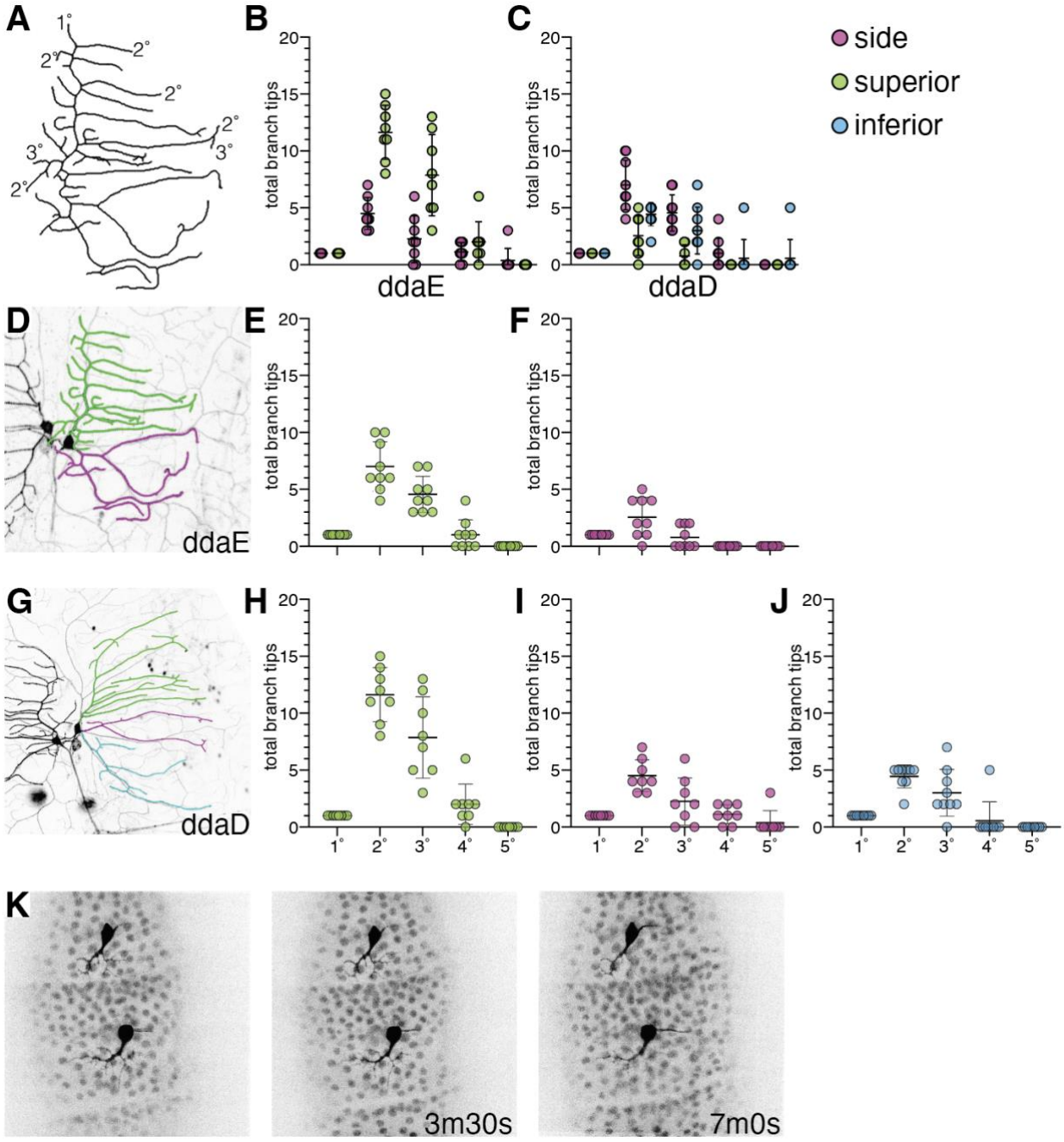

Fig. 18.0 Features of class I dendrite development and in-vivo dynamics

In collaboration with the Mjolness Lab (Dept. of Computer Science), we have been working on developing accurate simulations of class I dendrite development. On our end, we have been

providing their lab biological data such as branch tips of various branching orders for class I ddaD and ddaE to help generate more accurate simulations (A-J). We also conducted in vivo time lapse imaging of drosophila embryos using the class I driver ($gal4^{2\text{-}21}$) (K). To image drosophila embryos we deshelled drosophila embryos, placed them onto double-sided tape, and placed a drop of diH_2O. We imaged directly through the water without using a cover slip, using an upright immersion scope.

APPENDIX F: Dendrotomy induces ER fragmentation and calcium influx

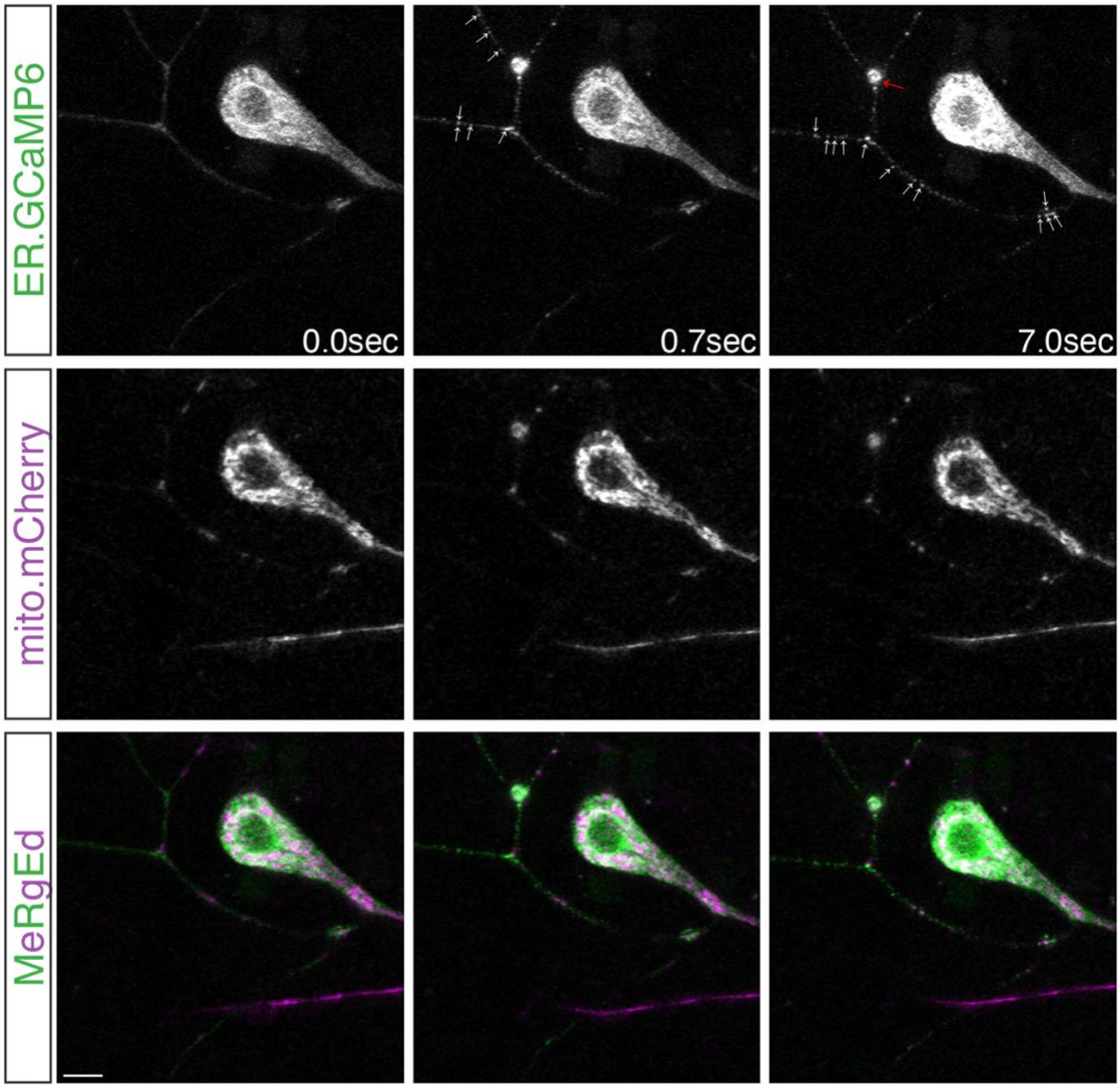

Fig. 19.0 Dendrotomy induces ER fragmentation and calcium influx

Mitochondrial-endoplasmic reticulum contact sites are known to regulate calcium exchange between mitochondria and ER. To better understand the cause of mitochondrial contraction, we simultaneously imaged ER calcium influx and mitochondria during dendrotomy. Under basal conditions, ER.GCaMP6 is not particularly bright or concentrated. Immediately after dendrotomy, ER fragment, accumulating calcium in a punctate manner. This injury-induced ER fragmentation

originated at and propagated as a wave away from the injury site (similar to injury-induced mitochondrial contraction). Interestingly, I observed changes in ER calcium flux in the absence of mitochondrial contraction, suggesting that the contraction response is not due to changes in ER calcium levels. Additionally, I observed instances where ER fragmentation propagated farther than mitochondrial contraction. Since we know that injury induces cytosolic, mitochondrial, and ER calcium influx I have no definitive interpretation of these observations. However, there were instances where ER fragmentation propagated farther than mitochondrial contraction, which informs me that, the change in ER morphology and subsequently changes in MERCS is not the driver of injury-induced mitochondrial contraction.